UNIVERSITY OF COPENHAGEN

Master's Thesis

Christian Holm Christensen

Lattice Quantum Chromodynamics with Quark Chemical Potential

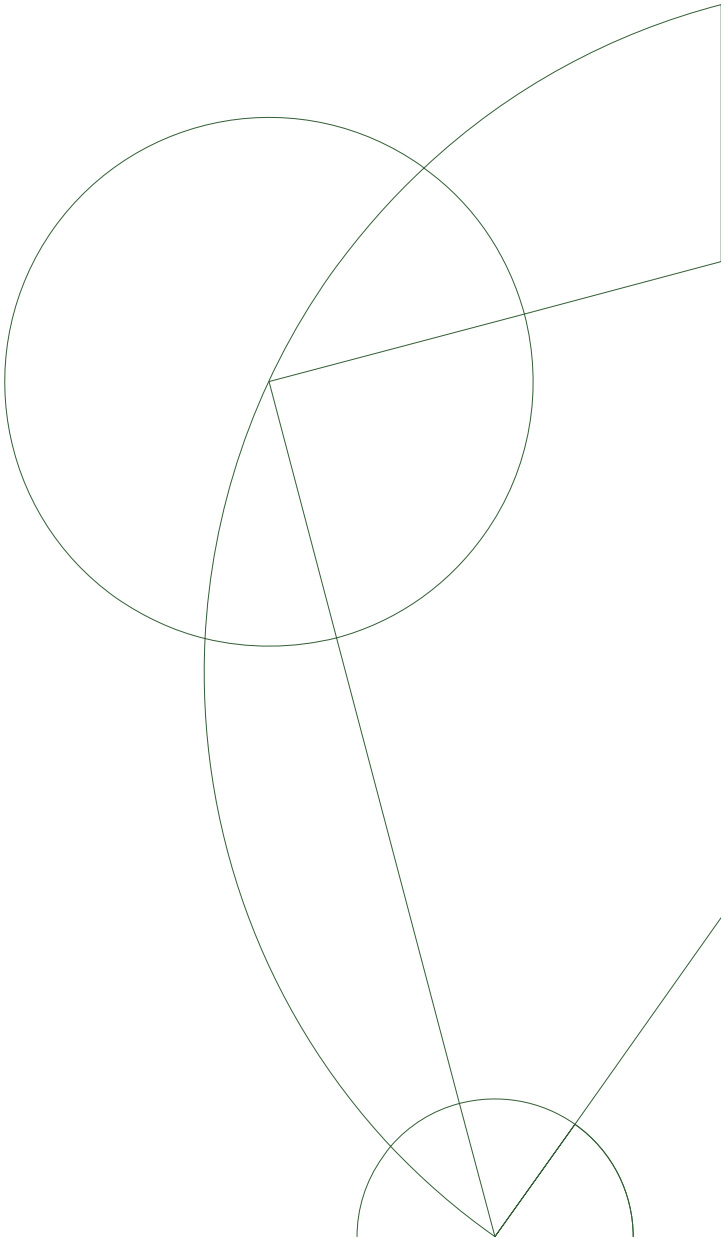

Supervisors:
Poul Henrik Damgaard
Kim Splittorff

Submitted May 1, 2012

Abstract

In this project the idea of Wilson's lattice action for quantum chromodynamics is presented together with an amount of group theory sufficient to make analytical calculations possible. Considering a lattice with a periodic temporal direction, the effective theory of Polyakov loops is derived based on the strong-coupling expansion of the theory. Both leading order and higher order terms are discussed. Finally a quark chemical potential μ is introduced and the expectation value of the Polyakov loop is calculated based on self-consistency equations and the similarity of $U(N_c)$ and $SU(N_c)$ in the large-N_c limit. Surprisingly the free energy turns out to be μ-independent and subsequently a vanishing expectation value of the quark number density operator is found. The findings of the project have given rise to a paper (arXiv:1204.2466) currently pending approval at Physics Letters B.

Acknowledgement

I would like to thank my supervisors Poul Henrik Damgaard and Kim Splittorff for the helpful and encouraging discussions we have had during my thesis, especially during the rough spots encountered along the way.
Furthermore I would like to thank the Niels Bohr Institute as a whole for supplying the foundation for what has been some of the greatest years of my life, both with regards to learning, personal growth and the forging of social connections.
Finally, I would like to thank Hjalte Frellesvig and Mizio Spatafora Andersen for proof reading.

Christian H. Christensen
Niels Bohr Institute
May 2012

Dansk Resume (Danish Summary)

Det primære fokus for dette speciale er introduktionen af Wilsons gitter-formulering af kvantekromodynamikken (QCD), den effektive "Polyakov-loop"-teori og bestemmelsen af forventningsværdien af den såkaldte Polyakov-loop variabel for stærk kobling og endelig temperatur.
Da kvantefeltteori imidlertid almindeligvis er en kontinuumsteori og beregninger ofte foretages perturbativt, gennemgås grundideerne bag pathintegraler og perturbationsteori ganske kort og bruges til at introducere endelig temperatur, samt til at forklare hvorfor perturbationsteorien bryder sammen ved stærk kobling. Ydermere introduceres gaugeteorier ved at modificere den frie feltteori for Dirac-spinorer, så den bliver invariant under gaugetransformationer. Fordelen ved denne indgangsvinkel er at *komparatoren*, der i en diskretiseret version danner grundlaget for gitterteorien, bliver introduceret.
For at kunne gennemgå de analytiske beregninger i gitterteorien introduceres nogle nødvendige gruppeteoretiske resultater, heriblandt det invariante integrale over grupper, samt ekspansionen af funktioner i termer af de repræsentationsafhængige *characters*.
På dette tidspunkt er det faglige fundament på plads og gitterteorien kan introduceres, først i form af en ren gaugeteori, men senere også med fermioner. I forbindelse med introduktionen af fermioner diskuteres den uønskede fermionfordobling, der kan fjernes ved introduktionen af de såkaldte Wilson-led i teorien. Det kvark-kemiske potentiale bliver introduceret i gitterteorien ud fra en beregning af den frie energi. Da det endelige mål er beregningen af forventningsværdien af Polyakov-loops bliver gitterteorien omskrevet til en effektiv teori for Polyakov-loops for stærk kobling og lille hopping parameter - herunder diskuteres også højereordens bidrag.
Efter et lille matematisk sidespring for at kunne evaluere et $U(N_c)$ integrale i $N_c \to \infty$ grænsen beregnes forventningsværdien for Polyakovloopet når et kvark-kemisk potentiale er påtrykt. Det grundlæggende trin her er at indse at teorien med det kvark-kemiske potentiale kan formuleres som en teori uden potentialet - herefter kan forventningsværdierne bestemmes analogt med tidligere resultater, ved brug af selvkonsistensligninger. For at få et indtryk af konvergenshastigheden af $U(N)$ integralet, når det er underlagt selvkonsistensligningerne, blev en numerisk beregning foretaget.
Endeligt blev den frie energi beregnet, hvilket ledte til den forventede opdagelse af en tredjeordens faseovergang i overensstemmelse med tidligere resultater. Overraskende var den frie energi helt uafhængigt af det påtrykte kvark-kemiske potentiale, hvilket betyder at forventningsværdien af kvarkdensiteten må være lig nul.
Beregningerne har givet ophav til en artikel der ligger på arXiv:1204.2466 og er indsendt til Physics Letters B.

Contents

Introduction

In this thesis I have tried to present the concepts of lattice-QCD in a way which makes contact with the continuum theory and which enables a reader without previous knowledge of lattice-QCD to follow the calculations. In order to do so I start with a chapter on continuum theory with emphasis on how the requirement of gauge invariance of a free field theory leads to the introduction of the comparator, which later, in a discretized version, becomes the fundamental degree of freedom on the lattice. An introduction to the essentials of group theory and group integrals is given before continuing to discuss lattice gauge theory and how both fermions and a quark chemical potential are introduced into it.
At this point the effective theory of Polyakov loops can be derived and my calculations and results on the large-N expectation value of the Polyakov loop with quark chemical potential are presented.

Chapter 1

Quantum Field Theory

1.1 Fundamentals

The sign convention used for the metric while in Minkowski space is

$$\eta^{\mu\nu} = \begin{bmatrix} 1 & 0 & 0 & 0 \\ 0 & -1 & 0 & 0 \\ 0 & 0 & -1 & 0 \\ 0 & 0 & 0 & -1 \end{bmatrix} \tag{1.1}$$

with the typical Minkowski spacetime indices running over $0, 1, 2, 3$. For the gamma matrices the Weyl/chiral representation will be used i.e.

$$\gamma^\mu = \begin{bmatrix} 0 & \sigma^\mu \\ \bar{\sigma}^\mu & 0 \end{bmatrix} \tag{1.2}$$

with

$$\sigma^\mu = (\mathbb{1}, \boldsymbol{\sigma}), \quad \bar{\sigma}^\mu = (\mathbb{1}, -\boldsymbol{\sigma}) \tag{1.3}$$

and

$$\sigma^1 = \begin{bmatrix} 0 & 1 \\ 1 & 0 \end{bmatrix}, \quad \sigma^2 = \begin{bmatrix} 0 & -i \\ i & 0 \end{bmatrix}, \quad \sigma^3 = \begin{bmatrix} 1 & 0 \\ 0 & -1 \end{bmatrix} \tag{1.4}$$

Most of this thesis will, however, be spent in Euclidean space, which can be rotated to by taking $x_0 \to -ix_4$, meaning that the Euclidean Lorentz indices run over $1, 2, 3, 4$. The motivation for this change is that it takes an ordinary inner product

$$x_{\mathrm{M}}^2 = \eta_{\mu\nu} x^\mu x^\nu = x_0^2 - \mathbf{x}^2 \to -\left(\mathbf{x}^2 + x_4^2\right) = -x_{\mathrm{E}}^2 \tag{1.5}$$

meaning that the Euclidean metric is simply

$$\eta^{\mu\nu} = \mathbb{1}_{4\times 4} = \begin{bmatrix} 1 & 0 & 0 & 0 \\ 0 & 1 & 0 & 0 \\ 0 & 0 & 1 & 0 \\ 0 & 0 & 0 & 1 \end{bmatrix} \tag{1.6}$$

so that time and space are treated on equal footings. Due to the form of the Euclidean metric, Lorentz indices can be lowered and raised at no cost. The form of the metric also has an impact on the gamma matrices, since in Minkowski space they need to fulfill the anti-commutator relation

$$\{\gamma^\mu, \gamma^\nu\} = 2\eta_M^{\mu\nu} \mathbb{1}_{4\times 4} \tag{1.7}$$

which becomes

$$\{\gamma^\mu, \gamma^\nu\} = 2\delta^{\mu\nu} \mathbb{1}_{4\times 4} \tag{1.8}$$

in Euclidean space. To accomodate this a simple change of the gamma matrices $i\gamma_i \to \gamma_i$ would suffice, but following the notation of Creutz [5] however, the substitution $\gamma^0 \to \gamma^4$ will be made, with

$$\gamma_4 \equiv \begin{bmatrix} \mathbb{1} & 0 \\ 0 & -\mathbb{1} \end{bmatrix} \tag{1.9}$$

and $\gamma^i \to \gamma_i' \equiv \gamma^4\gamma^i$. These new matrices satisfy the Euclidean space anti-commutator relations, which is most easily seen by realizing that $\gamma_4^2 = \mathbb{1}$ and $\gamma_4\gamma_i\gamma_4 = -\gamma_i$. Dropping the prime on the new spatial gamma matrices they are

$$\gamma_i = \begin{bmatrix} 0 & \sigma_i \\ \sigma_i & 0 \end{bmatrix} \tag{1.10}$$

from which it can be seen that all the new gamma matrices, aside from being unitary, are also Hermitian. Notice that the changes also apply to $\bar{\psi} \equiv \psi^\dagger\gamma^0$ and γ^5, the latter of which now can be written as

$$\gamma_5 = \gamma_1\gamma_2\gamma_3\gamma_4 = i\begin{bmatrix} 0 & -\mathbb{1} \\ \mathbb{1} & 0 \end{bmatrix} \tag{1.11}$$

by making the above-mentioned substitutions and moving γ_4 through at the cost of a sign.

1.2 Euclidean Path Integral

Since lattice theory takes place in a discretized space it is instructive to go through the path integral formulation - additionally this presents a chance to point out the correspondence betweeen statistical and quantum mechanics in a four dimensional Euclidean space. Chosing a simple Hamiltonian

$$\hat{H} = \frac{\hat{p}^2}{2m} + V(\hat{q}) \tag{1.12}$$

the probability amplitude of a particle moving from point q' to q within a time interval $\tau' - \tau$ is given by

$$\mathcal{A}(q', q) = \langle q'(\tau')|e^{-\hat{H}(\tau'-\tau)}|q(\tau)\rangle \tag{1.13}$$

which cannot be evaluated straightforwardly since the potential term $V(\hat{q})$ is position, and thus time, dependent. Subdiving the time interval into N_τ pieces of length $\epsilon = \frac{\tau'-\tau}{N_\tau}$ as shown in fig. 1.1a and writing $\tau_j = \tau + j\epsilon$ it is possible to calculate the transition amplitude between two neighbouring times

$$\begin{aligned}
\mathcal{A}(q(\tau_{j+1}), q(\tau_j)) &= \langle q(\tau_{j+1})|e^{-\hat{H}\epsilon}|q(\tau_j)\rangle && (1.14)\\
&= \int \frac{dp(\tau_{j+1})}{2\pi}\langle q(\tau_{j+1})|p(\tau_{j+1})\rangle\langle p(\tau_{j+1})|e^{-\hat{H}\epsilon}|q(\tau_j)\rangle && (1.15)\\
&\approx \int \frac{dp(\tau_{j+1})}{2\pi}e^{ip(\tau_{j+1})(q(\tau_{j+1})-q(\tau_j))-\epsilon H(p(\tau_{j+1}),q(\tau_j))} && (1.16)\\
&= \sqrt{\frac{m}{2\pi\epsilon}}e^{-\frac{m}{2\epsilon}(q(\tau_{j+1})-q(\tau_j))^2-\epsilon V(q(\tau_j))} && (1.17)
\end{aligned}$$

Since the approximation used relies on

$$e^{-\epsilon\hat{H}} = e^{-\epsilon\frac{\hat{p}^2}{2m}}e^{-\epsilon V(\hat{q})} + \mathcal{O}(\epsilon^2) \tag{1.18}$$

it is valid only as long as ϵ is sufficiently small. The whole transition amplitude is then expressible as

$$\mathcal{A}(q',q) = \left(\frac{m}{2\pi\epsilon}\right)^{\frac{N_\tau}{2}} \int \left[\prod_{j=0}^{N_\tau} dq(\tau_j)\right] e^{-\int_\tau^{\tau'} d\tau\left[\frac{m}{2}\dot{q}^2+V(q)\right]} \tag{1.19}$$

which, when ϵ is kept finite, is a lattice formulation of quantum mechanics. To reach the continuum the $N_\tau \to \infty$ limit is taken, resulting in

$$\mathcal{A}(q',q) = \int \lim_{N_\tau\to\infty}\left(\frac{m}{2\pi\epsilon}\right)^{N_\tau/2} \prod_{j=0}^{N_\tau} dq(\tau_j) e^{-\int_\tau^{\tau'} d\tau\left[\frac{m}{2}\dot{q}^2+V(q)\right]} \tag{1.20}$$

$$= \int \mathcal{D}q e^{-S_E}, \quad \mathcal{D}q = \lim_{N_\tau\to\infty}\left(\frac{m}{2\pi\epsilon}\right)^{N_\tau/2} \prod_{j=0}^{N_\tau} dq(\tau_j) \tag{1.21}$$

where S_E is the action in Euclidean space and the infinite dimensional integral is called the *path integral*. In order to see how this corresponds to a statistical system, let $\{|n\rangle\}$ be a orthonormal set of energy eigenstates with energy eigenvalues $\{E_n\}$ where $E_n \geq 0$. The transition amplitude can now be written as

$$\langle q',\tau'|q,\tau\rangle = \langle q'|e^{-H(\tau'-\tau)}|q\rangle = \sum_n \langle q'|n\rangle e^{-\epsilon N_\tau E_n}\langle n|q\rangle \tag{1.22}$$

Taking the endpoints to be equal, $q' = q$, as displayed in fig. 1.1b and integrating over q leads to

$$\mathcal{A} = \int dq\langle q,\tau'|q,\tau\rangle = \sum_n \langle n|\int dq|q\rangle\langle q|n\rangle e^{-\epsilon N_\tau E_n} = \sum_n e^{-\epsilon N_\tau E_n} \tag{1.23}$$

$$= \mathrm{Tr}[e^{-\epsilon N_\tau H}] = \int \mathcal{D}q e^{-S_E}, \quad S_E = \oint d\tau L_E(q,\dot{q}) \tag{1.24}$$

From which we see that the partition function of a quantum field theory with a temporal periodicity ϵN_τ is indistinguishable from that of a thermodynamic system, $Z = \mathrm{Tr}[e^{-\frac{1}{T}H}]$. It is thus possible to identify the temporal size of the lattice with a temperature $T = \frac{1}{\epsilon N_\tau}$.

1.3 Gauge Theory

A *gauge theory* is a theory with a Lagrangian which is invariant under a continuous group of local transformations. Historically it was first the theory of electromagnetism, which was found to be invariant under local $U(1)$ transformations but later

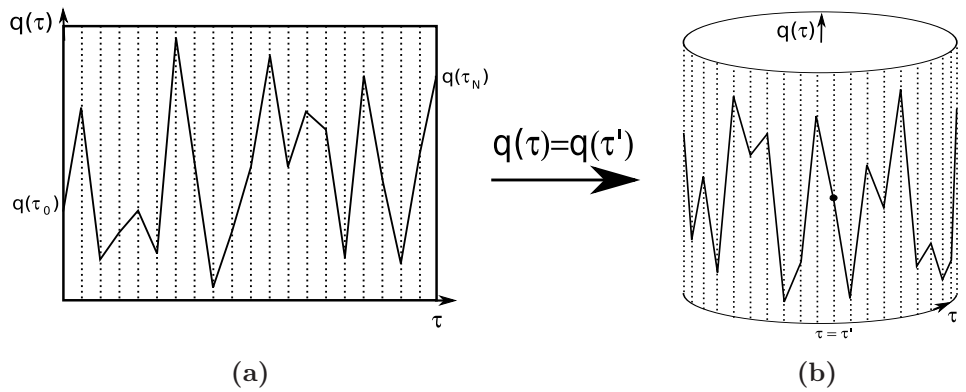

Figure 1.1: Path-Integrals (a) before and (b) after setting $q(\tau') = q(\tau)$. In each figure an example of a path have been drawn.

on, with the discovery of more general invariances ($SU(2)$ and $SU(3)$), gauge invariance rose to be regarded as a fundamental requirement of a theory of elementary particles. In this section $U(N)$ will be considered and it will be shown how to modify (*gauge*) the free field Lagrangian of Dirac spinors to be invariant under such a transformation. The section is based on chap. 15 of Peskin & Schroeder [10]. The starting point is the free field Lagrangian, which takes the form

$$\mathcal{L} = \bar{\psi}(x)\left(i\gamma^\mu\partial_\mu - m\right)\psi(x) \tag{1.25}$$

where flavour, colour and spinor indices have been left implicit. This theory is seen to be invariant under a global transformation $\psi_a(x) \to V_{ab}\psi_b(x)$ of the spinor fields, where V_{ab} is an element of the symmetry group $U(N)$ in some representation R (left implicit for ease of notation). This happens since the matrices V_{ij} are coordinate independent (commutes with ∂^μ), acts as an identity on the spinor space (commutes with γ_μ) and

$$\psi_a^\dagger\psi_a \to \left[V_{ab}\psi_b\right]^\dagger V_{ac}\psi_c = \psi_b^\dagger V_{ba}^* V_{ac}\psi_c = \psi_b^\dagger\delta^{bc}\psi_c = \psi_b^\dagger\psi_b \tag{1.26}$$

meaning that each term of the Lagrangian is invariant. The idea is now to make the Lagrangian invariant under a local version of this transformation i.e.

$$\psi_i(x) \to V_{ij}(x)\psi_j(x) \tag{1.27}$$

where $V_{ij}(x)$ are local elements of a representation of a general gauge group $\mathcal{G}$. As usual[1] it is possible to write a generic element as $V(x) = \exp(i\theta(x)_a T^a)$ with t^a being the generators of the group, which in the case of $U(N)$ are Hermitian. We want the variation of the Lagrangian (1.25) under the gauge transformation (1.27)

$$\delta\mathcal{L} = \mathcal{L}(V_{ab}(x)\psi_b(x)) - \mathcal{L}(\psi_a(x)) = i\bar{\psi}_b(x)\gamma^\mu V_{ab}^\dagger(x)(\partial_\mu V_{ac}(x))\psi_c(x) \tag{1.28}$$

[1]According to [11] page 14 a generic group element of a compact Lie group can be written in exponential form given an appropriate parametrization and a connection with the identity.

to vanish and the partial derivative to regain its intuitive meaning. The problem with the partial derivative is that by definition

$$n^\mu \partial_\mu \psi(x) = \lim_{\epsilon \to 0} \frac{1}{\epsilon} \left[\psi(x + \epsilon n) - \psi(x)\right] \tag{1.29}$$

but under a gauge transformation the two terms transform independently of each other due to their spacetime separation. To regain the comparability of the two points after a gauge transformation define a new derivative D_μ, called the *covariant derivative*, which transforms in such a way that $D_\mu \psi(x) \to V(x) D_\mu \psi(x)$. The easiest way to do this is to write

$$n^\mu D_\mu \psi(x) = \lim_{\epsilon \to 0} \frac{1}{\epsilon} \left[\psi(x + \epsilon n) - U(x + \epsilon n, x)\psi(x)\right] \tag{1.30}$$

where $U(x + \epsilon n, x)$ is called a *comparator* and chosen to transform as

$$U(y, x) \to V(y) U(y, x) V^\dagger(x) \tag{1.31}$$

such that the two terms in the covariant derivative transform in the same way under a gauge transformation. For simplicity we choose $U(x, x) = \mathbb{1}$ and restrict $U(y, x)$ to be a unitary matrix. This in turns means that close to the identity the comparator can be expanded in terms of its generators, t^a, as

$$U(x + \epsilon n, x) = \mathbf{1} + ig\epsilon n^\mu A^a_\mu(x) t^a + \mathcal{O}(\epsilon^2) \tag{1.32}$$

which, by insertion into (1.30), means that $D_\mu = \partial_\mu - igA^a_\mu t^a$. Here $A^a_\mu(x)$ are known as the *gauge fields* as they arise as a consequence of gauge invariance, but for ease of notation the contracted form $A_\mu(x) = A^a_\mu(x) t^a$ will generally be used. Since the needed transformation properties of D_μ are known it is possible to determine how A_μ transforms:

$$\begin{aligned} D_\mu(x) &\to V(x) D_\mu(x) V^\dagger(x) \\ \partial_\mu - igA_\mu(x) &\to V(x) \left(\partial_\mu - igA_\mu(x)\right) V^\dagger(x) \\ A_\mu(x) &\to V(x) A_\mu(x) V^\dagger(x) + \frac{i}{g} V(x) (\partial_\mu V^\dagger(x)) \end{aligned} \tag{1.33}$$

where $VV^\dagger = \mathbb{1}$ and $\partial_\mu V^\dagger = (\partial_\mu V^\dagger) + V^\dagger \partial_\mu$ have been used. The resulting Lagrangian

$$\mathcal{L} = \bar{\psi}(x) \left(i\gamma^\mu D_\mu - m\right) \psi(x) \tag{1.34}$$

is now invariant under gauge transformations. However, the question arises if more gauge invariant terms could be added to the theory; specifically terms involving only the gauge fields $A^a_\mu(x)$. Given the gauge transformation of the comparator (1.31), there is in fact a easy way to construct such a term, namely by considering the product of comparators around a very small loop[2]. However, first an exact form of the comparator for finite separations will be needed.

[2]Small due to the wish for locality

1.3.1 The Comparator

Starting by simply postulating a possible form of the comparator between two points, $x(0) = y$ and $x(1) = z$, along a specific path, $x(s)$, parametrized by the parameter s:

$$U_P(z,y) = P\left\{\exp\left[ig\int_0^1 ds\frac{dx^\mu}{ds}A^a_\mu(x(s))t^a\right]\right\} \tag{1.35}$$

where $P\{\}$ is the *path-ordering*, which orders the factors in each term such that lower values of s stand to the right. $U_P(z,y)$ is also known as the *Wilson line* and its Hermitian conjugate fulfills that $U^\dagger(z,y) = U(y,z)$, since the generators of a unitary group are Hermitian. At this point there are two things to show: That this expression has the appropriate gauge transformation (1.31) and that the comparator between infinitesimally separated points can be expressed as (1.32). The latter is easily seen by chosing the straight path between the two points, as

$$U_P(y+\epsilon n, y) = \exp\left[ig\epsilon n^\mu A^a_\mu(y)t^a\right] \tag{1.36}$$

where n^μ is a unit vector, has the appropriate power-series. The former statement requires a bit more work since it is not at all obvious that (1.35) transforms correctly. Using the small trick of noticing that the Wilson line can be expressed as a first order differential equation by

$$\begin{aligned}\frac{d}{ds}U_P(x(s),y) &= \left(ig\frac{dx^\mu}{ds}A^a_\mu(x(s))t^a\right)U_P(x(s),y) \qquad \Rightarrow \\ \frac{dx^\mu}{ds}D_\mu U_P(x,y) &= \frac{dx^\mu}{ds}\left(\frac{d}{dx^\mu} - igA^a_\mu(x(s))t^a\right)U_P(x(s),y) = 0\end{aligned} \tag{1.37}$$

where the integration range of eq. (1.35) is no longer $[0,1]$ but $[0,s]$ with s as a free parameter. Denoting by A^V and $U_P(z,y,A^V)$ the gauge transformed of the field configuration, A, and the Wilson line, $U_P(z,y,A)$, respectively, then the transformation we want to prove is

$$U_P(z,y,A^V) = V(z)U_P(z,y,A)V^\dagger(y) \tag{1.38}$$

However, from the infinitesimal form of the comparator the transformation properties of the covariant derivative are already known to be

$$D_\mu(A^V)V(x) = V(x)D_\mu(A) \tag{1.39}$$

which means that if $U_P(z,y,A)$ satisfies the differential equation, then so does $U_P(z,y,A^V)$. However, since the solution to a first order differential equation with a fixed boundary condition is unique, then eq. (1.38) is indeed the correct transformation property of the finitely separated comparator and eq. (1.35) the correct expression for finitely separated points

1.3.2 The Field Strength

With an explicit expression for the comparator at hand it is about time to consider the aforementioned loop. Representing $U(y, x)$ by a line pointing from x to y as

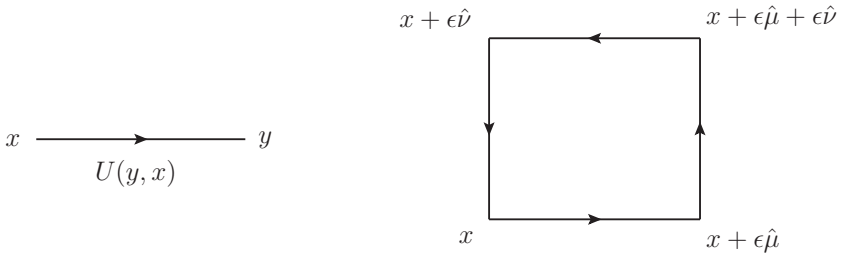

Figure 1.2: (a) The graphical representation of the comparator and (b) four/a comparator(s) forming a small loop.

depicted in figure 1.2a, the loop, $U_P(x, x)$ in figure 1.2b translates to

$$U_P(x,x) = P\left\{\exp\left[ig\epsilon\left(A_\mu(x+\frac{\epsilon}{2}\hat{\mu}) + A_\nu(x+\epsilon\hat{\mu}+\frac{\epsilon}{2}\hat{\nu})\right.\right.\right. \tag{1.40}$$

$$\left.\left.\left. -A_\mu(x+\frac{\epsilon}{2}\hat{\mu}+\epsilon\hat{\nu}) - A_\nu(x+\frac{\epsilon}{2}\hat{\nu})\right)\right]\right\} \tag{1.41}$$

$$= 1 + ig\epsilon^2\left(-\partial_\nu A_\mu(x) + \partial_\mu A_\nu(x)\right) - \frac{g^2\epsilon^2}{2}(-2)\left[A_\mu(x), A_\nu(x)\right] + \mathcal{O}(\epsilon^3) \tag{1.42}$$

$$= 1 + ig\epsilon^2\left(\partial_\mu A_\nu(x) - \partial_\nu A_\mu(x) - ig\left[A_\mu(x), A_\nu(x)\right] + \mathcal{O}(\epsilon^3)\right) \tag{1.43}$$

In this derivation there is a subtlety to be aware of both of which is related to the power series expansions performed, namely the effect of the path-ordering on the power series expansion of the gauge fields. Doing the naive power series expansion of the fields before the path-ordering leads to another result than path-ordering and then doing the power series expansion. The reason for this apparent discrepancy between the results arise from the group structure of the terms involved; path-ordering also reorders the group elements, which means that doing the power series expansion of the fields while within the path-ordering leads to an incorrect ordering of the, generally non-commuting, group elements. This detail also means that interpreting figure 1.2b as four, path-ordered comparators

$$U_P(x,x) = U_{P_1}(x+\epsilon\hat{\mu}, x)U_{P_2}(x+\epsilon\hat{\mu}+\epsilon\hat{\nu}, x+\epsilon\hat{\mu})U_{P_3}(x+\epsilon\hat{\nu}, x+\epsilon\hat{\mu})U_{P_4}(x, x+\epsilon\hat{\nu}) \tag{1.44}$$

where P_i denotes the different straight-line segments, yields the same result as previously where it was seen as a single comparator running in a loop[3] (at least to second order in ϵ). From the result of both calculations the second order term in ϵ is found to be

$$F_{\mu\nu}(x) = \partial_\mu A_\nu(x) - \partial_\nu A_\mu(x) - ig\left[A_\mu(x), A_\nu(x)\right] \tag{1.45}$$

which necessarily transforms as the comparator, i.e.

$$F_{\mu\nu}(x) \to V(x) F_{\mu\nu}(x) V^\dagger(x) \tag{1.46}$$

The quantity $F_{\mu\nu}$ is known as the *field strength tensor* and is a generalized curl of the gauge fields. Writing $F_{\mu\nu} = F^a_{\mu\nu} t^a$ it is possible to write $F^a_{\mu\nu}$ as

$$F^a_{\mu\nu}(x) = \partial_\mu A^a_\nu(x) - \partial_\nu A^a_\mu(x) + g f^{abc} A^b_\mu(x) A^c_\nu(x) \tag{1.47}$$

since the generators fulfill the commutator relation $[t^a, t^b] = i f^{abc} t^c$, where f^{abc} is the *structure constants* and is antisymmetric in its indices. Due to the transformation properties the field strength tensor is useful in constructing gauge invariant terms for the Lagrangian; the simplest term for the case of $SU(N)$, which displays both gauge and Lorentz invariance is $\mathrm{Tr}[F^2_{\mu\nu}] = \frac{1}{2}(F^a_{\mu\nu})^2$, assuming that the generators are in the fundamental representation and normalized such that $\mathrm{Tr}[t^a t^b] = \frac{1}{2}\delta^{ab}$. The final, gauge-invariant SU(N) Lagrangian is then

$$\mathcal{L} = \bar{\psi}(x)\left(i\gamma^\mu D_\mu - m\right)\psi(x) - \frac{1}{4}(F^a_{\mu\nu})^2 \tag{1.48}$$

where sums over both Lorentz and group indices are implied. In the physical theory of QCD then the gauge group is $SU(3)$ in the fundamental representation. Going to the Euclidean space formulation by taking $x_0 \to -ix_4$, changing the gamma matrices and taking $iS_M \to -S_E$ results in a Lagrangian

$$\mathcal{L} = \bar{\psi}(x)\left(\gamma^\mu D_\mu + m\right)\psi(x) + \frac{1}{4}(F^i_{\mu\nu})^2 \tag{1.49}$$

provided a simultaneous transformation $A_0 \to -iA_4$ is performed. This latter transformation was implied by the Lorentz index of the gauge field and ensures that the pure gauge term of the Lagrangian remains real. That this is indeed the correct Lagrangian can is most easily seen by considering eq. (1.48) and taking $i\gamma_i \to \gamma_i$.

1.4 Perturbation Theory

A tool which has proven immensely powerful within quantum field theories is that of perturbation theory and, although not applicable to the case in question, it deserves

[3]The commutator in the four-line case comes from the application of the Baker-Campbell-Hausdorff formula.

a brief mentioning - if for nothing else then to explain why it cannot be applied at strong coupling. The section is based on [1] and will contain a quick and dirty description of the fundamentals of perturbation theory and Feynman diagrams.
The basic principle behind perturbation theory is to split up the action into two parts

$$S[\psi] = S_0[\psi] + S_I[\psi] \tag{1.50}$$

where the first term S_0 is known as the *free* part and is an action for which the theory is exactly solvable and S_I is 'all the rest' i.e. terms which, when added to S_0 makes the theory unsolvable. The idea of perturbation theory is then to consider the case where S_I can be considered small i.e. a perturbation to the theory S_0. To get a bit more specific consider a theory

$$S(\bar{\psi}, \psi) = \bar{\psi} \cdot S_F^{-1} \cdot \psi + S_I(\bar{\psi}, \psi) \tag{1.51}$$

where ψ is a fermionic field and S_F^{-1} is an operator for which the inverse is known. The $\langle \cdot \rangle$ denotes contractions over all indices; spacetime, colour, spin, flavour etc but will be left implicit from now on. Adding source terms $\bar{\eta}\psi$ and $\bar{\psi}\eta$ to the action allows for correlation functions to be calculated by using functional derivatives

$$Z(\bar{\eta}, \eta) = \exp(-\bar{\psi} S_F^{-1} \psi - S_I(\bar{\psi}, \psi) + \bar{\eta}\psi + \bar{\psi}\eta) \tag{1.52}$$

$$\langle \psi \bar{\psi} \rangle = -\frac{\delta}{\delta \bar{\eta}} \frac{\delta}{\delta \eta} Z(\bar{\eta}, \eta) \tag{1.53}$$

where the minus sign is due to the anticommuting nature of Grassman numbers. Considering the free part of the action with applied source terms, then

$$\begin{aligned} Z_0(\bar{\eta}, \eta) &= \int \mathcal{D}\bar{\psi}\mathcal{D}\psi \exp(-\bar{\psi} S_F^{-1} \psi + \bar{\eta}\psi + \bar{\psi}\eta) \\ &= Z(0,0) \exp(\bar{\eta} S_F \eta) \end{aligned} \tag{1.54}$$

where a normalization such that $Z(0,0) = 1$ is usually chosen. Assuming that S_I is small the partition function of the full theory can be written as

$$\begin{aligned} Z(\bar{\eta}, \eta) &= \exp(-S_I(-\frac{\delta}{\delta \bar{\eta}}, \frac{\delta}{\delta \eta})) Z_0(\bar{\eta}, \eta) \\ &= \exp(-S_I(-\frac{\delta}{\delta \bar{\eta}}, \frac{\delta}{\delta \eta})) \exp(\bar{\eta} S_F \eta) \end{aligned} \tag{1.55}$$

by using Wick's theorem. Using Coleman's lemma this can be rewritten into a more convenient form

$$Z(\bar{\eta}, \eta) = \exp(-\frac{\delta}{\delta \psi} S_F \frac{\delta}{\delta \bar{\psi}}) \exp(-S_I(\bar{\psi}, \psi) + \bar{\eta}\psi + \bar{\psi}\eta) \Big|_{\bar{\psi}=\psi=0} \tag{1.56}$$

Consider the case where a bosonic field is present with the Yukawa interaction $\mathcal{L}_I(\bar{\psi}, \psi, \phi) = g\bar{\psi}\psi\phi$ with g assumed small. The partition function, after having applied Wick's theorem, is then

$$Z(\bar{\eta}, \eta, J) = e^{\frac{1}{2}\frac{\delta}{\delta\phi}\Delta\frac{\delta}{\delta\phi}} e^{-\frac{\delta}{\delta\bar{\psi}}S_F\frac{\delta}{\delta\psi}} \exp(-g\bar{\psi}\psi\phi + \bar{\eta}\psi + \bar{\psi}\eta + J\phi)\Big|_{\bar{\psi}=\psi=0} \tag{1.57}$$

where Δ is the bosonic propagator. The fermionic two-point function to leading order in g and with no external sources is now simply

$$\langle\psi\bar{\psi}\rangle = -\frac{\delta}{\delta\psi}S_F\frac{\delta}{\delta\bar{\psi}}\psi(x)\bar{\psi}(y) = S_F(x, y) \tag{1.58}$$

which can be represented diagrammatically as in fig. 1.3a. Another example is the fermionic two-point, bosonic one point, which, to lowest non-vanishing order in g, is

$$\begin{aligned}\langle\phi\psi\bar{\psi}\rangle &= \frac{1}{4}\frac{\delta}{\delta\phi}\Delta\frac{\delta}{\delta\phi}(-\frac{\delta}{\delta\psi}S_F\frac{\delta}{\delta\bar{\psi}})(-\frac{\delta}{\delta\psi}S_F\frac{\delta}{\delta\bar{\psi}})\left[\int d^4w' \left(-g\bar{\psi}\psi\phi\right)\right]\phi(x)\psi(y)\bar{\psi}(z) \\ &= gS_F(w, w)\Delta(w, x)S_F(y, z) + -gS_F(y, w)S_F(w, z)\Delta(w, x)\end{aligned} \tag{1.59}$$

The diagram corresponding to the first term is displayed in fig. 1.4a and the second in fig. 1.4b.

(a) Fermionic propagator **(b)** Bosonic propagator

Figure 1.3: Propagators corresponding to (a) $\langle\psi\bar{\psi}\rangle$ and (b) $\langle\phi\phi\rangle$.

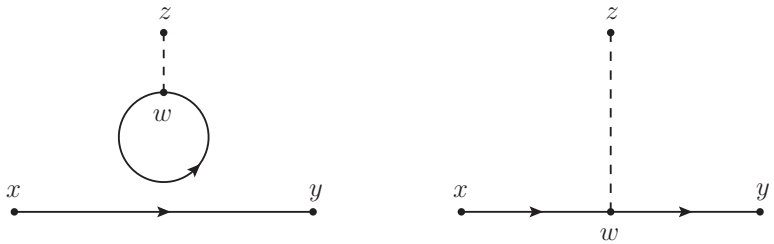

(a) Disconnected **(b)** Connected

Figure 1.4: Leading order contributions to $\langle\phi\psi\bar{\psi}\rangle$.

The procedure illustrated here can in principle be applied to any correlation function as long as the Taylor expansion of the exponential is convergent i.e. for sufficiently

small g. 'In principle' since the gluon-gluon interactions of QCD make even low order perturbative computations rather complicated. Another problem is that the value of the coupling constant g is not constant; rather, as a consequence of the renormalization necessary to get non-divergent integrals, the coupling is a function of energy. In the case of quantum chromodynamics this problem is especially devastating, since the low-energy coupling is too large for the perturbative methods of Feynman diagrams to be applied. Instead other methods need to be used, one of which is the lattice formulation of QCD which will be the focus of this thesis.
As this approach relies heavily on integrals over symmetry groups it is necessary to first take a detour into the world of group theory and its integrals.

Chapter 2

Groups

In this chapter the basics of group theory, group integration and character expansions will be introduced based on [2], [3] and, for the character expansions, [4]. Since integration over the group $SU(N)$ lies at the heart of lattice QCD a section dedicated to the evaluation of such integrals is included following the steps of [5]. The sections on group theory and integration over groups have been formulated somewhat mathematically and is largely self-contained, albeit without proofs. For the character expansion and the $SU(N)$ integration a much less rigorous formulation has been used, in part reflecting the nature of their sources.

2.1 Basics

Definition 1. A group $\mathcal{G}$ is a set of elements $\{G_i\}$ with an associated binary operator (denoted $\cdot$) such that

(i) $G_i \cdot G_j \in G$ (**closure**)

(ii) $G_i \cdot (G_j \cdot G_k) = (G_i \cdot G_j) \cdot G_k$ (**associativity**)

(iii) there exists a unique element $I \in G$ such that $I \cdot G_i = G_i = G_i \cdot I$ (**identity**)

(iv) there exists an element G_i^{-1} such that $G_i \cdot G_i^{-1} = I = G_i^{-1} \cdot G_i$ (**inverse**)

for all i, j, k.

A simple example of a group is $GL(N, C)$ which contains all complex, invertable matrices of dimension N and has matrix multiplication as its group operator. Another group, which has special relevance in particle physics is that of $U(N)$ which is the group of all unitary matrices of dimension N i.e. matrices fulfilling $UU^\dagger = \mathbb{1} = U^\dagger U$ where $U^\dagger$ is the complex conjugate and transposed of U. In this case the binary operator is matrix multiplication and the group can easily be seen to have both closure, associativity, an identity $I = \mathbb{1}$ and inverse matrices that are in the group $U^\dagger = U^{-1}$. The group $SU(N) \subseteq U(N)$ has the added requirement that $\det U = 1$.

Definition 2. A matrix representation $D : \mathcal{G} \to D(\mathcal{G}) \subseteq GL(n, \mathbb{C})$ of a group G is an assignment of a non-singular square $n \times n$ matrix $D(G_i)$ to each element $G_i \in G$, such that

(i) $D(I) = \mathbb{1}$

(ii) $D(G_i)D(G_j) = D(G_iG_j)$

When this is fulfilled D is said to be an n-dimensional representation of G

A simple representation of $U(N)$ is the *fundamental* representation, in which the representation matrices are $N \times N$.

Definition 3. A matrix representation D is said to be faithful if $D(G_i) \neq D(G_j)$ for every $G_i \neq G_j$.

An example of a representation which is not faithful is the *trivial* representation which maps every element of $\mathcal{G}$ into the identity.

Theorem 1. *The Rearrangement Theorem: For any fixed element $G' \in \mathcal{G}$ the sets $\{G'G|G \in \mathcal{G}\}$ and $\{GG'|G \in \mathcal{G}\}$ each contain every element of $\mathcal{G}$ once and only once.*

Definition 4. A set of elements $\{G_i\} \subseteq \mathcal{G}$ is said to form a conjugacy class if for any two elements in the set there exists a $X \in \mathcal{G}$ such that

$$G_i = XG_jX^{-1} \tag{2.1}$$

The elements G_i are said to be conjugate to each other.

Definition 5. The set of elements

$$Z(\mathcal{G}) = \{z \in \mathcal{G} | \forall G \in \mathcal{G}, zG = Gz\} \tag{2.2}$$

is called the center of $\mathcal{G}$.

In the case of $SU(N)$ the requirement that $\det U = 1$ for $U \in SU(N)$ restricts the center to be isomorphic to the cyclic group of order N denoted by Z_N. In the case that $SU(N)$ is in the fundamental representation i.e. $D(SU(N)) = SU(N)$ the elements of the center are $z = \exp(\frac{2\pi n}{N})\mathbb{1}_{N\times N}$ for $n \in \{0, 1, ..., N-1\}$.

2.2 Linear Lie Groups

Definition 6. Linear Lie group of dimension N

In order for a group $\mathcal{G}$ to be a linear Lie group it has to satisfy four conditions:

(I) *$\mathcal{G}$ must possess at least one faithful finite-dimensional representation $D(\mathcal{G})$*

Suppose $D(\mathcal{G})$ has dimension m. A metric, $d(G, G')$ between elements, G, G' can then be *defined* as

$$d(G, G') = \left[\sum_{i=1}^{m} \sum_{j=1}^{m} \left| D(G)_{ij} - D(G')_{ij} \right|^2 \right] \tag{2.3}$$

which implies that the group has been equipped with the topology of the m^2-dimensional complex Euclidean space $\mathbb{C}^{m^2}$. This metric has a number of properties

$$d(G, G') = d(G', G) \tag{2.4}$$
$$d(G, G) = 0 \tag{2.5}$$
$$d(G, G') > 0 \text{ for } G \neq G' \tag{2.6}$$
$$d(G, G'') \leq d(T, T') + d(T, T'') \tag{2.7}$$

Let S be the set of elements $G \in \mathcal{G}$ such that $d(G, E) < \delta$ for $\delta > 0$. These elements are said to *lie in a sphere of radius δ centered on the identity E.*

(II) *There must exist a $\delta > 0$ such that every element S can be parametrized by N real parameters $x_1, x_2..., x_N$ with no such two sets of parameters corresponding to the same element of S. The identity E is parametrized by $x_1 = x_2 = ... = x_N = 0$.*

This means that every element in S corresponds to one and only one point in a N-dimensional real Euclidean space $\mathbb{R}^N$.

(III) *There must exist a $\eta > 0$ such that every point in R^N for which*

$$\sum_{i=1}^{N} x_i^2 < \eta^2 \tag{2.8}$$

corresponds to some element G in S.

Denote the set of points fulfilling (III) by R_η. As a consequence of conditions (II) and (III) there is a one-to-one mapping of elements in S to points in R_η. Defining $G(x)$ to be the element $G \in \mathcal{G}$ corresponding to a point $x \in R_\mu$ and $D(x) = D(G(x))$. The last condition is then

(IV) *Each of the matrix elements of $D(x)$ must be an analytical function of $x \in R_\mu$.*

Here 'analytic' means expressible as a power series in $x_1 - x_1^0, x_2 - x_2^0, ..., x_N - x_N^0$

for all $x^0 \in R_\mu$, which in turn implies that all derivatives $\frac{\partial D_{ij}}{\partial x_k}$ must exist for all $i, j = 1, .., m$ and $x \in R_\mu$. Define the N $m \times m$ matrices $a_1, a_2, ..., a_N$ by

$$(a_p)_{ij} = \left(\frac{\partial D_{ij}}{\partial x_p} \right)_{x=0} \tag{2.9}$$

Theorem 2. *The matrices $a_1, a_2, ..., a_N$ form the basis for a N-dimensional real vector space.*

Theorem 3. *A maximal set of elements $\{G\}$ of a linear Lie group $\mathcal{G}$ that can be obtained from each other by continuously varying one or more of the matrix elements $D(G)_{ij}$ of the faithful finite dimensional representation D is said to form a 'connected component' of $\mathcal{G}$. A linear Lie group is said to be 'connected' if it has only one such component.*

Every connected component of a linear Lie group of dimension n can be parametrized by n real numbers $y_1, y_2, ..., y_n$ which form a connected set in $\mathbb{R}^n$ such that all the matrix elements $D(G)_{ij}$ in the connected component are continous functions of the parameters.

2.3 Invariant Integration

Since the formal definition of 'compact' is rather difficult then, for the purpose of this project, the following theorem will instead be used as the definition of compact:

Theorem 4. *A subset of points of a real or complex finite dimensional Euclidean space is 'compact' if and only if it is closed and bounded.*

As the continuous image of a compact set is always another compact set then

Theorem 5. *A linear Lie group of dimension N is compact if it has only a finite number of connected components and the parameters $y_1, y_2..., y_N$, which parametrize the group, range over closed, finite intervals $a_i \leq y_i \leq b_i$, $i = 1, 2, ..., N$.*

Due to the Rearrangement Theorem (theorem 1) it would be natural to assume that integrals over groups fulfill the same requirement. The problem however lies in whether a measure can be found such that this is fulfilled. This question was answered by Haar in (1933):

Theorem 6. *For linear Lie groups there always exists a left-invariant integral and a right-invariant integral.*

Let

$$\int_{\mathcal{G}} f(G) d_l G \equiv \int_{a_i}^{b_i} d^N y f(G(y)) \sigma_l(y) \tag{2.10}$$

$$\int_{\mathcal{G}} f(G) d_r G \equiv \int_{a_i}^{b_i} d^N y f(G(y)) \sigma_r(y) \tag{2.11}$$

be the left and right invariant integrals of a linear Lie group $\mathcal{G}$ such that

$$\int_{\mathcal{G}} f(G'G)d_lG = \int_{\mathcal{G}} f(G)d_lG \tag{2.12}$$

$$\int_{\mathcal{G}} f(GG')d_rG = \int_{\mathcal{G}} f(G)d_rG \tag{2.13}$$

for any $G' \in \mathcal{G}$ and any function $f(G)$ for which the integrals are well defined. The left- and right-invariant integrals are *finite* if

$$\int_{\mathcal{G}} d_lG \quad \text{and} \quad \int_{\mathcal{G}} d_rG \tag{2.14}$$

are finite. The left and right invariant measures are known as *Haar measures*. If the weight factors, σ_l, σ_r are equal up to a multiplicative constant so that the integrals are both left and right invariant, $\mathcal{G}$ is said to be *unimodular*. Peter and Weyl (1927) proved that

Theorem 7. *If $\mathcal{G}$ is a compact Lie group, then $\mathcal{G}$ is unimodular and the invariant integral*

$$\int_{\mathcal{G}} f(G)dG \equiv \int_{a_i}^{b_i} d^N y f(G(y))\sigma(y) \tag{2.15}$$

exists and is finite for every continuous function $f(G)$. Consequently $\sigma(y)$ can be chosen such that

$$\int_{\mathcal{G}} dG = 1 \tag{2.16}$$

which is the normalization assumed for the rest of the thesis.

2.4 Irreps and Characters

Theorem 8. *Let D be a d-dimensional representation of a group $\mathcal{G}$ and let S be any $d \times d$ non-singular matrix. Then the set of matrices given by*

$$D'(G) = S^{-1}D(G)S \tag{2.17}$$

for each $G \in \mathcal{G}$ also form a representation of $\mathcal{G}$. D and D' are said to be equivalent and the transformation is a 'similarity transformation'.

Theorem 9. *Every representation of a finite or compact Lie group is equivalent to a unitary representation.*

Definition 7. Any representation which can be brought into block-diagonal[1] form by a similarity transformation is said to be reducible.

Definition 8. A representation which is not reducible is said to be *irreducible*.

The irreducible representations are often referred to as the *irreps* of a group.

Theorem 10. *Orthogonality of unitary, irreducible representations: Let* $\hat{D}^{(\lambda)}$ *and* $\hat{D}^{(\mu)}$ *be two unitary, irreducible representations of the group* $\mathcal{G}$ *- it then follows that*

$$\int \left[\hat{D}^{(\lambda)}(G)\right]^*_{ab} \left[\hat{D}^{(\mu)}(G)\right]_{cd} dG = \frac{1}{d_\lambda}\delta_{ac}\delta_{bd}\delta_{\lambda\mu} \tag{2.18}$$

where a, c *denotes the rows and* b, d *the columns of the matrices and* d_λ *is the dimension of the representation(s).*

However, since the representations and irreps change with the choice of coordinate basis and as such are not unique, the trace of the matrices is a more convenient quantity to consider since it is invariant under similarity transformations.

Definition 9. The characters $\chi(G)$ of a representation D of a group $\mathcal{G}$ is defined as the traces of the matrices $D(G)$ i.e. $\chi(G) = \mathrm{Tr}[D(G)]$.

Since the characters are representation specific they might occasionally be written as $\chi_r(G)$ to state their relation to the representation r explicitly. Notice that all elements within a conjugacy class is given the same character - functions where all elements of a conjugacy class are given the same value are known as *class functions*. The orthogonality of irreducible representations and the definition of characters lead to:

Theorem 11. *Orthogonality of characters: The characters* χ_λ *and* χ_μ *of two irreducible representations,* λ *and* μ*, of the group* $\mathcal{G} = \{G\}$ *fulfills*

$$\int [\chi_\lambda(G)]^* [\chi_\mu(G)]\, dG = \delta_{\lambda\mu} \tag{2.19}$$

Proof. Starting from the left hand side of 2.19 by simply inserting the definition of the characters:

$$\begin{aligned}\int dG\, [\chi_\lambda(G_i)]^* [\chi_\mu(G)] &= \int dG \sum_{a=1}^{n_\lambda}\sum_{c=1}^{n_\mu} \left[\hat{D}^{(\lambda)}(G)\right]^*_{aa} \left[\hat{D}^{(\mu)}(G)\right]_{cc} \\ &= \frac{1}{n_\lambda}\sum_{a=1}^{n_\lambda}\sum_{c=1}^{n_\mu}\delta_{ac}\delta_{ac}\delta_{\lambda\mu} = \frac{1}{n_\lambda}\sum_{a=1}^{n_\lambda}\delta_{\lambda\mu} = \delta_{\lambda\mu}\end{aligned} \tag{2.20}$$

where n_λ, n_μ are the dimensions of the representations. □

[1] Block-diagonal is here understood as consisting only of diagonal submatrices of smaller dimension than the full matrix.

Theorem 12. *The characters χ_r form a basis for every square integrable class function $f(G)$, meaning that*

$$f(G) = \sum_r \alpha_r \chi_r(G), \quad \alpha_r = \int \chi_r^*(G) f(G) dG \tag{2.21}$$

where α_r are known as the expansion coefficients.

A well-known example of this arises in the case of $U(1)$, where the representations are labelled by integers such that $\chi_n(e^{i\theta}) = e^{in\theta}$ and the expansion is

$$f(\theta) = \sum_n \alpha_n e^{in\theta}, \quad \alpha_n = \frac{1}{2\pi} \int e^{-in\theta} f(\theta) d\theta \tag{2.22}$$

which is just a regular Fourier transformation.

2.5 Integration over SU(N)

Since the Wilson action, which will be introduced later, is expressed by special unitary matrices in the fundamental representation, it will be sufficient to consider integration over group elements in this representation. Following the steps of [7] a general approach to calculating the integral over a product of elements $U, U^\dagger \in SU(N)$ in the fundamental representation can be derived. Defining a generating function

$$W(J,K) = \int dU \exp(\mathrm{Tr}[JU + KU^\dagger]) \tag{2.23}$$

where J and K are arbitrary $N \times N$ matrices, an integral I over a product of group elements can be expressed as derivatives of $W(J,K)$ as

$$\begin{aligned} I &= \int dU U_{i_1 j_1} \cdots U_{i_n j_n} U^\dagger_{k_1 l_1} \cdots U^\dagger_{k_m l_m} \\ &= \left(\frac{\partial}{\partial J_{i_1 j_1}} \cdots \frac{\partial}{\partial J_{i_n j_n}} \frac{\partial}{\partial K_{k_1 l_1}} \cdots \frac{\partial}{\partial K_{k_m l_m}} \right) W(J,K) \Big|_{J=K=0} \end{aligned} \tag{2.24}$$

A simplification of this expression is possible by expressing $U^\dagger = U^{-1}$ in terms of the adjugate (transpose of the cofactor) of U as

$$\begin{aligned} (U^{-1})_{ij} &= \frac{1}{\det(U)} \mathrm{adj}(U)_{ij} = (\mathrm{cof}(U))_{ji} \\ &= \frac{1}{(N-1)!} \epsilon_{j i_1 \ldots i_{n-1}} \epsilon_{i j_1 \ldots j_{n-1}} U_{i_1 j_1} \cdots U_{i_{n-1} j_{n-1}} \end{aligned} \tag{2.25}$$

using $\det(U) = 1$ for $SU(N)$. This means that the K derivatives in eq. (2.24) can be replaced with J-derivatives and K dropped entirely from the equations. Writing

$W(J) = W(J, K = 0)$ and using a result from [8], which is based on the left and right invariance of the measure, $W(J)$ can be shown to only depend on powers of the determinant of J. Writing

$$W(J) = \sum_{i=0}^{\infty} a_i (\det J)^i \tag{2.26}$$

a direct consequence of the normalization of the Haar measure is that $a_0 = 1$. Using a combinatorial result from [9]:

$$\left(\det(\frac{\partial}{\partial J})\right)(\det J)^i = \frac{(i+N-1)!}{(i-1)!}(\det J)^{i-1} \tag{2.27}$$

together with

$$(\det \frac{\partial}{\partial J})W(J) = W(J) \tag{2.28}$$

which follows from $\det(U) = 1$, a recursive relation for the a_i-coefficients can be found by

$$\begin{aligned} W(J) &= \left(\det(\frac{\partial}{\partial J})\right) W(J) \\ &= \sum_{i=0}^{\infty} a_i \left(\det(\frac{\partial}{\partial J})\right)(\det J)^i \\ &= \sum_{i=1}^{\infty} a_i \frac{(i+N-1)!}{(i-1)!}(\det J)^{i-1} \end{aligned} \tag{2.29}$$

which, by moving the summation limits, means that

$$a_i = \frac{(i-1)!}{(i+N-1)!} a_{i-1} \tag{2.30}$$

from which a closed form is easily found knowing that $a_0 = 1$

$$\begin{aligned} a_i &= \prod_{m=1}^{i} \frac{(m-1)!}{(m+N-1)!} \\ &= \prod_{m=0}^{i-1} \frac{m!}{(m+N)!} \\ &= \frac{2!3!...(i-1)!}{N!(N+1)!...(i+N-1)!} \\ &= \frac{2!3!...(N-1)!}{i!(i+1)!...(i+N-1)!} \end{aligned} \tag{2.31}$$

$$= \prod_{m=0}^{N-1} \frac{m!}{(i+m)!} \tag{2.32}$$

Inserting the expression into (2.26) gives

$$W(J) = \sum_{i=0}^{\infty} \left(\prod_{m=0}^{N-1} \frac{m!}{(i+m)!} \right) (\det J)^i \tag{2.33}$$

Now everything is in place for evaluation of integrals of the type (2.24) given that we remember that for an arbitrary $N \times N$ matrix M the determinant can be written as

$$\det(M) = \frac{1}{N!} \epsilon_{i_1 \ldots i_n} \epsilon_{j_1 \ldots j_n} M_{i_1 j_1} \ldots M_{i_n j_n} \tag{2.34}$$

To summarize; replace factors of $U^\dagger$ with Us using eq. (2.25), replace Us with J derivatives and let the derivatives act on (2.33) to evaluate the integral finishing of by setting $J = 0$. Due to the nature of the Haar measure doing the opposite i.e. replacing Us with $U^\dagger$s etc. is also an option - and occationally preferable.

2.5.1 Evaluation of integrals

Starting off by a few simple consequences of the rules derived - first off then

$$\begin{aligned} I &= \int dU U_{i_1 j_1} \cdots U_{i_m j_m} U^\dagger_{k_1 l_1} \cdots U^\dagger_{k_n l_n} \\ &= 0 \quad \text{for} \quad [(n-m) \bmod N] \neq 0 \end{aligned} \tag{2.35}$$

which reflects the fact that the only term, which survives setting $J = 0$, is the one with exactly as many J-derivatives as is contained in one of the $(\det J)^i$ terms; a multiple of N. Since each $U^\dagger$ term leads to a cofactor and each of these contain $N-1$ derivatives w.r.t. J the final result becomes $(n-m) \mod N$. Applying this to a simple integral in the case of SU(3)

$$I_3 = \int dU U_{i_1 j_1} U_{i_2 j_2} U_{i_3 j_3} \tag{2.36}$$

it can be evaluated using the system described in the previous subsection. Then

$$\begin{aligned} I_3 &= \frac{\partial}{\partial J_{i_1 j_1}} \frac{\partial}{\partial J_{i_2 j_2}} \frac{\partial}{\partial J_{i_3 j_3}} W(J,K) \Big|_{J=K=0} \\ &= \frac{\partial}{\partial J_{i_1 j_1}} \frac{\partial}{\partial J_{i_2 j_2}} \frac{\partial}{\partial J_{i_3 j_3}} W(J) \Big|_{J=0} \\ &= \frac{1}{6} \frac{\partial}{\partial J_{i_1 j_1}} \frac{\partial}{\partial J_{i_2 j_2}} \frac{\partial}{\partial J_{i_3 j_3}} \det J \\ &= \frac{1}{6} \epsilon_{i_1 i_2 i_3} \epsilon_{j_1 j_2 j_3} \end{aligned} \tag{2.37}$$

However, keeping track of all the indices soon becomes a rather cumbersome affair - luckily an alternative to writing out all of the equations exists.

2.5.2 Diagrammatic Representation

To simplify the integrations, diagrammatic rules can be introduced as described in [9]. Here U_{ij} is depicted as an upwards arrow, $U^{\dagger}_{ij}$ as a downwards arrow and the identity δ_{ij} as a vertical line as shown in figure 2.1.

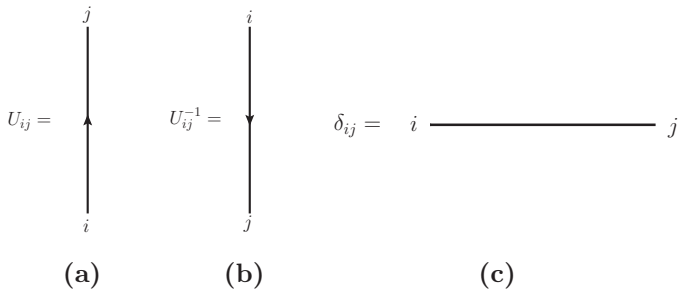

Figure 2.1: The diagrammatic representation of (a) the group element U_{ij}, (b) the inverse, U^{-1}_{ij}, and (c) the identity/Kronecker delta δ_{ij}.

These conventions means that the general $SU(N)$ integral (2.24) can be drawn as in figure 2.2.

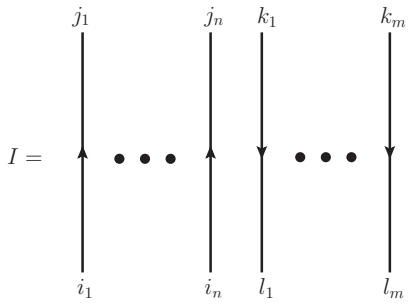

Figure 2.2: Representation of the general SU(N) integral (2.24).

Adding to the collection a diagram for the Levi-Civita symbol as in figure 2.3a the invariance of the Kronecker and Levi-Civita symbols under the operations

$$U_{ij}\delta_{jk}U^{-1}_{kl} = \delta_{il} \tag{2.38}$$

$$U_{i_1j_1}...U_{i_Nj_N}\epsilon_{j_1...j_N} = \epsilon_{i_1...i_N} \tag{2.39}$$

can be represented as in figs. 2.3b and 2.3c.
Using eq. (2.25) to express U^{-1} in terms of Us is depicted in fig. 2.4. Finally, it will be convenient to have some expressions for contractions of indices on Levi-Civita

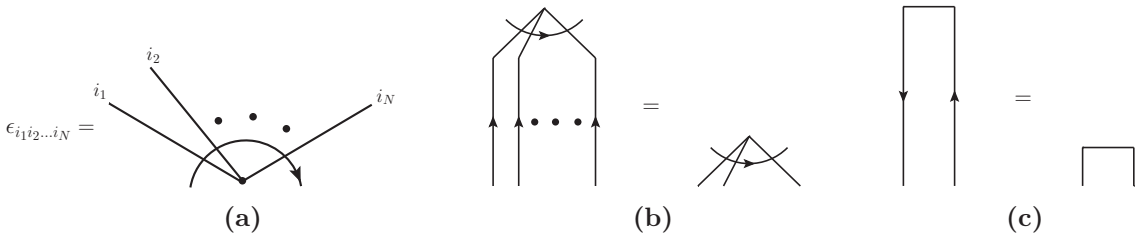

Figure 2.3: (a) The representation of the Levi-Civita symbol and invariance of (b) the Levi-Civita symbol and (c) the Kronecker delta symbol.

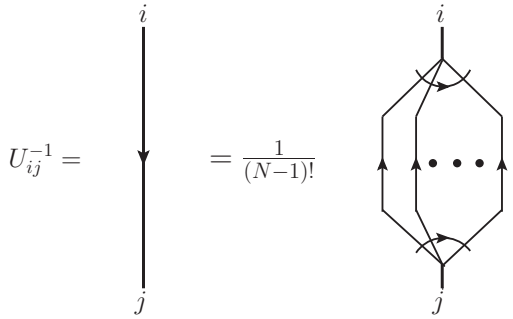

Figure 2.4: Replacing the inverse by the cofactor.

symbols:

$$\epsilon_{i_1 \ldots i_N} \epsilon_{i_1 \ldots i_N} = N! \tag{2.40}$$

$$\epsilon_{i, i_1 \ldots i_{N-1}} \epsilon_{j i_1 \ldots i_{N-1}} = (N-1)! \delta_{ij} \tag{2.41}$$

$$\epsilon_{ij i_1 \ldots i_{N-2}} \epsilon_{kl i_1 \ldots i_{N-2}} = (N-2)! \left(\delta_{ik}\delta_{jl} - \delta_{il}\delta_{jk}\right) \tag{2.42}$$

which are also shown in fig. 2.5. Expressions for contractions with fewer indices can easily be deduced; if n indices are contracted there is a combinatorial factor $n!$ followed by a combination of delta functions with the same index symmetry as that of the Levi-Civita symbols.

Finally, the last piece of the puzzle is the actual integration over a number of aligned lines. As a consequence of eq. (2.35) only a multiple of N lines is non-vanishing, so considering Np aligned lines where $p \in \mathbb{N}$, the result is as shown in fig. 2.6. To explain the figure consider how the Np differentiations acts on the determinants; naively the chain rule leads to $(Np)!$ different terms, but since it does not matter which of the p determinants a pairing of N group elements act on, there will be $p!$ cases where a specific pairing into p sets of N elements appear. Furthermore, within a given set of N group elements the matrix indices on each individual U_{ij} element is put in the same position on separate Levi-Civita symbols, meaning that each ordering within the set of N elements gives rise to the same factor. The combinatorial factor of $N!$ arising from this is however cancelled by the

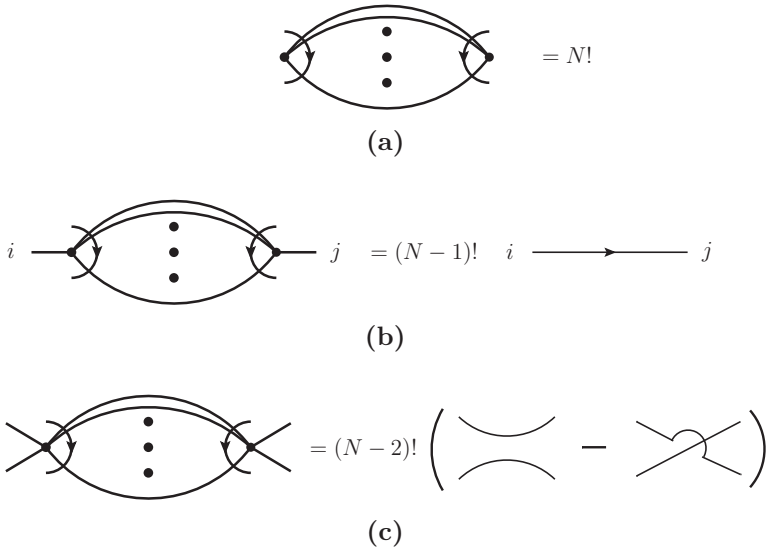

Figure 2.5: Three different $\epsilon_{i_1 i_2 \ldots i_N}$ contractions. corresponding to (a) eq. (2.40), (b) eq. (2.41) and (c) eq. (2.42)

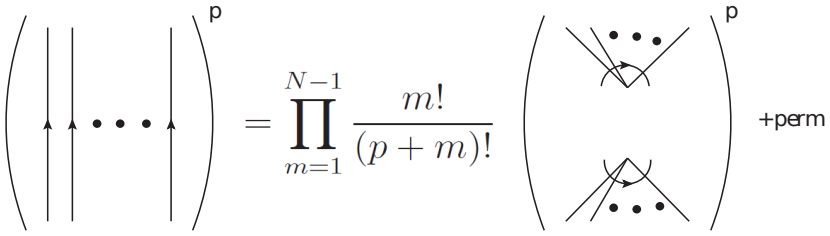

Figure 2.6: Integration of Np group elements - the permutations are over all other groupings of the indices.

$\frac{1}{N!}$ coming from the expression for the determinant. Finally, the differentiation leads to a splitting of first and second indices onto separate Levi-Civita symbols within a set of N elements leading to a complete separation of upper and lower indices in the diagram. Each of the resulting $\frac{(Np)!}{(N!)^p p!}$ unique combinations of indices are the permutations referred to in fig. 2.6.

2.5.3 Diagrammatical Integration

At this point everything is set up for the diagrammatic evaluation of group integrals! For instance the result

$$\int dU U_{ij} U^{-1}_{kl} = \frac{1}{N} \delta_{il} \delta_{jk} \tag{2.43}$$

can be derived as displayed in fig. 2.7. A quick summary: First fig. 2.4 was used to express U^{-1}_{kl} in terms of Us, then fig. 2.6 was used to evaluate the integrals and

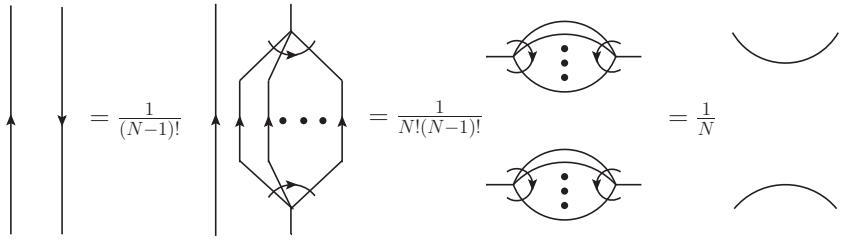

Figure 2.7: Evaluation of the integral $\int dU U_{ij} U_{kl}^{-1}$.

finally fig. 2.5b was used to express the result in terms of Kronecker symbols. Considering the more complicated case of

$$\int dU U_{ij} U_{kl}^{-1} U_{mn} U_{op}^{-1} \tag{2.44}$$

it is possible to again perform the diagrammatic integration as displayed in fig. 2.8. That the terms come in pairs of two follows from the original symmetry of the problem; switching U_{kl}^{-1} with U_{op}^{-1} makes no difference to the calculations and as such diagrams related by this symmetry should have the same coefficients. Furthermore no contraction between indices on U_{ij} and U_{mn} or U_{kl}^{-1} and U_{op}^{-1} appear; this is a direct consequence of fig. 2.5c, which splits the lines into different contractions.

Determining the value of a and b can either be done through a tedious combinatorial

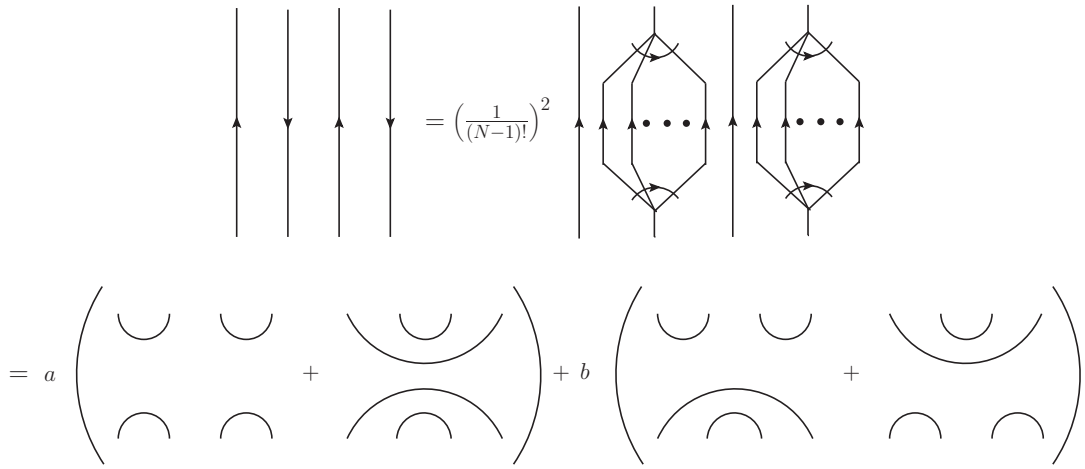

Figure 2.8: Evaluation of the integral $\int dU U_{ij} U_{kl}^{-1} U_{mn} U_{op}^{-1}$.

excercise or by contracting two of the free indices. Going with the latter and using the result of fig. 2.7, the evaluation is as displayed in fig. 2.9. From the figure the

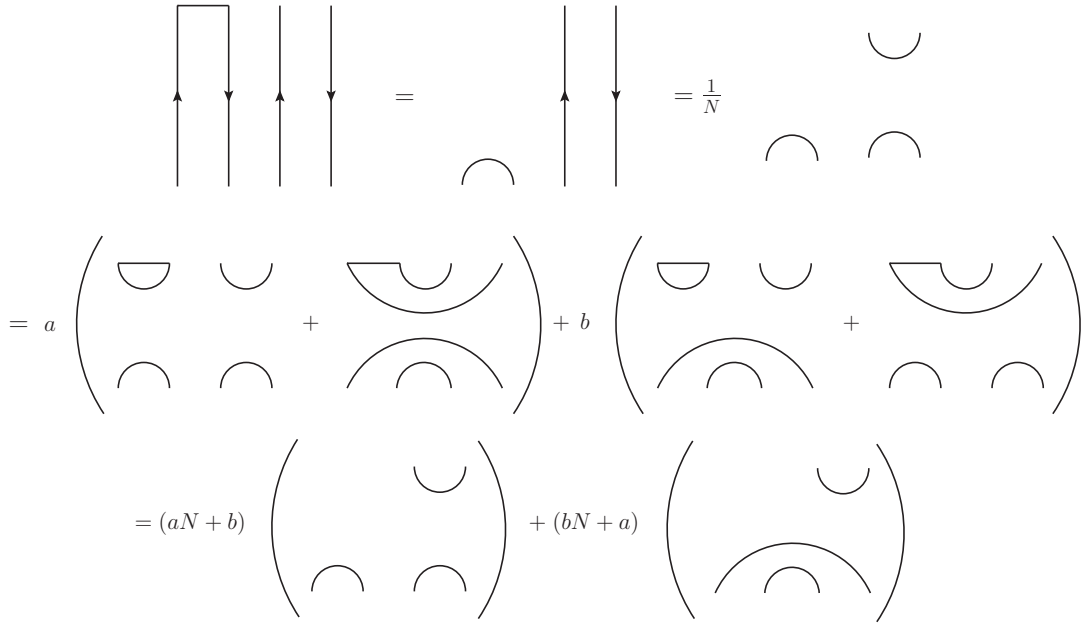

Figure 2.9: Evaluation of the coefficients a and b - closed circles represent $\delta_{ii} = N$.

coefficients can be determined as

$$aN + b = \frac{1}{N} \quad \wedge \quad bN + a = 0 \tag{2.45}$$

$$\Leftrightarrow a = \frac{1}{N^2 - 1} \quad \wedge \quad b = -\frac{1}{N(N^2 - 1)} \tag{2.46}$$

The final value of the integral is then

$$\begin{aligned} \int dU U_{ij} U^{-1}_{kl} U_{mn} U^{-1}_{op} = \quad & \frac{1}{N^2 - 1} \quad [\delta_{il}\delta_{jk}\delta_{mp}\delta_{no} + \delta_{ip}\delta_{jo}\delta_{ml}\delta_{nk}] \\ & - \frac{1}{N(N^2 - 1)} [\delta_{il}\delta_{jo}\delta_{mp}\delta_{nk} + \delta_{ip}\delta_{jk}\delta_{ml}\delta_{no}] \end{aligned} \tag{2.47}$$

Chapter 3

Lattice QCD

Due to the growth of the strong coupling parameter and with this the breakdown of perturbation theory for QCD at low energies, an alternative approach was necessary in order to understand the quark and gluon interactions in this limit. The approach which will be introduced in this chapter was conceived by Wilson [7] and formulates QCD on a spacetime lattice. The chapter is based on [4, 5, 12]

3.1 The Lattice

Several forms of lattices could be considered, but the most used (and straightforward) is that of the hypercube, occasionally however with a different lattice separation in the temporal direction than in the spatial ones. Here we will use the simple hypercube with a spacetime lattice separation constant denoted by a. Since the spacetime points are discrete we can choose the coordinates so that any point can be written as multiples of a:

$$x_\mu = m_\mu a \text{ for } m_\mu \in \mathbb{Z}^4 \tag{3.1}$$

In this way the directionality of the lattice axes are chosen to coincide with that of the spacetime system (i.e. all axes are either perpendicular or parallel) and one of the lattice points are chosen to be placed in the origo of the spacetime system. Notice that no generality is lost doing this since rotational and translational invariance of Euclidean space allows for any choice of spacetime reference frame. The m_μ values themselves are intrinsic coordinates known as *lattice coordinates* and represent another way of denoting the lattice sites.
While discussing spacetime symmetries it is worth noticing that as spacetime passes from a continuum to a discrete system, so does the symmetries; instead of continuous translational and rotational symmetry, these become discrete; for $n \in \mathbb{Z}$ translations by na along the lattice axes and rotations of $\frac{\pi}{2}n$ in the planes spanned by any two of the lattice axes are the only remaining symmetries of the system. Naturally, when passing back to the continuum, the original symmetries are recovered.

3.2 Wilson Action

In this section a brief introduction of the theory of gauge fields on a space-time lattice which Wilson proposed in 1974 will be presented based on [13]. The theory relies on the fact that a gauge field can be seen as a path-dependent phase factor as is evident from the explicit form of the comparator (1.35). Defining a lattice version of the comparator is done by making a simple approximation to the integral involved, which will become exact when the $a \to 0$ limit is taken. Writing

$$U_{ij} = \exp(igA_\mu(x)a) \tag{3.2}$$

where i and j are lattice coordinates denoting the endpoints of the comparator, defines a gauge field A_μ as a function of the spacetime coordinate x_μ. Here x_μ needs to converge to the appropriate point in the continuum limit, which can be ensured by using a suitable convention - for instance

$$x_\mu = \frac{1}{2}a(i_\mu + j_\mu) \tag{3.3}$$

By this procedure every lattice link is associated with a group element, U_{ij}, in one direction and its inverse, $U_{ji} = U_{ij}^{-1}$ in the opposite direction. At this point, due to the method used in section 1.3.2 of deriving the field strength term of the QCD Lagrangian based on the requirement of gauge invariance, it has already been shown that the field strength tensor can be formulated on a lattice in terms of loops $U_{ij}U_{jk}U_{kl}U_{li}$ circling around the fundamental, $a \times a$ squares (known as *plaquettes*) on the lattice. Wilson's proposal was then an action of the form

$$S = \sum_{\square} S_{\square}$$
$$S_{\square} = \beta\left(1 - \frac{1}{N}\operatorname{Re}\operatorname{Tr}[U_{ij}U_{jk}U_{kl}U_{li}]\right) \tag{3.4}$$

where N is the dimension of the representation matrices of the symmetry group in question and the sum runs over all oriented plaquettes to give the spacetime integration. The additive constant is chosen such that the action vanishes near the identity and β will be fixed by requiring the action to behave correctly in the continuum limit. The action is real, positive (since the eigenvalues of a unitary matrix have modulus one) and gauge invariant due to the transformation property of the comparator.

3.2.1 Retrieving the Yang Mills Action

Picking up from section 1.3.2, where an infinitesimal loop was considered, it should be clear that multiplying out the link variables U_{ij} leads to

$$S_{\square} = \beta\left(1 - \frac{1}{N}\operatorname{Re}\operatorname{Tr}[\exp(iga^2F_{\mu\nu} + O(a^3))]\right) \tag{3.5}$$

something which is more explicitly shown in the appendix A. Limiting ourselves to consider unitary groups means that every term in the exponent is an imaginary number times a Hermitian matrix due to $[t^a, t^b] = if^{abc}t^c$. Since Hermitian matrices have purely real eigenvalues, odd-order terms in the expansion of the exponential will have purely imaginary traces and thus contribute nothing to the action after the real part has been extracted. This leaves only even-order terms, specifically

$$\begin{aligned} S_\square &= \beta \left(1 - \frac{1}{N} \operatorname{Re} \operatorname{Tr}[\mathbf{1} - \frac{1}{2} g_0^2 a^4 F_{\mu\nu}^2] + \mathcal{O}(a^5)\right) \\ &= \frac{\beta g^2}{2N} a^4 \operatorname{Tr}[F_{\mu\nu}^2] + \mathcal{O}(a^5) \end{aligned} \tag{3.6}$$

which means that the full action in the continuum limit becomes

$$S = \sum_\square S_\square = \frac{\beta g_0^2}{4N} \int d^4x \operatorname{Tr}[F_{\mu\nu}^2] \tag{3.7}$$

by using $a^4 \sum_\square \to \int d^4x$. The extra factor of $\frac{1}{2}$ is due to $F_{\mu\nu}^2$ now having an implicit sum over the indices, which leads to a double counting. At this point a quick check with section 1.3.2 confirms that the correct action is indeed retrieved by choosing

$$\beta = \frac{2N}{g_0^2} \tag{3.8}$$

meaning that the Wilson action is a valid lattice Yang-Mills action.

3.2.2 Integrating over links

Here, a short intermezzo to discuss some cases of what happens when links that are shared between plaquettes are integrated out. Consider first two plaquettes with the same orientation lying next to each other as depicted in fig. 3.1a and perform

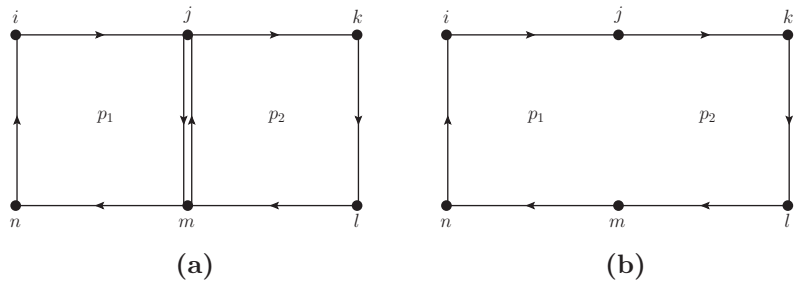

Figure 3.1: Integration over a link shared by two neighbouring plaquettes with the same orientation: (a) Before and (b) after integration.

an integration over the link, U_{jm}, that they share:

$$\int dU_{jm}\mathrm{Tr}[U_{p_1}^{(r_1)}]\mathrm{Tr}[U_{p_2}^{(r_2)}] = \int dU_{jm}\mathrm{Tr}[U_{mnij}^{(r_1)}U_{jm}^{(r_1)}]\mathrm{Tr}[U_{jklm}^{(r_2)}U_{mj}^{(r_2)}] \tag{3.9}$$

where the shorthand $U_{ijkl} = U_{ij}U_{jk}U_{kl}$ has been used and the characters have been allowed to be in different representations for generality. Writing the matrix indices and using the orthogonality relation (2.18) leads to

$$\begin{aligned}\int dU_{jm}\mathrm{Tr}[U_{p_1}^{(r_1)}]\mathrm{Tr}[U_{p_2}^{(r_2)}] &= \int dU_{jm}\left[U_{mnij}^{(r_1)}\right]_{ab}\left[U_{jm}^{(r_1)}\right]_{ba}\left[U_{jklm}^{(r_2)}\right]_{cd}\left[U_{jm}^{(r_2)}\right]^*_{cd} \\ &= \frac{1}{N}\delta^{r_1r_2}\left[U_{mnij}^{(r_1)}\right]_{ab}\left[U_{jklm}^{(r_1)}\right]_{ba} \\ &= \frac{1}{N}\delta^{r_1r_2}\mathrm{Tr}[U_{mnij}^{(r_1)}U_{jklm}^{(r_1)}] \\ &= \frac{1}{N}\delta^{r_1r_2}\mathrm{Tr}[\prod_{ij\in C}U_{ij}^{r_1}]\end{aligned} \tag{3.10}$$

meaning that the integration merges the two plaquettes into one loop as depicted graphically in figure 3.1b. The C denotes the contour indicated in the figure. From

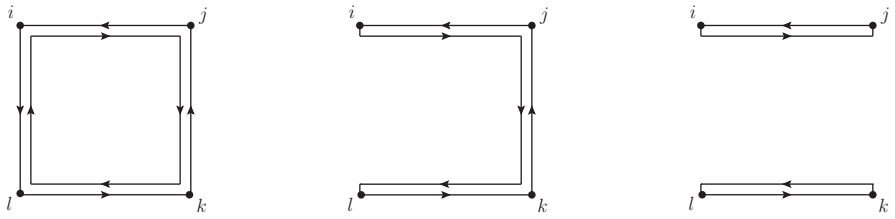

(a) **(b)** **(c)**

Figure 3.2: Integration of links for two oppositely oriented plaquettes placed on top of each other (a) before and (b) after the first and (c) after two integrations. As can be seen (b) corresponds to a 'folding' of fig. 3.1b.

here it is easy to consider the case of fig. 3.2a with two oppositely oriented loops placed on top of each other. In this case

$$\begin{aligned}\int dU\mathrm{Tr}[U_p^{(r_1)}]\mathrm{Tr}[U_p^{*(r_2)}] &= \frac{1}{N^2}\delta^{r_1r_2}\int dU_{ij}dU_{kl}\left[U_{ij}\right]_{ab}\left[U_{ij}^*\right]_{ab}\left[U_{kl}\right]_{cd}\left[U_{kl}^*\right]_{cd} \\ &= \frac{1}{N^4}\delta^{r_1r_2}(\delta^{aa})^4 = \delta^{r_1r_2}\end{aligned} \tag{3.11}$$

Considering another example, namely the case of N overlapping plaquettes with the same orientation in the fundamental representation of $SU(N)$, then

$$\begin{aligned}\int dU(\mathrm{Tr}U_p)^N &= \int dU\,[U_{ij}]_{a_1b_1}\,[U_{jk}]_{b_1c_1}\,[U_{kl}]_{c_1d_1}\,[U_{li}]_{d_1a_1}\cdot\ldots\\ &\quad\cdot\ldots[U_{ij}]_{a_Nb_N}\,[U_{jk}]_{b_Nc_N}\,[U_{kl}]_{c_Nd_N}\,[U_{li}]_{d_Na_N}\\ &= \int dU_{ij}\,[U_{ij}]_{a_1b_1}\,[U_{ij}]_{a_2b_2}\cdots[U_{ij}]_{a_Nb_N}\int dU_{jk}\,[U_{jk}]_{b_1c_1}\ldots[U_{li}]_{d_Na_N}\\ &= \left(\prod_{l=0}^{N-1}\frac{1}{1+l}\right)^4(\epsilon_{a_1\ldots a_N})^2(\epsilon_{b_1\ldots b_N})^2(\epsilon_{c_1\ldots c_N})^2(\epsilon_{d_1\ldots d_N})^2\\ &= \left(\frac{1}{N!}\right)^4(N!)^4 = 1 \end{aligned} \tag{3.12}$$

where the results of section 2.5 have been used. In the case of $SU(3)$ this can be depicted as in fig. 3.3.

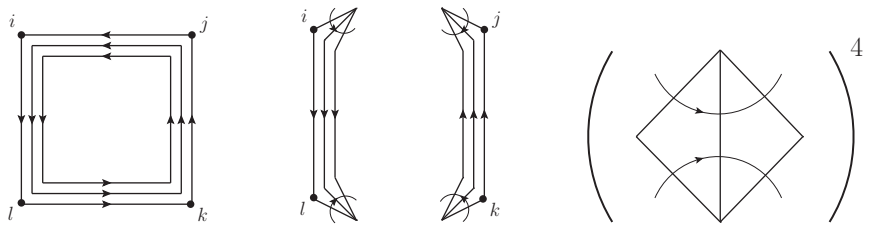

(a) **(b)** **(c)**

Figure 3.3: Diagrams for the integration over three plaquettes with the same orientation placed on top of each other in the case of $SU(3)$: (a) Before integration, (b) after two integrations and (c) after all integrations. Prefactors not included.

3.2.3 Strong Coupling Expansion

At strong couplings the parameter $\beta = \frac{2N}{g^2}$ gets small enough that a power series expansion of the exponential around zero becomes possible. From now on we will be working with a slightly simplified version of eq. (3.4)

$$S = -\frac{\beta}{2N}\sum_P\left(\mathrm{Tr}U_p + \mathrm{Tr}U_p^*\right) \tag{3.13}$$

where the constant term has been included in the normalization of the partition function. Unless otherwise stated then the group elements $U, U^\dagger$ are in the fundamental representation of $SU(N)$ with $N > 2$. Given this action the expansion

is

$$\begin{aligned} Z &= \int dU e^{-S} = \int dU e^{\frac{\beta}{2N}\sum_p \left(\mathrm{Tr}U_p + \mathrm{Tr}U_p^*\right)} \\ &= \int dU \sum_{m=0}^{\infty} \frac{1}{m!} \left(\frac{\beta}{2N} \sum_p (\mathrm{Tr}U_p + \mathrm{Tr}U_p^*) \right)^m \\ &= \int dU \prod_p \left(\sum_{m=0}^{\infty} \frac{1}{m!} \left[\frac{\beta}{2N} \mathrm{Tr}U_p \right]^m \right) \left(\sum_{n=0}^{\infty} \frac{1}{n!} \left[\frac{\beta}{2N} \mathrm{Tr}U_p^* \right]^n \right) \\ &= \int dU \prod_p \sum_{m,n=0}^{\infty} \frac{1}{m!n!} \left(\frac{\beta}{2n} \right)^{m+n} (\mathrm{Tr}U_p)^m (\mathrm{Tr}U_p^*)^n \end{aligned} \tag{3.14}$$

where $\sum_p$ is over all the plaquettes in the lattice and $U_p = U_{ij}U_{jk}U_{kl}U_{li}$ is the product of links around a single plaquette. Recalling eq. (2.35) then the integral will vanish if any single link-site on the lattice does not fulfill $\frac{m-n}{N} \in \mathbb{Z}$, meaning that the lowest order, non-trivial contribution will be for $m = n = 1$ i.e. second order in β, so that

$$\begin{aligned} Z &= \int dU \prod_p \left(1 + \frac{\beta^2}{4N^2} \mathrm{Tr}U_p \mathrm{Tr}U_p^* + \mathcal{O}(\beta^3) \right) \\ &= \int dU \left(1 + \frac{\beta^2}{4N^2} \sum_p \mathrm{Tr}U_p \mathrm{Tr}U_p^* + \mathcal{O}(\beta^3) \right) \\ &= 1 + \frac{\beta^2}{4N^2} N_p + \mathcal{O}(\beta^3) \end{aligned} \tag{3.15}$$

where N_p is the total number of plaquettes. An exception is for $SU(2)$ for which $m = 2$, $n = 0$ and $m = 0$, $n = 2$ also contributes. Since the matrices are real in this case the partition function is

$$\begin{aligned} Z_{SU(2)} &= \int dU \left(1 + \frac{\beta^2}{2N^2} \sum_p (\mathrm{Tr}U_p)^2 + \mathcal{O}(\beta^4) \right) \\ &= 1 + \frac{\beta^2}{2N^2} N_p + \mathcal{O}(\beta^3) \end{aligned} \tag{3.16}$$

The diagrammatical representation of these lowest order terms have already been shown in fig. 3.2 for $SU(N)$ and 3.3 for $SU(3)$. Some higher order, non-vanishing terms are shown in fig. 3.4. From the calculations above it should be easy to see that all closed surface structures, built by pairing two oppositely oriented links at each link-site, will be non-vanishing.

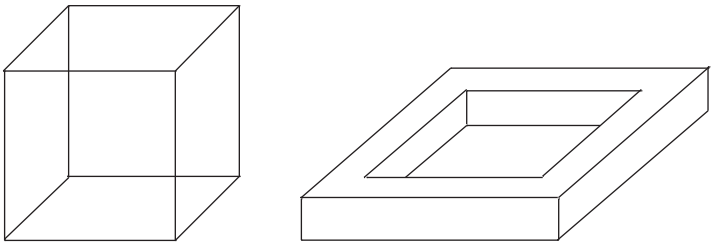

(a) **(b)**

Figure 3.4: Two types of higher order, non-vanishing terms in the strong coupling expansion; each line represents the pairing of two oppositely oriented lines of links that has not yet been integrated out.

3.2.4 Wilson Loops

The expectation value of a Wilson loop in the pure $SU(N_c)$ lattice gauge is given by:

$$\langle W \rangle = Z^{-1} \int dU \frac{1}{N} e^{-S} \mathrm{Tr} \prod_{ij \in C} U_{ij} \tag{3.17}$$

where the $\frac{1}{N}$ is introduced for later convenience. Considering the case of a 3×3 loop as depicted in fig. 3.5a. At strong coupling the lowest order contribution becomes that of fig. 3.5b since each link needs to be paired up with one of the opposite orientation (for $N > 2$). The expansion brings down a factor of $\frac{\beta}{2N}$ for each plaquette, integration of each pair of oppositely oriented links gives $\frac{1}{N}$ and finally each site leads to a factor N as can be seen from fig. 3.5d. For a more general $I \times J$ loop then it is straightforward to see that to lowest order in β

$$\langle W \rangle = \frac{1}{N} \left(\frac{\beta}{2N} \right)^{IJ} \frac{1}{N^{I(J+1)+J(I+1)}} N^{(I+1)(J+1)} = \left(\frac{\beta}{2N^2} \right)^{IJ} \tag{3.18}$$

In the case of $SU(2)$ there is the additional option of bringing down plaquttes such that pairs of links of the same orientation get matched - in this case the expectation value is

$$\langle W \rangle = \left(\frac{\beta}{N^2} \right)^{IJ} = \left(\frac{\beta}{4} \right)^{IJ} \tag{3.19}$$

From these equations it is evident that - at least to leading order - there is an area law

$$\langle W \rangle = K^A, \quad K = \begin{cases} \frac{\beta}{2N^2} & \text{for } N > 2 \\ \frac{\beta}{4} & \text{for } N = 2 \end{cases} \tag{3.20}$$

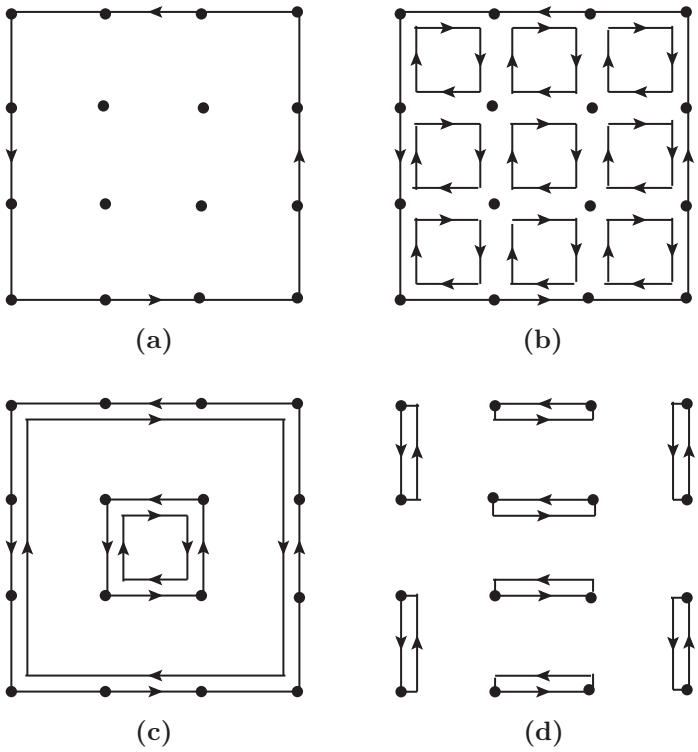

Figure 3.5: When calculating the expectation value of a 3×3 Wilson loop (a) the lowest order contribution is to fill it with oppositely oriented plaquettes as in (b). Integration can then proceed as shown by (c) and (d).

at play but that it generalizes to arbitrarily-shaped Wilson loops is implied by fig. 3.6 - simply removing one square at a time along the perimeter gives a factor of K per plaquette. The next to leading order terms will depend on the theory - for $SU(3)$ there is the option of replacing one of the tiling plaquettes of fig. 3.5b with two going in the opposite direction as displayed in fig. 3.7a. Since this can be done anywhere within the Wilson loop it leads to

$$\langle W \rangle = \left(\frac{\beta}{2N^2}\right)^{IJ} \left(1 + IJ\frac{\beta}{4N} + \mathcal{O}(\beta^2)\right) = \left(\frac{\beta}{18}\right)^{IJ} \left(1 + IJ\frac{\beta}{12} + \mathcal{O}(\beta^2)\right) \quad (3.21)$$

The next order includes diagrams as displayed in figs. 3.7b and 3.7c. Eventually also non-planar terms, like figs. 3.8a and 3.8b, will contribute - in these figures every drawn plaquette-site is occupied such that each line without arrows represent two oppositely oriented links.
Disconnected diagrams are generally removed by the $\frac{1}{Z}$-factor but in some cases too much is removed by this procedure - specifically whenever the diagram for a term in Z overlaps with the connected diagram of the nominator. The contribution from

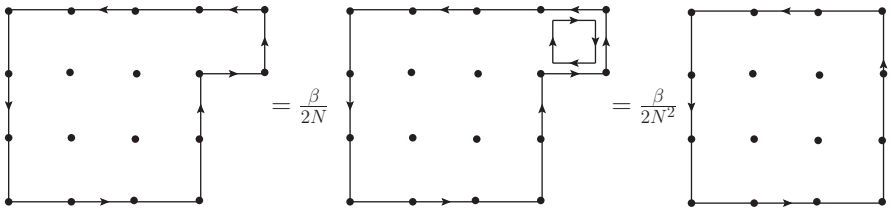

Figure 3.6: Removing one plaquette at a time leads to a factor of K per fundamental square within the loop. Here displayed for the case of $N > 2$.

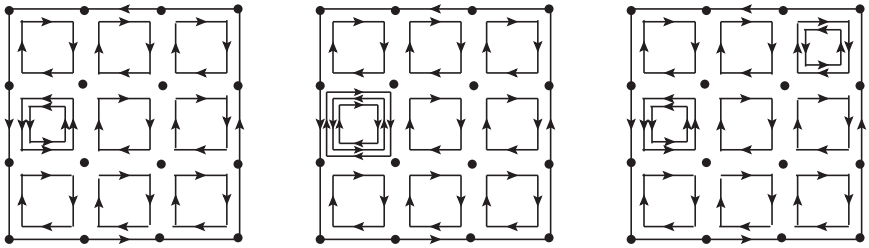

Figure 3.7: Higher order, planar contributions to $\langle W \rangle$ for $SU(3)$. (a) Next to leading order and (b) and (c) both next-to-next leading order in β

fig. 3.9 is

$$\langle W \rangle_{Z^{-1}\text{correct}} = -\left(\frac{\beta}{2N^2}\right)^{IJ} \left(\frac{\beta}{2N}\right)^2 IJ = -81\left(\frac{\beta}{18}\right)^{11} \tag{3.22}$$

where the IJ factor stems from the fact that there is exactly one overlap for every plaquette within the Wilson loop.

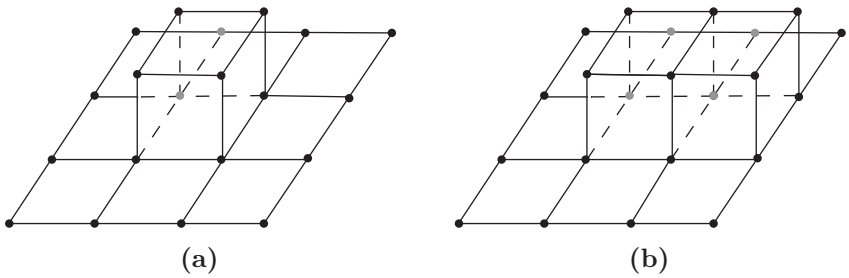

Figure 3.8: Higher order, non-planar contributions to $\langle W \rangle$ for $SU(N)$. (a) $\mathcal{O}(\beta^4)$ and (b) $\mathcal{O}(\beta^6)$ higher than the leading order term

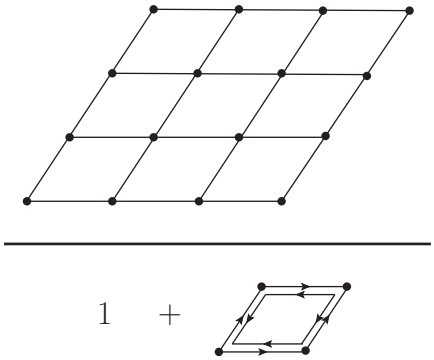

Figure 3.9: Correction to $\langle W \rangle$ stemming from Z^{-1}

Characters Applied

Another way to deal with the integrations is by using the character expansion of eq. (2.21). Writing

$$Z = \int dU e^{-S} = \int dU \prod_P \exp\left[\frac{\beta}{2N}\left(\mathrm{Tr}U_p + \mathrm{Tr}U_p^*\right)\right] \tag{3.23}$$

and performing the character expansion

$$Z = \int dU \prod_P \left(1 + \sum_{r\neq 0} \alpha_r \chi_r(U_P)\right) \tag{3.24}$$

$$\alpha_r = \int dU \chi_r^*(U) \exp\left[\frac{\beta}{2N}\left(\mathrm{Tr}U + \mathrm{Tr}U^*\right)\right] \tag{3.25}$$

it should be clear that, using the character expansion, the problem of how the plaquette sites are tiled has been simplified greatly. Every representation have an expansion coefficient α_r, which needs to be computed, but this only involves a single integral over the group in question. After that there is a product which only involves each plaquette once. However, the problem of tiling has been substituted with a different one; the integration over products of characters in different representations. Performing these integrals turns out to be rather hard and with the group theoretical insights presented so far only two of the expansion coefficients can be calculated in the strong coupling expansion:

$$\alpha_0 = \int dU \exp\left[\frac{\beta}{2N}\left(\mathrm{Tr}U + \mathrm{Tr}U^*\right)\right] \tag{3.26}$$

$$= 1 + \frac{\beta^2}{4N^2} + \frac{\beta^3}{24N^3} + \mathcal{O}(\beta^4) \tag{3.27}$$

$$\alpha_f = \int dU \chi_f^*(U) \exp\left[\frac{\beta}{2N}\left(\mathrm{Tr}U + \mathrm{Tr}U^*\right)\right] \tag{3.28}$$

$$= \frac{\beta}{2N} + \frac{\beta^2}{8N^2} + \frac{\beta^4}{64N^4} + \mathcal{O}(\beta^5) \tag{3.29}$$

where for the integration the choice of $SU(3)$ was made to provide an explicit example. For other representations symmetry and the orthogonality of characters (2.19) can be invoked to realize that $\alpha_r = \mathcal{O}(\beta^2)$ or higher. Applied to the case of the 3×3 Wilson loop then the lowest order, non-vanishing contribution comes from filling it with plaquettes in the fundamental representation i.e.

$$\langle W \rangle = Z^{-1} \int dU \frac{1}{N} e^{-S} \mathrm{Tr} \prod_{ij \in C} U_{ij} \tag{3.30}$$

$$= \alpha_f^{IJ} \frac{1}{N^{IJ}} \tag{3.31}$$

with non-fundamental representations contributing terms of $\mathcal{O}(\beta^{2IJ})$ or higher and contributions from Z^{-1} at least $\mathcal{O}(\beta^{IJ+2})$. A quick check verifies that result is in agreement with eq. (3.18).

3.3 Fermions on the lattice

Introducing quarks to in the lattice theory [14, 15] seems rather simple; instead of having fields $\psi(x)$ associated with each spacetime point, they will now be associated with points j on the lattice and written as ψ_j instead. Differentiation will be replaced by difference quotients for which we will be using the symmetric version

$$\partial_\mu \psi(x) \to \frac{1}{2a} \left(\psi_{m_\nu + \delta_{\mu\nu}} - \psi_{m_\nu - \delta_{\mu\nu}} \right) \tag{3.32}$$

which means that the covariant derivative can written as

$$D_\mu \psi(x) \to \frac{1}{2a} \left(U_{m_\nu, m_\nu + \delta_{\mu\nu}} \psi_{m_\nu + \delta_{\mu\nu}} - U_{m_\nu, m_\nu - \delta_{\mu\nu}} \psi_{m_\nu - \delta_{\mu\nu}} \right) \tag{3.33}$$

The quark-part of the QCD action is then

$$S = \sum_{m,n} \bar{\psi}_m M_{mn} \psi_n \tag{3.34}$$

with the quark mass matrix

$$M_{mn} = \frac{1}{2} a^3 \sum_\mu \gamma_\mu \left(\delta^4_{m_\nu + \delta_{\nu\mu}, n_\nu} - \delta^4_{m_\nu - \delta_{\nu\mu}, n_\nu} \right) U_{mn} + a^4 m \delta^4_{mn} \tag{3.35}$$

However, as we shall see, this naive approach to a lattice QCD action has a rather unfortunate defect; it describes 16 times the intended number of fermions!

3.3.1 Fermion Doubling

Particles represent themselves through minima in the energy-spectrum of the propagator which are directly connected to the poles of the propagators. However, since it is easier to invert M_{mn} in momentum space, we will first make the suitable Fourier transformation

$$\begin{aligned}
&a^{-4}\sum_{m,n} M_{mn} e^{-iaqm+iapn} \\
&= \sum_{m,n}\left[\frac{1}{2}a^{-1}\sum_{\mu}\gamma_\mu\left(\delta^4_{m_\nu+\delta_{\nu\mu},n_\nu}-\delta^4_{m_\nu-\delta_{\nu\mu},n_\nu}\right)+m\delta^4_{mn}\right]e^{-iaqm+iapn} \\
&= \sum_{m}\left[\frac{1}{2}\sum_{\mu}\gamma_\mu a^{-1}\left(e^{iap_\mu}-e^{-iap_\mu}\right)+m\right]e^{ia(p-q)m} \\
&= \left(ia^{-1}\sum_{\mu}\gamma_\mu\sin(aq_\mu)+m\right)\delta(p-q)
\end{aligned} \tag{3.36}$$

meaning that

$$\tilde{M}_q = ia^{-1}\sum_{\mu}\gamma_\mu\sin(aq_\mu)+m \tag{3.37}$$

from which it is fairly easy to find the propagator to be

$$\tilde{M}_q^{-1} = \frac{m-ia^{-1}\sum_\mu\gamma_\mu\sin(aq_\mu)}{m^2+a^{-2}\sum_\mu\sin^2(aq_\mu)} \tag{3.38}$$

The usual continuum propagator is retrieved near $aq_\mu = 0$:

$$\tilde{M}_q^{-1} = \frac{m-ia^{-1}\not{s}}{m^2+a^{-2}s^2} \tag{3.39}$$

but since sine also vanishes for $aq_\mu = \pi$ there is $2^4 = 16$ poles in total (all situated near the zeros). A bit more rigorously the poles are solutions to

$$\sin^2(aq_4) = -\left(\mathbf{s}^2+a^2m^2\right) \tag{3.40}$$

i.e. $q_4 = \pm i\omega$ and $q_4 = \pm i\omega + a^{-1}\pi$ with ω defined by

$$\sinh(a\omega) \equiv \sqrt{\mathbf{s}^2+a^2m^2} \tag{3.41}$$

Performing a Fourier transform back to position space to determine the time dependence

$$\begin{aligned}
S(\mathbf{x},t) &= \int_{-\frac{\pi}{a}}^{\frac{\pi}{a}}\frac{d^4q}{(2\pi)^4}e^{iaqx}\frac{m-ia^{-1}\not{s}}{m^2+a^{-2}s^2} \\
&= \int_{-\frac{\pi}{a}}^{\frac{\pi}{a}}\frac{d^3q}{(2\pi)^3}e^{ia\mathbf{q}\cdot\mathbf{x}}\int_{-\frac{\pi}{a}}^{\frac{\pi}{a}}\frac{dq_4}{2\pi}e^{iaq_4t}\frac{m-ia^{-1}\not{s}}{m^2+a^{-2}s^2}
\end{aligned} \tag{3.42}$$

the temporal part can be found via a substitution $z = e^{iaq_4}$ by which the integration countour becomes the unit circle

$$\begin{aligned} S(\mathbf{q},t) &= \oint \frac{dz}{2\pi i} z^{t-1} \frac{m - ia^{-1}\sum_i \gamma_i s_i - \frac{1}{2}a^{-1}\gamma_4 (z - z^{-1})}{m^2 + a^{-2}\mathbf{s}^2 - \frac{1}{4}a^{-2}(z-z^{-1})^2} \\ &= -4a \oint \frac{dz}{2\pi i} z^t \frac{z(am - i\gamma\mathbf{s}) - \frac{1}{2}\gamma_4(z^2-1)}{z^4 - 2fz^2 + 1} \end{aligned} \tag{3.43}$$

with $f = 2(a^2m^2 + \mathbf{s}^2) + 1$. The roots are then

$$(z_\pm)^2 = f \pm \sqrt{f^2 - 1}, \quad z_\pm = e^{\pm a\omega} \tag{3.44}$$

For $t > 0$ the two roots $\pm z_-$, corresponding to $q_4 = i\omega$ and $q_4 = i\omega + a^{-1}\pi$, contribute[1] meaning the integral can be evaluated as

$$\begin{aligned} S(\mathbf{x},t) = \int_{-\frac{\pi}{a}}^{\frac{\pi}{a}} \frac{d^3\mathbf{q}}{(2\pi)^3} \frac{e^{ia\mathbf{q}\cdot\mathbf{x} - a\omega t}}{\sinh(2a\omega)} \Big(&\left[m - ia^{-1}\gamma\mathbf{s} + a^{-1}\gamma_4 \sinh(a\omega)\right] \\ &+ (-1)^t \left[m - ia^{-1}\gamma\mathbf{s} - a^{-1}\gamma_4 \sinh(a\omega)\right]\Big) \end{aligned} \tag{3.45}$$

displaying a doubling of the number of fermionic species from the discretization of space. However, identifying particles with local minima in the excitation energy spectrum, $\omega(\mathbf{q})$, a further doubling as displayed in fig. 3.10 for each spatial dimension is seen making a total of 16 particles. That these particles are indeed in-

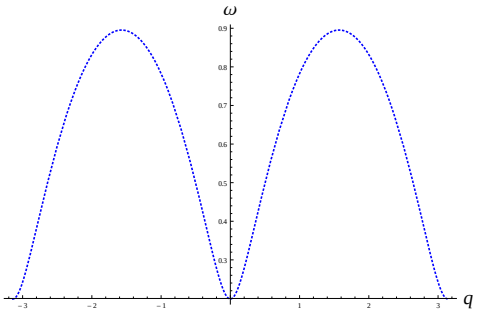

Figure 3.10: The excitation energy spectrum for the naive fermionions with $\mathbf{q} = (q, 0, 0)$, $m = 0.2$ and $a = 1$ (lattice units).

dependent is most easily seen by subdividing the intervals and shifting the integrals, such that

$$\int_{-\frac{\pi}{a}}^{\frac{\pi}{a}} \frac{d^4q}{(2\pi)^4} \tilde{M}_q = \sum_{l=1}^{16} \int_{-\frac{\pi}{2a}}^{\frac{\pi}{2a}} \frac{d^4q^{(l)}}{(2\pi)^4} \tilde{M}_{q^{(l)}} \tag{3.46}$$

[1] This is most easily seen from (3.42) where the contour needs to be closed upwards, since e^{iq_4} is only vanishing in that part of the complex plane.

A few comments on the theory is in order at this point; first of the fermionic doublers cannot simply be ignored since they interact with each other - momentum conservation is for instance only obeyed when all particles are taken into account. Furthermore, to obtain smooth behaviour for the theory it is necessary to make the time-steps twice as large as the other separation distances due to the rapidly oscillating factor $(-1)^t$. Luckily there exists ways of removing the time doublers, the two most popular being the Kogut-Susskind method of staggered fermions and the Wilson's method of heavy fermions [4, 5, 12]. For the purpose of this project Wilson's method will be used.

3.3.2 Wilson's Method: Heavy Fermions

Since the problem of fermion doubling arises due to the sine function in the momentum space propagator (3.38), a possible solution would be to introduce a term into the Lagrangian which suppresses all the particles but the one at $q_4 = i\omega$. Wilson's solution was then to write

$$\tilde{M}_q = m + ia^{-1}\sum_\mu \gamma_\mu \sin(aq_\mu) + a^{-1}r\sum_\mu (1-\cos(aq_\mu)) \tag{3.47}$$

where r is an arbitrary parameter. The effect of the new term is an increase of the mass of all the doublers by $a^{-1}rN_\pi$ where N_π is the number of components of q_μ which lie near $\frac{\pi}{a}$. In the case of $aq_\mu \approx 0$ the leading order, non-vanishing contribution is

$$a^{-1}r\sum_\mu (1-\cos(aq_\mu)) = ar\sum_\mu q_\mu^2 \tag{3.48}$$

i.e. $\mathcal{O}(a)$ meaning that in the continuum limit this term will drop out. Being a bit more thorough let us examine the denominator of the propagator

$$\begin{aligned}
\tilde{M}_q\tilde{M}_q^* &= a^{-2}s^2 + m^2 + 2a^{-1}mr\sum_\mu (1-c_\mu) + a^{-2}r^2\left(\sum_\mu (1-c_\mu)\right)^2 \\
&= a^{-2} + a^{-2}\mathbf{s}^2 + \Sigma^2 - 2a^{-1}r\Sigma c_4 + a^{-2}(r^2-1)c_4^2 \\
\Sigma &= m + a^{-1}r + a^{-1}\sum_i (1-c_i)
\end{aligned} \tag{3.49}$$

which, for the choice of $r = 1$ is linear in $\cos(aq_4)$ and hence does not show doubling. The roots for an arbitrary choice of r are

$$\cosh(a\omega_\pm) = \frac{a^{-1}r\Sigma \pm \sqrt{a^{-2}\Sigma^2 - a^{-2}(r^2-1)(1+a^{-2}\mathbf{s}^2)}}{a^{-2}(r^2-1)} \tag{3.50}$$

In the limit where $r \to 1$ the energy of the time doublers, ω_+, goes to infinity, whereas the local energy minima for the rest of the doublers simply vanish already before the

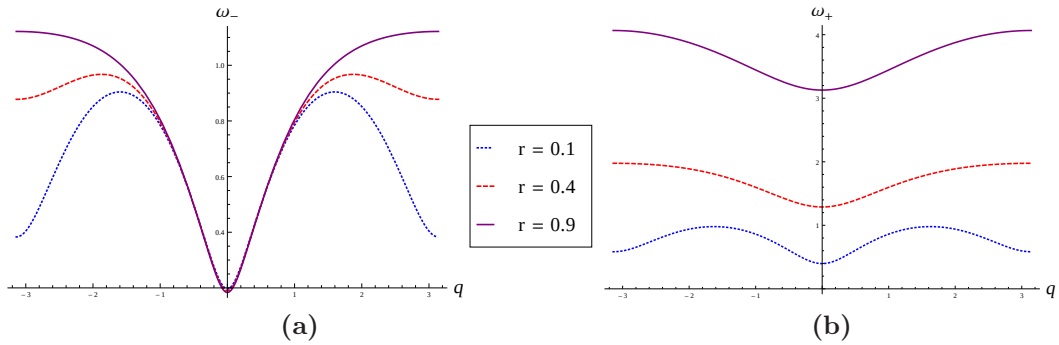

Figure 3.11: The excitation energy spectrum for (a) ω_- and (b) ω_+ for three different values of r and with $\mathbf{q} = (q, 0, 0)$, $m = 0.2$ and $a = 1$ (lattice units).

limit is reached, as depicted in figs. 3.11a and 3.11b. Having now introduced a way of eliminating the doublers it is about time to find the position space representation corresponding to $\tilde{M}_q$ - for this it is only necessary to focus on the newly introduced term and run a calculation similar to eq. (3.36) in reverse:

$$\begin{aligned}
\tilde{M}_q\delta(p-q) &= ra^{-1}\sum_\mu(1-\cos(aq_\mu))\delta(p-q) \\
&= ra^{-1}\left(4-\frac{1}{2}\sum_\mu(e^{iaq_\mu}+e^{-iaq_\mu})\right)\delta(p-q) \\
&= ra^{-1}\sum_m\left(4-\frac{1}{2}\sum_\mu(e^{iaq_\mu}+e^{-iaq_\mu})\right)e^{ia(p-q)m} \\
&= ra^{-1}\sum_{m,n}\left(4\delta^4_{m,n}-\frac{1}{2}\sum_\mu(\delta^4_{m_\nu+\delta_{\nu\mu},n_\nu}+\delta^4_{m_\nu,n_\nu+\delta_{\nu\mu}})\right)e^{iapn-iaqm} \\
&= a^{-4}\sum_{m,n}M_{mn}e^{iapn-iaqm}
\end{aligned} \tag{3.51}$$

The operator M_{mn} can be written even more compactly by introducing the forward derivative

$$\begin{aligned}
(\partial^{(f)}_\mu)_{mn}\psi_n &= a^{-1}(\delta^4_{m_\nu+\delta_{\nu\mu},n_\nu}-\delta^4_{m_\nu,n_\nu})\psi_n \\
&= a^{-1}(\psi_{m_\nu+\delta_{\nu\mu}}-\psi_{m_\nu})
\end{aligned} \tag{3.52}$$

with which

$$\begin{aligned}
M_{mn} &= \frac{ra^3}{2}\sum_{l\mu}(\delta^4_{l_\nu+\delta_{\nu\mu},m_\nu}-\delta^4_{l_\nu,m_\nu})(\delta^4_{l_\nu+\delta_{\nu\mu},n_\nu}-\delta^4_{l_\nu,n_\nu}) \\
&= \frac{ra^5}{2}\sum_{l\mu}(\partial^{(f)}_\mu)_{lm}(\partial^{(f)}_\mu)_{ln}
\end{aligned} \tag{3.53}$$

The full fermionic Lagrangian can then be written as

$$S = \left(a^4 m + 4a^3 r\right) \bar{\psi}_m \psi_m - a^3 \sum_{m\mu} \left(\bar{\psi}_{m_\nu + \delta_{\nu\mu}} \frac{r + \gamma_\mu}{2} \psi_{m_\nu} + \bar{\psi}_m \frac{r - \gamma_\mu}{2} \psi_{m_\nu + \delta_{\nu\mu}} \right) \tag{3.54}$$

Noticing that the operators defined as $P^\mu_\pm = \frac{1 \pm \gamma_\mu}{2}$ are rank two orthogonal projectors

$$(P^\mu_\pm)^2 = P^\mu_\pm, \quad P^\mu_\pm P^\mu_\mp = 0, \quad \mathrm{Tr}[P^\mu_\pm] = 2, \quad P^\mu_+ + P^\mu_- = 1 \tag{3.55}$$

where no sum over μ is implied, reveals that only part of the spinor field is propagating for the choice $r = 1$ leading to the observed removal of doublers. Introducing gauge invariance is a simple matter introducing U-factors in every term with spinors at different positions on the lattice i.e.

$$\begin{aligned} S_F &= \left(a^4 m + 4a^3 r\right) \bar{\psi}_m \psi_m - a^3 \sum_{\mu} \left(\bar{\psi}_{m_\nu + \delta_{\nu\mu}} \frac{r + \gamma_\mu}{2} U_{m_\nu + \delta_{\nu\mu}, m_\nu} \psi_{m_\nu} \right. \\ &\qquad \left. + \bar{\psi}_m \frac{r - \gamma_\mu}{2} U_{m_\nu, m_\nu + \delta_{\nu\mu}} \psi_{m_\nu + \delta_{\nu\mu}} \right) \\ &= \left(a^4 m + 4a^3 r\right) \bar{\psi}_m \psi_m - \frac{1}{2} a^3 \sum_{\{i,j\}} \bar{\psi}_i \left(r + \gamma_\mu e_\mu\right) U_{ij} \psi_j \end{aligned} \tag{3.56}$$

where the sum over $\{i, j\}$ is over all nearest-neighbour pairs of points on the lattice and includes one term for each direction. $e_\mu = (i - j)_\mu$ is a unit vector in the direction of the ij link.

3.3.3 Hopping Expansion

Considering the action (3.56) it can be written as

$$S_F = \bar{\psi}_i M_{ij} \psi_j \tag{3.57}$$

$$M_{ij} = K_{ij} + H_{ij} = K_{fg} \left(\delta_{ij} - \kappa_{gh} H_{ij}\right) \tag{3.58}$$

$$H_{ij} = \frac{1}{2} \left(r + \gamma_\mu e_\mu\right) U_{ij} (\delta^4_{i_\nu, j_\nu + \delta_{\nu\mu}} + \delta^4_{i_\nu + \delta_{\nu\mu}, j_\nu}) \tag{3.59}$$

$$K_{fg} = \left(a^4 m_f + 4a^3\right) \delta_{fg}, \qquad \kappa_f = \frac{1}{a m_f + 4} \tag{3.60}$$

where the flavour indices f, g have been explicitly written to emphasize that K_{fg} and κ_f are flavour-dependent and does not depend on the lattice coordinates. κ_f is known[2] as the *hopping parameter*. Rescaling the spinor fields $\psi_f \to M^{-\frac{1}{2}}_{fg} \psi_g$ and

[2] I use a slightly different convention than the normal one - typically $\kappa_f = \frac{1}{2am_f + 8}$ but mine rids the equations of some unnecessary factors of 2.

introducing source terms leads to

$$S_F = \bar{\psi}_i \left(\delta_{ij} - \kappa_{fg} H_{ij}\right) \psi_j + \sum_i (b_i \psi_i - \bar{\psi} c_i) \tag{3.61}$$

Performing the fermionic integral leads to

$$\int d\bar{\psi} d\psi e^{-S_F} = \det(1 - \kappa_f) \exp\left[- \sum_i (b_i \left(1 - \kappa_f H\right)^{-1}_{ij} c_j) \right] \tag{3.62}$$

Using the identity $\det(B) = \exp(\mathrm{Tr}\log(B))$ and performing what is known as the hopping expansion in κ_f

$$\begin{aligned} \det(1 - \kappa_f H) &= \exp\left(\mathrm{Tr}\log\left(1 - \kappa_f H\right)\right) \\ &= \exp\left(- \sum_{L=1}^{\infty} \frac{\kappa_f^L}{L} \mathrm{Tr}[H^L] \right) \end{aligned} \tag{3.63}$$

where $(H^L)_{ij}$ corresponds to moving along a line, the trace makes it a sum over all closed loops of length L and the sum is over all the different loop lengths possible. Since H is a function of both the link variables U_{ij} and has spinor indices, then this expansion includes a sum over both Wilson and spin loops. For $r = 1$ the spin loop and the Wilson loop has no back-tracking due to the projectors $P_{\pm}$. Furthermore it is important to notice that there is also a sum over all starting positions, which for a loop of length L not covering any link sites multiple times is L, which cancels the $\frac{1}{L}$ factor. In the case of both strong coupling and hopping expansions a generating function can be found by combining eqs. (3.63) and (3.14):

$$\begin{aligned} Z(c, b, J, \bar{J}) = \int dU \exp\left(- \sum_{L=1}^{\infty} \frac{\kappa_f^L}{L} \mathrm{Tr}[H^L] \right) \exp\left[- \sum_i (b_i \left(1 - \kappa_f H\right)^{-1}_{ij} c_j) \right] \\ \cdot \prod_p \sum_{m,n=0}^{\infty} \frac{1}{m! n!} \left(\frac{\beta}{2N} \right)^{m+n} (\mathrm{Tr} U_p)^m (\mathrm{Tr} U_p^*)^n \exp\left(\sum_{\{i,j\}} \mathrm{Tr}[U_{ij} J_{ij} + U_{ji} \bar{J}_{ij}] \right) \end{aligned} \tag{3.64}$$

From this expression general expectation values can be found by taking derivatives with respect to the sources and afterwards setting the source terms equal to zero. A diagrammatic representation of the individual terms of eq. (3.64) are found by making an expansion of M^{-1} in terms of κ_f

$$M^{-1}_{ij} = \left(\frac{1}{1 - \kappa_f H} \right)_{ij} = \sum_L \kappa_f^L H^L_{ij} \tag{3.65}$$

which, due to H connecting neighbouring sites on the lattice, corresponds to lines on the lattice. For a concrete example consider $\langle\bar{\psi}_i\gamma_5\psi_i\bar{\psi}_j\gamma_5\psi_j\rangle$:

$$\begin{aligned}\langle\bar{\psi}_i\gamma_5\psi_i\bar{\psi}_j\gamma_5\psi_j\rangle &= Z^{-1}\frac{\partial}{\partial c_i}\gamma_5\frac{\partial}{\partial b_i}\frac{\partial}{\partial c_j}\gamma_5\frac{\partial}{\partial b_j}Z\Big|_{b=c=0} \\ &= Z^{-1}\int dU\left[\left(\gamma_5 M^{-1}\right)_{ii}\left(\gamma_5 M^{-1}\right)_{jj}+\left(\gamma_5 M^{-1}\right)_{ij}\left(\gamma_5 M^{-1}\right)_{ji}\right] \\ &\cdot\prod_p\sum_{m,n=0}^{\infty}\frac{1}{m!n!}\left(\frac{\beta}{2n}\right)^{m+n}(\mathrm{Tr}U_p)^m(\mathrm{Tr}U_p^*)^n \\ &\cdot\exp\left(-\sum_{L=1}^{\infty}\frac{(\kappa_f)^L}{L}\mathrm{Tr}[H^L]\right)\end{aligned} \tag{3.66}$$

Here the $(\gamma_5 M^{-1})_{ij}(\gamma_5 M^{-1})_{ji}$ term consists solely of diagrams where the i and j coordinates are connected whereas $(\gamma_5 M^{-1})_{ii}(\gamma_5 M^{-1})_{jj}$ consists of two loops, one which always goes through i another which always goes through j (they may, however, overlap). One of the leading order terms contributing to the $(\gamma_5 M^{-1})_{ij}(\gamma_5 M^{-1})_{ji}$ term is displayed in fig. 3.12a. For the integration to give a non-vanishing contri-

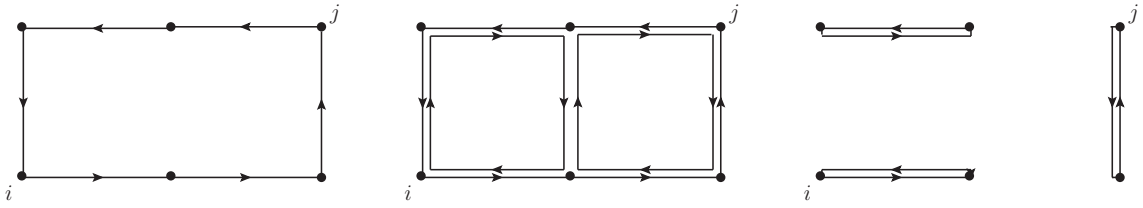

Figure 3.12: The leading order contribution to $\left(\gamma_5 M^{-1}\right)_{ij}\left(\gamma_5 M^{-1}\right)_{ji}$. (a) The initial expansion of M^{-1}, (b) filling the loop with plaquettes and (c) integration.

bution the loop is tiled by using the strong-coupling expansion, which means that the leading order contribution to $(\gamma_5 M^{-1})_{ij}(\gamma_5 M^{-1})_{ji}$ becomes

$$\begin{aligned}\Delta M_{\text{fig}} &= \kappa_f^6\mathrm{Tr}\left[\gamma_5\left(\frac{1-\gamma_1}{2}\right)^2\frac{1-\gamma_4}{2}\gamma_5\left(\frac{1+\gamma_1}{2}\right)^2\frac{1+\gamma_4}{2}\right]\frac{1}{N}\left(\frac{\beta}{2N}\right)^2 \\ &= \frac{\kappa_f^6}{N}\mathrm{Tr}\left[\frac{1+\gamma_1}{2}\frac{1+\gamma_4}{2}\frac{1+\gamma_1}{2}\frac{1+\gamma_4}{2}\right]\left(\frac{\beta}{2N}\right)^2 \\ &= \frac{\kappa_f^6}{2N}\left(\frac{\beta}{2N}\right)^2\end{aligned} \tag{3.67}$$

This procedure is shown diagrammatically in fig. 3.12. Furthermore, associated with this diagram there is a another diagram with all the arrows reversed which has the exact same contribution to the expansion.

3.4 Gauge Fixing

Since the gauge group $SU(N)$ is compact, it is not necessary to gauge fix to attain finite results as it is in the continuum theory. In some cases it can prove advantageous however since it can greatly simplify computations. Under a gauge transformation the link variables transform as

$$U(x,y) \to U'(x,y) = g^{-1}(x)U(x,y)g(y) \tag{3.68}$$

with $g \in SU(N)$ which means that fixing a link at a particular value $U(b)$ can be easily done through for instance

$$g(y) = U^{-1}(x,y)g(x)U(b) \tag{3.69}$$

Consider doing this one link at a time all the way around a loop. Since the gauge fixing of every link depends on the previous one, then the final gauge fixing would be defined in terms of itself and consequently the last link cannot be chosen freely like the others. This means that only configuration of links not containing loops can be gauge fixed to an arbitrary group element. Two concrete examples of gauge choices are the maximal tree in fig. 3.13a and the temporal gauge in fig. 3.13b. The maximal tree is defined such that no more links can be fixed without creating a loop, whereas the temporal gauge fixes all time-oriented link variables to one[3] and still leaves some gauge freedom intact.

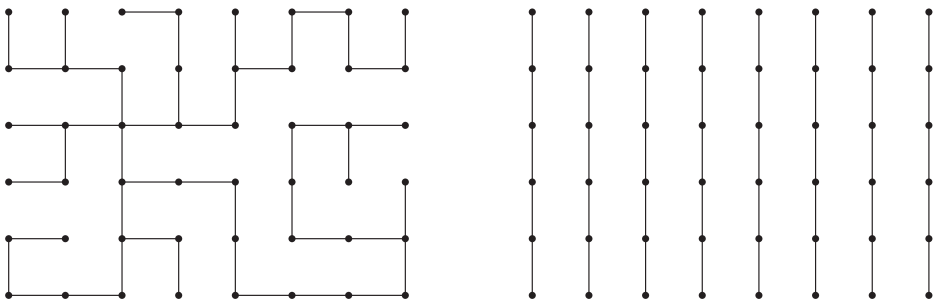

Figure 3.13: Two different ways of gauge fixing: (a) The maximal tree and (b) the temporal gauge. Note that the boundaries of the figures are assumed non-periodic.

[3]Except in the case of periodic time/finite temperature where a single temporal link is left.

In order to see that the gauge fixing does not affect the expectation values, consider a Green's function

$$G(P) = Z^{-1} \int dU e^{-S(U)} P(U) \tag{3.70}$$

where $P(U)$ is a gauge invariant polynomial in the link variables. Define the delta function on the gauge group by

$$\int dg \delta(g, g') f(g) = \int dg \delta(g', g) f(g) = f(g') \tag{3.71}$$

$$\delta(g, g') = \delta(g_0 g g_1, g_0 g' g_1) \tag{3.72}$$

and perform a integration over all links except U_{ij}, which will be fixed at g:

$$I(P, g) = Z^{-1} \int [dU] \delta(U_{ij}, g) e^{-S(U)} P(U) \tag{3.73}$$

The original Green's function is retrived by a integration over g, but since the action $S(U)$, the polynomial $P(U)$ and the measure are all gauge invariant, then so is $I(P, g)$, meaning

$$G(P) = \int dg I(P, g) = \int dg I(P, g_i g g_j) \tag{3.74}$$

As g_i and g_j can be chosen arbitrarily, $G(P)$ is independent of the value of the link U_{ij}. This generalizes to gauge fixing of any number of links as long as they do not form closed loops (as discussed above).

3.5 Confinement

Since there is a strong analogy between the pure gauge lattice action and models of magnetism in statistical mechanics, it could be asked if the equivalent of a spontaneous magnetization can arise in lattice gauge theory. In a ferromagnet the phase-transition is indicated by the spins which develope a non-zero expectation value - since the equivalent of the spins are the link-variables, the imagined phase transition would mean that

$$\langle U_{ij} \rangle \neq 0 \tag{3.75}$$

In an ordinary magnet such an expectation value arises due to the breaking of a global symmetry. However, in QCD such a non-zero expectation value is in direct violation with gauge symmetry - to see this make a change of variables on all other links from site i

$$U_{ik} \to U_{ij} U_{ik} \tag{3.76}$$

i.e. multiply all these links with the value of the ij link. Since the same number of link variables are ordered away as towards i then the dependence in the action cancels within each traced plaquette, implying that

$$\langle U_{ij} \rangle = \int dU_{ij} U_{ij} e^{-S(U)} = \int dU_{ij} U_{ij} = 0 \tag{3.77}$$

In other words the gauge invariance forces us to look for gauge invariant quantities, which can indicate the confinement/deconfinement transition. One such quantity is the Wilson loop which was introduced in section 3.2.4 and treated by use of the strong coupling expansion. The physical interpretation of a rectangular loop of spatial extent S and temporal extent T would be a quark and an anti-quark being created and instantly separated, maintained staticly at a distance S and then after a time T instantly moved together and annihilated. For large T the act of separating can be disregarded, which means that to leading order in the pure gauge theory the potential between the charges is

$$e^{-V(R)T} = \langle W \rangle = e^{-\sigma \cdot ST} \tag{3.78}$$

$$\Rightarrow V = \sigma S, \quad \sigma = \ln(\frac{2N_c^2}{\beta}) \tag{3.79}$$

using eq. 3.18. This means that in the strong coupling limit the potential grows linearly with the spatial separation showing that confinement is occuring. A special case of the Wilson loop which is of interest for this thesis is the Polyakov loop, which arises due to the periodic time direction. It is defined as

$$\hat{L}(\mathbf{x}) \equiv \prod_{\tau=1}^{N_\tau} U(\mathbf{x}, \tau), \quad L(\mathbf{x}) = \mathrm{Tr}\hat{L}(\mathbf{x}) \tag{3.80}$$

i.e. a product of links at fixed spatial coordinates $\mathbf{x}$ which wind around the periodic time direction. In the pure gauge case it probes the screening properties of the surrounding gluonic medium and thereby gives an indication of whether the theory is in the confined or deconfined phase. As in the case of magnetism the phase transition is associated with the spontaneous breaking of a symmetry. Notice that the pure gauge action is invariant under the Z_{N_c} transformation

$$U_{x,\hat{4}} \to z U_{x,\hat{4}}, \quad \forall \mathbf{x}, \, x_4 \text{ fixed}, \quad z \in Z_N \tag{3.81}$$

While the usual Wilson loop is also invariant under such a transformation, the Polyakov loop is seen not to be; in fact

$$L(\mathbf{x}) \to z L(\mathbf{x}) \tag{3.82}$$

meaning that the transition from a zero to a non-zero value of $\langle L \rangle$ indicates the breaking of the Z_N symmetry and a transition from the confined to the deconfined phase, where complete gluonic colour screening occurs. In the case where quarks are added to the theory the Polyakov loop is no longer an exact order parameter, since the quarks are also capable of screening the colour charge of the loop.

3.6 Quark Chemical Potential

In order to consider a non-zero quark (number) density a chemical potential can be introduced to the theory. From standard thermodynamics the partition function for the grand canonical ensemble is

$$Z(T,\mu_q) \equiv \mathrm{Tr}[-\exp(\frac{1}{T}\,(H-\mu N_q))] \tag{3.83}$$

where N_q is the *number density operator*. In the case of QCD $N_q = \int d^4x\psi^\dagger(x)\psi(x)$ yields the number density of quarks. Since

$$\mu\psi^\dagger\psi = \mu\bar{\psi}\gamma_4\psi \tag{3.84}$$

and the gauge field normally couples as

$$i\gamma^\mu\bar{\psi}A_\mu\psi \tag{3.85}$$

it is natural to assume that the chemical potential should appear the same way as iA_4 does. The quark mass matrix can then be written as

$$M_{ij} = \delta_{ij} - \frac{1}{2}\kappa_f \sum_{n=\pm1}^{\pm3} \delta_{y,x+\hat{n}}(r+\gamma_\mu)U_{xn} \tag{3.86}$$

$$-\frac{1}{2}\kappa_f F(a\mu)\delta_{y,x+\hat{4}}(r+\gamma_\mu)U_{x4} - \frac{1}{2}\kappa_f G(a\mu)\delta_{y,x+\hat{4}}(r-\gamma_\mu)U_{x4} \tag{3.87}$$

where, by the aforementioned analogue, $F(a\mu) = e^{a\mu}$ and $G(a\mu) = e^{-a\mu}$ to $\mathcal{O}(a)$. To substantiate this claim a bit more consider the Helmholtz free energy density [16] given by

$$f(T,\mu) = -\frac{T}{V}\ln Z = -\frac{1}{a^4 N_{\mathbf{x}} N_\tau}\ln Z \tag{3.88}$$

in the absence of gauge interactions ($U = \mathbb{1}$). Performing the standard Grassmanian integration leading to

$$f(T,\mu) = -\frac{T}{V}\ln\det M = -\frac{T}{V}\ln\det\tilde{M} \tag{3.89}$$

where in the last step the unitary transformation

$$\tilde{M}_{lk} = \frac{1}{N_{\mathbf{x}} N_\tau}\sum_{ij} e^{-iyl+ixk} M_{yx} \tag{3.90}$$

has been used. By this transformation

$$\tilde{M}_{lk} = \delta(l-k)\Bigg[1 - \kappa_f \sum_{i=1}^{3}(r\cos k_i - i\gamma_\mu \sin k_i) +$$

$$-\frac{1}{2}\kappa_f F(a\mu)e^{-ik_4}(r+\gamma_4) - \frac{1}{2}\kappa_f G(a\mu)e^{ik_4}(r-\gamma_4)\Bigg] \tag{3.91}$$

From writing

$$\frac{1}{2}(F+G) = R\cosh(\theta), \qquad \frac{1}{2}(F-G) = R\sinh(\theta) \tag{3.92}$$

it follows that $R = \sqrt{FG}$ and $\tanh(\theta) = \frac{F-G}{F+G}$. From the identification of $F = Re^{\theta}$ and $G = Re^{-\theta}$ it then the last line of eq. (3.91) can be written as

$$-\kappa_f \left[2\cos(k_4 + i\theta) + 2i\sin(k_4 + i\theta)\right] \tag{3.93}$$

Due to the $\delta(l-k)$ factor the momentum space part of the determinant can be written as a product over the $l = k$ diagonal, which, due to the logarithm can be written as a sum over k. Writing the determinant in spinor and colour space by $\det_{sc}$ we get

$$f(T,\mu) = -\frac{T}{V}\sum_k \ln\det{}_{sc}\Bigg(1 - \kappa_f\Big[\sum_{i=1}^{3}(r\cos k_i - i\gamma_i \sin k_i) + rR\cos(k_4 + i\theta) - iR\gamma_4\sin(k_4 + i\theta)\Big]\Bigg) \tag{3.94}$$

Since no gauge interactions are considered the colour determinant leads to N_c equal contributions, leaving only the spinor determinant, which, after a bit of calculations, gives that

$$f(T,\mu) = -\frac{2N_cT}{V}\sum_k \ln\Bigg[\Big(1 - r\kappa_f\sum_{i=1}^{3}\cos k_i - rR\kappa_f\cos(k_4 + i\theta)\Big)^2 + \kappa_f^2\sum_{i=1}^{3}\sin^2 k_i + \kappa_f^2 R^2\sin^2(k_4 + i\theta)\Bigg] \tag{3.95}$$

To remove vacuum contributions from the expression the free energy density at $\mu = 0$

$$f(T,0) = \frac{2N_cT}{V}\sum_k \ln\left[\Big(1 - r\kappa_f\sum_{i=1}^{4}\cos k_i\Big)^2 + \kappa_f^2\sum_{i=1}^{4}\sin^2 k_i\right] \tag{3.96}$$

needs to be subtracted from $f(T,\mu)$. However, since $\kappa_f = \frac{1}{ma+4r} = \frac{1}{4r} - \frac{ma}{16r^2} + \mathcal{O}(a^2)$ for small a then the $f(T,0)$ term diverges in the continuum limit (where also $k_\mu = ap_\mu$)

$$f(T,0) = \frac{2N_cT}{V}\sum_k \ln\Bigg[\Big(1 - r(\frac{1}{4r} - \frac{ma}{16r^2} + \mathcal{O}(a^2))\sum_{i=1}^{4}(1 + \mathcal{O}(a^2))\Big)^2 \tag{3.97}$$

$$+(\frac{1}{4r} - \frac{ma}{16r^2} + \mathcal{O}(a^2))^2\sum_{i=1}^{4}(a^2p_i^2 + \mathcal{O}(a^3))\Bigg] \tag{3.98}$$

$$= \frac{2N_cT}{V}\sum_k \ln\left[\frac{a^2}{16r^2}\left(m^2 + p^2\right) + \mathcal{O}(a^3)\right] \tag{3.99}$$

The only way to avoid this divergence is to set

$$R = 1, \qquad \theta(a\mu) = a\mu + \mathcal{O}[(a\mu)^2] \tag{3.100}$$

which is mostly simply fulfilled by choosing $F = e^{a\mu}$ and $G = e^{-a\mu}$ in agreement with the earlier argument. For this choice simply taking $p_4 \to p_4 + i\mu$ leads from $f(T, 0)$ to the leading order term in $f(T, \mu)$ i.e.

$$f(T,\mu) = \frac{2N_c T}{V} \sum_k \ln \left[\frac{a^2}{16r^2} \left(m^2 + \sum_{i=1}^{3} p_i^2 + (p_4 + i\mu)^2 \right) \right] \tag{3.101}$$

from which the free energy without vacuum contributions can be calculated

$$f(T,\mu) - f(T,\mu) = \frac{2N_c}{(2\pi)^4} \int d^4p \ln \frac{m^2 + \sum_{i=1}^{3} p_i^2 + (p_4 + i\mu)^2}{m^2 + p^2} \tag{3.102}$$

3.7 Effective Theory of Polyakov Loops

As we have discussed in section 3.5 the expectation value of the Polyakov loop is an order parameter for confinement in the pure gauge theory due to its role as an indicator of $\mathbb{Z}(N)$ symmetry breaking. For this reason it is of interest to consider a theory with a periodic time direction in which the Polyakov loops are the fundamental degree of freedom. In this section and later on we will write the Polyakov loop as

$$\hat{W}_x = \prod_{\tau=1}^{N_\tau} U_{x,\tau;4} \tag{3.103}$$

Formally, what must be done to get to the effective theory, is then

$$\begin{aligned} Z &= \int \mathcal{D}U \exp(S[U]) \\ &= \int \mathcal{D}U \mathcal{D}W \prod_x \delta \left(\mathrm{Tr}\hat{W} - \mathrm{Tr} \prod_{\tau=1}^{N_\tau} U_{x,\tau;4} \right) \exp(S[U]) \\ &= \int \mathcal{D}W \exp(S_{eff}[\hat{W}]) \end{aligned} \tag{3.104}$$

i.e. integrate out all the links such that the remaining expression is only depending on the Polyakov loops. As earlier the integral is evaluated by considering contributing terms in the strong coupling expansion. The derivation for the leading order effective Polyakov action in the strong coupling limit will be presented based on [17] together with some discussion of higher order terms.

3.7.1 Leading order

Since it is possible to work in the temporal gauge where all non-loop temporal links are set to unity, $U_0 = 1$, it is clear that only loops winding around the time axis can contribute to the effective action. Splitting up the pure gauge partition function into time-like and space-like plaquettes

$$\begin{aligned} Z &= \int \mathcal{D}U \exp\left[\frac{\beta}{2N_c}\left(\sum_{t.p.}\mathrm{Tr}[U_{p_t} + H.c.] + \sum_{s.p}\mathrm{Tr}[U_{p_s} + H.c.]\right)\right] \\ &= \int \mathcal{D}U \exp\left(\frac{\beta}{2N_c}\sum_{t.p.}\mathrm{Tr}[U^{(\tau)}_{p_t} + H.c.]\right)\prod_{s.p}\exp\left(\frac{\beta}{2N_c}\mathrm{Tr}[U_{p_s} + H.c.]\right) \end{aligned} \quad (3.105)$$

it is immediately clear that the lowest order contribution to the effective action comes from the case where no spatial plaquettes are used. As such the lowest order contribution which winds around the time axis is

$$Z = \int \mathcal{D}U \left[1 + \left(\frac{\beta}{2N_c}\right)^{N_\tau}\sum_{\mathbf{x}}\left(\prod_{\tau=1}^{N_\tau}\mathrm{Tr}[U_{p_t}(\mathbf{x},\tau)] + \prod_{\tau=1}^{N_\tau}\mathrm{Tr}[U^\dagger_{p_t}(\mathbf{x},\tau)]\right)\right] \quad (3.106)$$

where the spatial links can be integrated out:

$$\begin{aligned} &\int \mathcal{D}U \left(\frac{\beta}{2N_c}\right)^{N_\tau}\prod_{\tau=1}^{N_\tau}\mathrm{Tr}[U_p(\mathbf{x},\tau)] \\ &= \int \mathcal{D}U \left(\frac{\beta}{2N_c}\right)^{N_\tau}\prod_{\tau=0}^{N_\tau}\mathrm{Tr}[U_i(\mathbf{x},\tau)U_4(\mathbf{x}+\hat{i},\tau)U_{-i}(\mathbf{x}+\hat{i},\tau+\hat{4})U_{-4}(\mathbf{x},\tau+\hat{4})] \\ &= \int \mathcal{D}U_4 \left(\frac{\beta}{2N_c^2}\right)^{N_\tau}\mathrm{Tr}[\prod_{\tau=1}^{N_\tau}U_4(\mathbf{x},\tau)]\mathrm{Tr}[\prod_{\tau=1}^{N_\tau}U_4^\dagger(\mathbf{x}+\hat{i},\tau)] \\ &= \int \mathcal{D}W \left(\frac{\beta}{2N_c^2}\right)^{N_\tau}\mathrm{Tr}[\hat{W}(\mathbf{x},\tau)]\mathrm{Tr}[\hat{W}^\dagger(\mathbf{x}+\hat{i},\tau)] \end{aligned} \quad (3.107)$$

The additional factors of $\frac{1}{N_c}$ come from the N_τ link integrations and that $\prod_\tau \mathcal{D}U_4 = \mathcal{D}W$ can be seen by going to the temporal gauge. This means that to leading order the effective action can be written as

$$S_{eff} = J\sum_{\mathbf{x},i}\left[W(\mathbf{x})W^\dagger(\mathbf{x}+\hat{i}) + W^\dagger(\mathbf{x})W(\mathbf{x}+\hat{i})\right] \quad (3.108)$$

where $W = \mathrm{Tr}[\hat{W}]$, $J = \left(\frac{\beta}{2N_c^2}\right)^{N_\tau}$ and i runs over positive spatial directions. To leading order in the hopping parameter the inclusion of fermions is straightforward;

once again only loops winding around the time axis have any dependency on the temporal links, so

$$S_q = -h \sum_{\mathbf{x}} \left[e^{a\mu N_\tau} W(\mathbf{x}) + e^{-a\mu N_\tau} W^\dagger(\mathbf{x}) \right] \tag{3.109}$$

where $h = 2N_f \kappa_f^{N_\tau}$ and $\kappa_f = \frac{1}{am_f+1+D}$ for N_f mass-degenerate fermions. Here the factor of 2 comes from the spinor trace since $P_\pm^\mu$, as discussed earlier, are rank 2 projectors.

3.7.2 Higher Order Corrections

In this section I will be presenting and evaluating some of the higher order contributions to the effective theory of Polyakov loops based on the strong coupling expansion and group integration as introduced in section 2.5. The procedure is completely analogous to that of [18, 19] but uses neither the character expansion nor the method of comulants and moments. The different types of contributions involves pure gauge, pure fermion and gauge-fermion corrections, which lead to corrections to the coefficients, couplings between more than nearest neighbours and Polyakov loops with multiple windings around the time axis. Exactly which term is the leading order correction will depend on the values of N_τ, N_c, β and the number of spatial dimensions D. The leading order coefficients will be referred to as J_0 and h_0, with corrections to these having other subscripts.

Pure Gauge Corrections

Ignoring the spatial plaquettes for a second, then the higher order corrections arise from replacing plaquettes with N_c-1 plaquettes with the opposite orientation and/or Polyakov loops winding around the axis multiple times. Considering the former then the first higher order term is displayed and evaluated in fig. 3.14 with a contribution of

$$J_1 = \frac{N_\tau}{N_c^2} \left(\frac{\beta}{2N_c} \right)^{N_c-1} \left(\frac{\beta}{2N_c^2} \right)^{N_\tau-2} \frac{\beta}{2N_c} = N_\tau \left(\frac{\beta}{2N_c} \right)^{N_c-2} J_0 \tag{3.110}$$

where N_τ stems from the freedom in choosing the position. The next contribution comes from using the same principle but on two plaquettes, leading to the diagrams 3.15a and 3.15b. The first gives a contribution

$$\begin{aligned} J_{2S} &= \frac{1}{2} \frac{N_\tau(N_\tau-3)}{N_c^4} \left(\frac{\beta}{2N_c} \right)^{2(N_c-1)} \left(\frac{\beta}{2N_c^2} \right)^{N_\tau-4} \left(\frac{\beta}{2N_c} \right)^2 \\ &= \frac{1}{2} N_\tau(N_\tau-3) \left(\frac{\beta}{2N_c} \right)^{2(N_c-2)} J_0 \end{aligned} \tag{3.111}$$

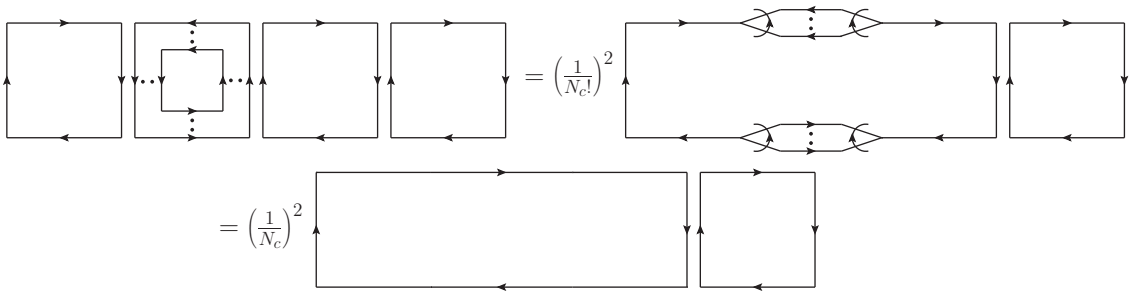

Figure 3.14: Leading order correction to J arising by replacing one of the plaquettes with $N_c - 1$ going in the opposite direction.

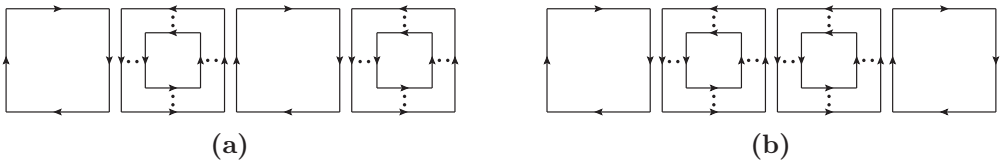

Figure 3.15: Two planar corrections to the coupling constant J both involving the replacement of plaquettes with $N_c - 1$ oppositely oriented plaquettes.

whereas the straightforward evaluation of the second diagram is rather hard due to the $2(N-1)$ group elements ($N-1$ in each direction) situated at the same link site. Luckily a choice of gauge can simplify the problem markedly! In fig. 3.16a the dashed lines represent group elements set to $\mathbb{1}$ by gauge fixing.

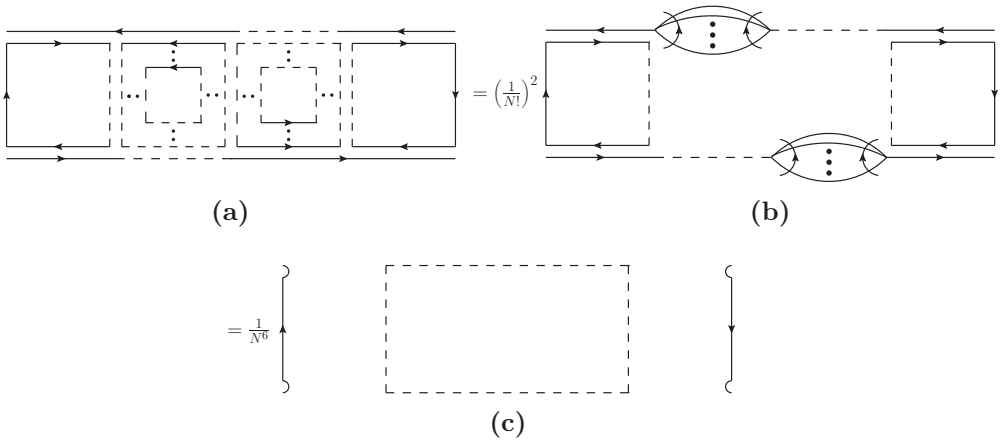

Figure 3.16: Evaluation by gauge fixing: (a) Gauge fixed version of fig. 3.15b, (b) $2 \times N_c$ aligned lines integrated and (c) only the usual integrations left.

After the steps illustrated by figs. 3.16b-3.16c only the usual integrations are left, which contributes a factor of $N_c^{5-N_\tau}$. Including the factors of $\frac{\beta}{2N_c}$ the contribution

can be evaluated to be

$$J_{2N} = N_\tau \left(\frac{\beta}{2N_c}\right)^{2(N_c-2)} \left(\frac{\beta}{2N_c^2}\right)^{N_\tau} \tag{3.112}$$

Another type of contribution stems from tiling each plaquette site twice with plaquettes with the same orientation as shown in fig. 3.17a - what kind of contributions does this give rise to? By gauge fixing as in fig. 3.17b it is possible to systematically integrate out the remaining links - starting from an end by using fig. 2.8 as shown in fig. 3.17c and continuing towards the right until fig. 3.17d and the last integration is reached. Here $a = \frac{1}{N_c^2-1}$, $b = -\frac{1}{N_c(N_c^2-1)}$ and A and B are the combined factors from the integrations, A containing all terms with even powers of b and B contains all odd powers of b.

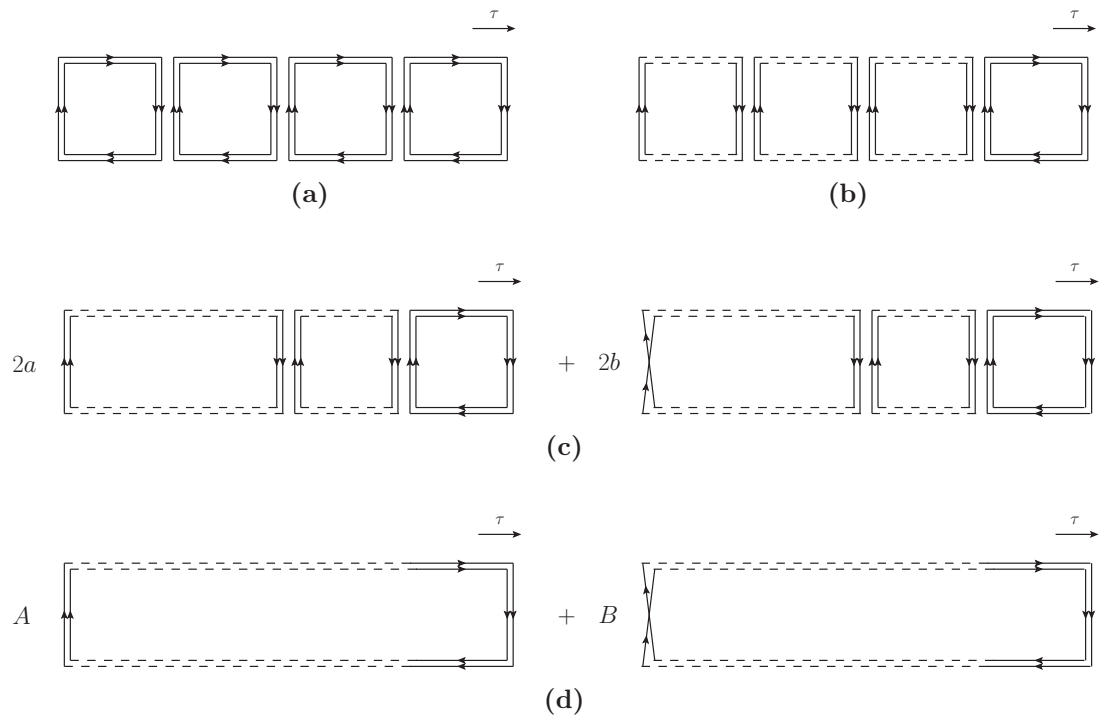

Figure 3.17: Evaluation of diagram leading to double winding loops: (a) The tiling, (b) gauge fixing, (c) start of integration and (d) only one link site left to integrate over.

The last integration can be performed leading to

$$S_1 = \frac{1}{2^{N_\tau}} \left(\frac{\beta}{2N_c}\right)^{2N_\tau} \sum_{\{ij\}} \left[C_1 W_i^2 (W_j^\dagger)^2 + C_2 W_i^2 \mathrm{Tr}[(\hat{W}_j^\dagger)^2]\right.$$

$$\left. + C_2 \mathrm{Tr}[\hat{W}_i{}^2](W_j^\dagger)^2 + C_1 \mathrm{Tr}[\hat{W}_i^2]\mathrm{Tr}[(\hat{W}_j^\dagger)^2]\right] \tag{3.113}$$

$$\tag{3.114}$$

where $\{ij\}$ is all nearest neighbour lines and

$$C_1 = Aa + Bb, \quad C_2 = Ab + Ba \tag{3.115}$$

and the A and B factors depend on N_τ. Considering $N_\tau = 4$ then

$$A = 8[a^3 + 3ab^2], \quad B = 8[b^3 + 3a^2b] \tag{3.116}$$

from which it is easy to generalize to higher N_τ.

Non-planar Contributions

Taking the spatial links into account the first non-planar higher order contribution stems from the diagram shown in fig. 3.18a. Since there is an addition of four

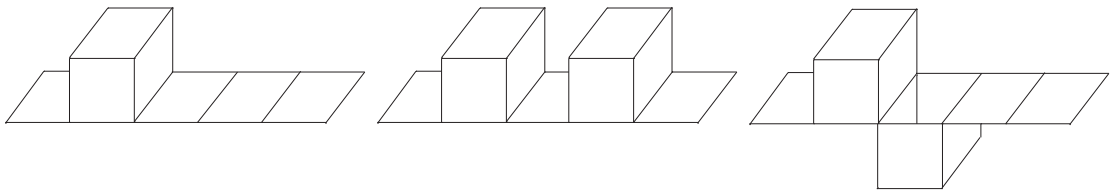

(a) **(b)** **(c)**

Figure 3.18: Higher order corrections to the effective Polyakov action.

plaquettes the contribution becomes

$$J_{NP,1} = 2(D-1)N_\tau \left(\frac{\beta}{2N_c^2}\right)^{N_\tau+4} = 2(D-1)N_\tau \left(\frac{\beta}{2N_c^2}\right)^4 J_0 \tag{3.117}$$

where the factor $2(D-1)$ is the number of directions the box can point in ('up' and 'down' in each spatial dimension except from the one the strip includes). The contributions from figs. 3.18b and 3.18c can be found to be

$$J_{NP,2} = 2(D-1)^2 N_\tau (N_\tau - 3) \left(\frac{\beta}{2N_c^2}\right)^8 J_0 \tag{3.118}$$

$$J_{NP,3} = 2(D-1)(2D-3)N_\tau \left(\frac{\beta}{2N_c^2}\right)^8 J_0 \tag{3.119}$$

in agreement with the findings of Langelage, Lottini & Philipsen[4] [18].

[4]There is a small typo in their eq. (2.11) but it is corrected in (2.12).

Non-Nearest Neighbour Loops

While it would have been natural to assume that the first non-nearest neighbour term would arise from a term as the one depicted in fig. 3.19a this term is already covered by the leading order effecting action (simply make a Taylor expansion and the 2nd order term will include this contribution). As such the leading order contribution involving non-nearest neighbours is the the one shown in fig. 3.19b with a leading order term

$$S_2 = N_\tau(N_\tau - 1)\left(\frac{\beta}{2N_c^2}\right)^{2N_\tau+2} \sum_{|k,l|} W_k W_l^\dagger \tag{3.120}$$

where the $|k,l|$ sum runs over all pairs of $\sqrt{2}a$ separated Polyakov loops. The leading order term for $2a$ separated lines arises as shown in fig. 3.19c and gives

$$S_3 = N_\tau\left(\frac{\beta}{2N_c^2}\right)^{2N_\tau+6} \sum_{[k,l]} W_k W_l^\dagger \tag{3.121}$$

where the sum this time is over pairs of $2a$ separated Polyakov loops. At even higher

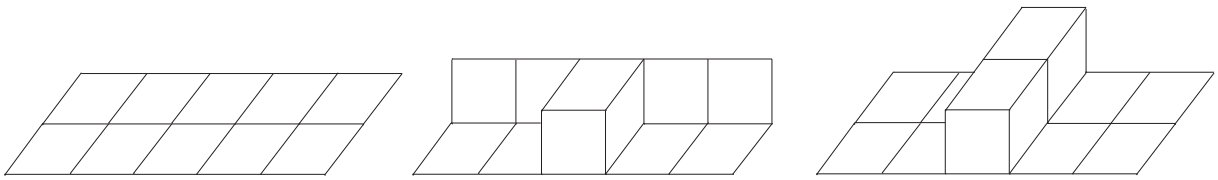

Figure 3.19: Pure gauge non-nearest neighbour contributions to the effective Polyakov action.(a) is already part of the leading order effective action, but (b) and (c) contributes with new terms.

orders, terms with even larger separations or a greater number of Polyakov loops will arise.

Fermionic Corrections

Adding fermions to the theory gives rise to a lot of new contributions both higher order corrections to h and J, but also terms with higher separations or multiple Polyakov loops. Especially, since the fermion loops can be plaquettes-sized they give rise to a whole family of contributions where they are replacing the gauge plaquettes. Some contributions giving rise to corrections to J and h are depicted in fig. 3.20. Their values are

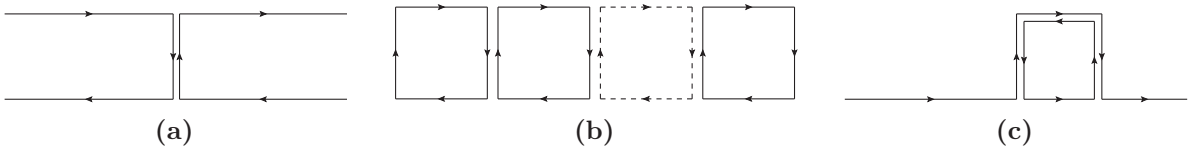

Figure 3.20: Three corrections to the couplings: (a) A purely fermionic correction to J, (b) A fermion-gauge correction to J (fermion is dashed) and (c) a correction to h, which is either fermion-gauge or purely fermionic.

$$J_{F1} = -N_\tau \frac{\kappa_f^{2N_\tau+2}}{2N_c} \tag{3.122}$$

$$J_{F2} = -N_\tau \frac{\kappa_f^4}{2N_c} \left(\frac{\beta}{2N_c^2} \right)^{N_\tau - 1} \tag{3.123}$$

$$h_1 = DN_\tau \kappa_f^{N_\tau+2} \left(\frac{\beta}{2N_c^2} - \frac{\kappa_f^4}{2N_c} \right) \tag{3.124}$$

where the negative signs stem from the spinor traces. These corrections can be extended quite easily to cover multiple additional plaquettes for fig. 3.20b and 3.20c and multiple crossings for 3.20a. Finally two examples which does not correspond to corrections to J and h are shown in figs. 3.21 and have coefficients

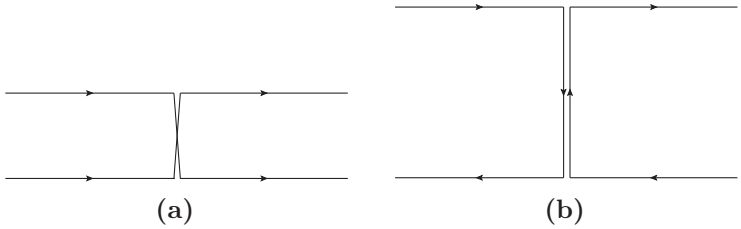

Figure 3.21: Two higher order fermionic corrections to the action: (a) Polyakov loops with the same orientation and (b) 2a separated loops.

$$S_4 = N_\tau \frac{\kappa_f^{2N_\tau+2}}{N_c} \sum_{\{ij\}} W_i W_j \tag{3.125}$$

$$S_3 = -N_\tau \frac{\kappa_f^{2N_\tau+4}}{N_c} \sum_{[ij]} W_i W_j^\dagger \tag{3.126}$$

where $\{ij\}$ are nearest neighbour pairs and $[ij]$ are $2a$ separated pairs just as earlier.

Chapter 4

Mathematical Interlude: A Unitary Integral

4.1 Derivation

In this section we will go through the calculations of [20], although in a slightly altered form, to derive the analytical expression for the integral

$$I(A,B) = \int\limits_{U(N)} dU e^{\mathrm{Tr}[AU]+\mathrm{Tr}[BU^\dagger]} \tag{4.1}$$

for $A, B \in GL(N,\mathbb{C})$. In doing so it will be necessary to rely on some group theoretical results which are more advanced than the ones introduced in the chapter on group theory, but due to the relevance of the results and the fact that several of the steps are possible based on what was previously introduced, I have decided to include the derivation nonetheless. Using the character expansion introduced in eq. (2.21) to write the integral as

$$I(A,B) = \sum_r \sum_{r'} \alpha_r \alpha_{r'} \int\limits_{U(N)} dU \chi_r(AU)\chi_{r'}(BU^\dagger) \tag{4.2}$$

and subsequently applying the orthogonality relation for irreducible representations eq. (2.18)

$$\begin{aligned} I(A,B) &= \sum_r \sum_{r'} \int\limits_{U(N)} dU \alpha_r \alpha_{r'} A_{ij} U^r_{ji} B_{kl} (U^{r'})^*_{kl} \\ &= \sum_r \sum_{r'} \alpha_r \alpha_{r'} A_{ij} B_{kl} \delta_{jk} \delta_{il} \delta_{rr'} \\ &= \sum_r \frac{\alpha_r^2}{d_r} \chi(AB) \end{aligned} \tag{4.3}$$

we have succesfully rewritten the expression in terms of the character coefficients and a trace. To simplify the expression further a few results from group theory are necessary. The first is Weyl's character formula as stated in [20]

$$\chi_r(AB) = \frac{\det(\lambda_j^{2(n_i+N-i)})}{\Delta(\lambda^2)} \tag{4.4}$$

where λ_i are the eigenvalues of the matrix AB, n_j with $j = 1, ..., N$ is the partition of the irreducible representation r i.e. a set $\{n_1, ..., n_N\}$ of non-negative, non-increasing numbers, which denotes the specific irrep. $\Delta(x)$ is the Vandermonde determinant given by

$$\Delta(x) = \prod_{i<j}^{N}(x_i - x_j) \tag{4.5}$$

Secondly, eqs. (3.2) and (3.3) of [21] give explicit expressions for the character coefficients

$$\alpha_r = \det \frac{1}{(n_i + j - i)!} \tag{4.6}$$

$$= \prod_{i=1}^{N} \frac{(N-i)!}{(n_i + N - i)!} d_r \tag{4.7}$$

where $d_r = \chi_r(\mathbb{1})$ is the dimension of the representation. This allows for the integral to be written as

$$\begin{aligned} I(A,B) &= \left[\prod_{n=1}^{N-1} n!\right] \frac{1}{\Delta(\lambda^2)} \sum_r \det\left(\frac{1}{(n_i+N-i)!(n_i+j-i)!}\right) \det(\lambda_j^{2(n_i+N-i)}) \\ &= \left[\prod_{n=1}^{N-1} n!\right] \frac{1}{\Delta(\lambda^2)} \sum_r \det\left(\frac{1}{k_i!(k_i-N+j)!}\right) \det(\lambda_j^{2k_i}) \end{aligned} \tag{4.8}$$

where $k_i = n_i + N - i$. Due to the Binet-Cauchy formula (eq. (B4) of [21]) the two determinants can be written as one with an ordinary sum over $k = 1, ..., N$ instead of the sum over representations. This means that the power series expansion of the modified Bessel function of the first kind

$$\frac{I_\sigma(2y)}{y^\sigma} = \sum_{k=0}^{\infty} \frac{y^{2k}}{k!(k+\sigma)!} \tag{4.9}$$

can be used to get

$$\begin{aligned} I(A,B) &= \left[\prod_{n=1}^{N-1} n!\right] \frac{1}{\Delta(\lambda^2)} \det\left[\lambda_i^{N-j} I_{j-N}(2\lambda_i)\right] \\ &= \left[\prod_{n=1}^{N-1} n!\right] \frac{1}{\Delta(\lambda^2)} \det\left[\lambda_i^{j-1} I_{j-1}(2\lambda_i)\right] \end{aligned} \tag{4.10}$$

where in the last line $I_j = I_{-j}$ and invariance of the determinant under $N - j \to j$ have been used. This is the final expression for the integral and the one which will become relevant in $N_c \to \infty$ limit. First, however, a slight rewriting for it to apply to the case in question.

4.2 Rewriting the Integral

As we will see later then the relevant case has $A = h_+ I$ and $B = h_- I$ where I is a $N_c \times N_c$ identity matrix. This means that $\lambda_i = \sqrt{h_+ h_-}$ and a problem due to factors of zero seems to arise in the denominator of eq. (4.10). However, since the numerator turns out to have the exact same number of zeros, taking the factors of $\frac{0}{0}$ to be limits enables a rewriting into derivatives:

$$\frac{f(\lambda) - f(\lambda)}{\lambda - \lambda} \to \lim_{\lambda_1 \to \lambda} \frac{f(\lambda) - f(\lambda_1)}{\lambda - \lambda_1} = f'(\lambda) \tag{4.11}$$

To do this a bit more explicitly notice that

$$\Delta(\lambda^2) = \prod_{i<j}^{N} (\lambda_i^2 - \lambda_j^2) = \prod_{i<j}^{N} (\lambda_i + \lambda_j)(\lambda_i - \lambda_j) \tag{4.12}$$

has $\frac{N(N-1)}{2}$ factors of $\lambda_j - \lambda_i$ and that, subtracting a row of $\lambda_i^{j-1} I_{\nu+j-1}(2\lambda_i)$ from any of the others and dividing by $\lambda - \lambda$ yields:

$$\begin{aligned}
&\lim_{\lambda_i, \lambda_j \to \lambda} \frac{\lambda_i^{j-1} I_{\nu+j-1}(2\lambda_i) - \lambda_{i'}^{j-1} I_{\nu+j-1}(2\lambda_{i'})}{\lambda_i - \lambda_{i'}} \\
&\quad = (j-1)\lambda^{j-2} I_{\nu+j-1}(2\lambda) + \lambda^{j-1} I'_{\nu+j-1}(2\lambda) \\
&\quad = (j-1)\lambda^{j-2} I_{\nu+j-1}(2\lambda) + \lambda^{j-1} \left[(2 I_{\nu+j-2}(2\lambda) - \frac{\nu + j - 1}{\lambda} I_{\nu+j-1}(2\lambda) \right] \\
&\quad = 2\lambda^{j-1} I_{\nu+j-2}(2\lambda) - \nu I_{\nu+j-1}(2\lambda)
\end{aligned} \tag{4.13}$$

The $\nu I_{\nu+j-1}(2\lambda)$-term can be removed by another row subtraction leaving only $2\lambda^{j-1} I_{\nu+j-2}(2\lambda)$. To systemize this choose first $i' = 1$ and $i = i' + 1, ..., N$, removing $N - 1$ zeros from both numerator and denominator. Repeat the process for $i' = 2, ..., N-1$ until all $\frac{N(N-1)}{2}$ zeros in both numerator and denominator have been removed. The end result of this calculation is:

$$\begin{aligned}
I(A, B, \nu) &= \left[\prod_{n=1}^{N-1} n! \right] (2\lambda)^{-\frac{N(N-1)}{2}} \det[2^{i-1} \lambda^{j-1} I_{\nu+j-i}(2\lambda)] \\
&= \left[\prod_{n=1}^{N-1} n! \right] \det[I_{\nu+j-i}(2\lambda)]
\end{aligned} \tag{4.14}$$

The normalization constant will however be irrelevant later on.

4.3 Numerical Check

To verify the rewriting a simple numerical check was performed by evaluating the integral

$$Z = \int dU e^{h_+ \mathrm{Tr}U + h_- \mathrm{Tr}U^\dagger} \tag{4.15}$$

in the case of $U(2)$ for $h_- = 1$ and varying values of h_+ both by ordinary numerical integration but also with the expression (4.14), although without the normalization i.e.

$$Z_B = \det[I_{\nu+j-i}(2\lambda)] \tag{4.16}$$

For the numerical integration a parametrization

$$U = e^{i\theta} \begin{bmatrix} e^{i\theta_1}\cos\phi & -e^{-i\theta_2}\sin\phi \\ e^{i\theta_2}\sin\phi & e^{-i\theta_1}\cos\phi \end{bmatrix} \tag{4.17}$$

with $\phi \in [-\pi, \pi[$, $\theta, \theta_1 \in [0, \pi[$ and $\theta_2 \in [-\pi, \pi[$ is used. This parametrization is chosen such that

$$\begin{aligned} h_+\mathrm{Tr}U + h_-\mathrm{Tr}U^\dagger &= h_+ e^{i\theta}(e^{i\theta_1} + e^{-i\theta_1}) + h_- e^{-i\theta}(e^{-i\theta_1} + e^{i\theta_1})\cos\phi \\ &= 2(h_+ e^{i\theta} + h_- e^{-\theta})\cos\theta_1\cos\phi \end{aligned} \tag{4.18}$$

Calculating the determinant of the Jacobian involved with the coordinate change

$$\begin{aligned} \det(J) &= -i^3 e^{4i\theta} \det \begin{bmatrix} e^{i\theta_1}\cos\phi & e^{i\theta_1}\cos\phi & 0 & e^{i\theta_1}\sin\phi \\ -e^{-i\theta_2}\sin\phi & 0 & e^{-i\theta_2}\sin\phi & e^{-i\theta_2}\cos\phi \\ e^{i\theta_2}\sin\phi & 0 & e^{i\theta_2}\sin\phi & -e^{i\theta_2}\cos\phi \\ e^{-i\theta_1}\cos\phi & -e^{-i\theta_1}\cos\phi & 0 & e^{-i\theta_1}\sin\phi \end{bmatrix} \\ &= ie^{4i\theta}\left[2\cos^3\phi\sin\phi + 2\sin^3\phi\cos\phi\right] = ie^{4i\theta}\sin(2\phi) \end{aligned} \tag{4.19}$$

which means that the numerically evaluated integral is

$$\int_{-\pi}^{\pi} d\phi \int_0^{\pi} d\theta \int_0^{\pi} d\theta_1 |\sin(2\phi)| e^{2\cos\theta_1\cos\phi(h_+ e^{i\theta} + h_- e^{-\theta})} \tag{4.20}$$

The result is plotted in fig. 4.1 and shows very good agreement; the variation present is very small and likely due to numerical imprecision.

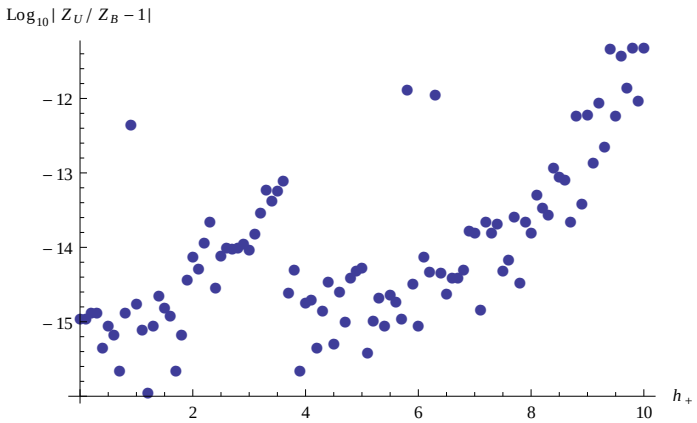

Figure 4.1: Comparison between numerical integration, Z_U, and the analytical expression Z_B in the case of $U(2)$ with $h_- = 1$ kept fixed.

Chapter 5

Expectation Value for the Polyakov Loop

Starting from the action for the effective theory of Polyakov loops with applied chemical potential introduced in section 3.7

$$\begin{aligned} S(J, he^{\bar{\mu}}, he^{-\bar{\mu}}) =& \frac{1}{2} J \sum_{\mathbf{x},j} [W(\mathbf{x}) W^\dagger(\mathbf{x}+\hat{j}) + W^\dagger(\mathbf{x}) W(\mathbf{x}+\hat{j})] \\ &+ hN_c \sum_{\mathbf{x}} [e^{\bar{\mu}} W(\mathbf{x}) + e^{-\bar{\mu}} W^\dagger(\mathbf{x})] \end{aligned} \tag{5.1}$$

where $\bar{\mu} = aN_\tau \mu$, $h = 2\frac{N_f}{N_c}\kappa_f^{N_\tau}$ and the j sum runs over positive directions only. In the following we will be interested in the $N_c \to \infty$ limit and we will keep the ration $\frac{N_f}{N_c}$ fixed. Retracing the steps of [22] the action above can be simplified by realizing that a rewriting

$$\begin{aligned} S(J,0,0) = \frac{1}{2} J \sum_{\mathbf{x},j} \big\{ &\langle W(\mathbf{x})\rangle W^\dagger(\mathbf{x}+j) + W(\mathbf{x}) \langle W^\dagger(\mathbf{x}+j)\rangle - \langle W(\mathbf{x})\rangle \langle W^\dagger(\mathbf{x}+j)\rangle \\ &+ [W(\mathbf{x}) - \langle W(\mathbf{x})\rangle][W^\dagger(\mathbf{x}+j) - \langle W^\dagger(\mathbf{x}+j)\rangle] + h.c \big\} \end{aligned} \tag{5.2}$$

is possible. Here the last term does not contribute due to large-N_c factorization. Below the bar in $\bar{\mu}$ will be dropped for convenience. Now, using translational invariance, the sum over j can be performed, leaving the expression

$$\begin{aligned} S(J, he^{\mu}, he^{-\mu}) = & JD \sum_{\mathbf{x}} [\langle W\rangle W^\dagger(\mathbf{x}) + \langle W^\dagger\rangle W(\mathbf{x}) - \langle W\rangle\langle W^\dagger\rangle] \\ &+ N_c \sum_{\mathbf{x}} [he^{\mu} W(\mathbf{x}) + he^{-\mu} W^\dagger(\mathbf{x})] \end{aligned} \tag{5.3}$$

Notice here that due to the chemical potential the action is non-Hermitian, meaning that $\langle W\rangle^\dagger \neq \langle W^\dagger\rangle$ - in fact $\langle W\rangle^\dagger = \langle W\rangle$. Defining

$$h_+ \equiv he^{\mu} + \frac{JD}{N_c}\langle W^\dagger\rangle, \qquad h_- \equiv he^{-\mu} + \frac{JD}{N_c}\langle W\rangle \tag{5.4}$$

the partition function can be written as

$$\begin{aligned} Z(J, he^{\mu}, he^{-\mu}) &= \exp[S(J, he^{\mu}, he^{-\mu})] \\ &= \exp[S(0, h_+, h_-) - JD \sum_{\mathbf{x}} \langle W \rangle \langle W^{\dagger} \rangle] \\ &= N(J) \exp[N_c \sum_{\mathbf{x}} h_+ W(\mathbf{x}) + h_- W^{\dagger}(\mathbf{x})] \end{aligned} \tag{5.5}$$

where $N(J) = \exp[-JD \sum_{\mathbf{x}} \langle W \rangle \langle W^{\dagger} \rangle]$ is an overall, J-dependent, normalization constant, which does not contribute to the expectation values of interest. The expectation values $\langle W \rangle$ and $\langle W^{\dagger} \rangle$ can now be written as

$$\langle W \rangle = \frac{1}{Z} \int_{SU(N)} W \exp[S(0, h_+, h_-)] = Z^{-1} \frac{1}{N_c V_{\mathbf{x}}} \frac{\partial}{\partial h_+} Z \tag{5.6}$$

$$\langle W^{\dagger} \rangle = \frac{1}{Z} \int_{SU(N)} W^{\dagger} \exp[S(0, h_+, h_-)] = Z^{-1} \frac{1}{N_c V_{\mathbf{x}}} \frac{\partial}{\partial h_-} Z \tag{5.7}$$

where $Z = Z(0, h_+, h_-)$ and $V_{\mathbf{x}} = \sum_{\mathbf{x}}$. Since $h_{\pm}$ are defined from the expectation values and the expectation values from $h_{\pm}$ eq. (5.4) are a set of self-consistency relations.

A few cases are worth considering before proceeding further. In the case where either $h = 0$ or $\mu = 0$ the action becomes Hermitian and as a consequence $\langle W \rangle = \langle W^{\dagger} \rangle$ and $h_+ = h_-$. Furthermore, if $h_+ = h_- = 0$ then $\langle W \rangle = \langle W^{\dagger} \rangle = 0$ since the integral over a single group element vanishes. As a consequence of the self-consistency relations, this also means that $h = 0$. In the case where only $h_- = 0$ then $he^{-\mu} = -\frac{JD}{N_c} \langle W \rangle$ and $h_+ = \frac{JD}{N_c} \left[\langle W^{\dagger} \rangle - \langle W \rangle e^{2\mu} \right]$ as a consequence. In the $N_c \to \infty$ limit $h_- = 0$ would mean that $\langle W \rangle = 0$ since no $W^{\dagger}$ is available and it would take an infinite number of Ws to get a non-vanishing contribution.

5.1 Application of Unitary Integral

Since the requirement for $SU(N)$ to have unit determinant becomes comparitatively weaker for larger N, the group integrations in the $N \to \infty$ limit can be replaced by $U(N)$ integrals. As such the unitary integral computed in the last chapter comes in handy; especially a single feature, namely that

$$Z(0, h_+, h_-) = Z(0, \sqrt{h_+ h_-}, \sqrt{h_+ h_-}) \tag{5.8}$$

which means that for $h_+, h_- \neq 0$ the expectation values (5.6-5.7) can be written as

$$\begin{aligned}\langle W\rangle &= Z^{-1}\frac{1}{N_c V_{\mathbf{x}}}\frac{\partial}{\partial h_+}Z(0,\sqrt{h_+h_-},\sqrt{h_+h_-}) \\ &= Z^{-1}\frac{1}{2N_c V_{\mathbf{x}}}\sqrt{\frac{h-}{h_+}}\frac{\partial}{\partial g}Z(0,g,g) \\ &= \sqrt{\frac{h-}{h_+}}\langle W\rangle_{h=\sqrt{h_+h_-},\mu=0} \\ \langle W^\dagger\rangle &= \sqrt{\frac{h+}{h_-}}\langle W\rangle_{h=\sqrt{h_+h_-},\mu=0} \end{aligned} \tag{5.9}$$

where $\langle W\rangle_{h=h',\mu=\mu'}$ is the expectation value calculated in a theory with $h=h'$ and $\mu=\mu'$. Remarkably, this means that the expectation values can be found from a theory without a chemical potential! Further consequences of these equations are that $h_-\langle W^\dagger\rangle = h_+\langle W\rangle$, which can be used with the self-consistency relations (5.4) to get a useful identity

$$h_+h_- = h_-\left(he^{\mu}+\frac{JD}{N_c}\langle W^\dagger\rangle\right) = h_+\left(he^{-\mu}+\frac{JD}{N_c}\langle W\rangle\right) \tag{5.10}$$

$$\Leftrightarrow h_-he^{\mu} = h_+he^{-\mu} \tag{5.11}$$

which means that for $h\neq 0$ then h_+ and h_- have the same sign, in turn meaning that the expectation values are purely real. Furthermore from this follows

$$\frac{h_+}{h_-} = \frac{\langle W^\dagger\rangle}{\langle W\rangle} = e^{2\mu} \tag{5.12}$$

when $h\neq 0$ (and $\langle W\rangle \neq 0$). In the case of $h=0$ then $\langle W\rangle = \langle W^\dagger\rangle$ and thus $\frac{h_+}{h_-}=1$, meaning that for eq. (5.12) to also cover $h=0$ then it is necessary to also set $\mu=0$ when setting $h=0$. Using the results from [22] and [23] the integral can be evaluated in a theory without an applied chemical potential in the $N_c\to\infty$ limit

$$\frac{1}{N_c}\langle W\rangle_{h=\sqrt{h_+h_-},\mu=0} = \begin{cases}\sqrt{h_+h_-} & \text{for } \sqrt{h_+h_-}<\frac{1}{2} \\ 1-\frac{1}{4\sqrt{h_+h_-}} & \text{for } \sqrt{h_+h_-}\geq\frac{1}{2}\end{cases} \tag{5.13}$$

which by direct insertion means

$$\frac{|h_+|\langle W\rangle}{N_c} = \frac{|h_-|\langle W^\dagger\rangle}{N_c} = \begin{cases}h_+h_- & \text{for } \sqrt{h_+h_-}<\frac{1}{2} \\ \sqrt{h_+h_-}-\frac{1}{4} & \text{for } \sqrt{h_+h_-}\geq\frac{1}{2}\end{cases} \tag{5.14}$$

Here the absolute value can be dropped straight away since $h_+, h_- \geq 0$, which follows from the self-consistency relations and the fact that both h and the expectation

values are greater or equal to zero. Solving the self-consistency equations (5.4) in the case of $\sqrt{h_+h_-} < \frac{1}{2}$ is straightforward

$$\frac{\langle W\rangle}{N_c} = h_- = \frac{h}{1-JD}e^{-\mu} \tag{5.15}$$

$$\frac{\langle W^\dagger\rangle}{N_c} = h_+ = \frac{h}{1-JD}e^{\mu} \tag{5.16}$$

In the $\sqrt{h_+h_-} \geq \frac{1}{2}$ case the expression (5.14) can be restated and the self-consistency inserted such that

$$\begin{aligned} 0 &= h_+\left(\frac{\langle W\rangle}{N_c} - \sqrt{\frac{h_-}{h_+}}\right) + \frac{1}{4} \\ &= \left(he^{\mu} + \frac{JD}{N_c}\langle W^\dagger\rangle\right)\left(\frac{\langle W\rangle}{N_c} - \sqrt{\frac{h_-}{h_+}}\right) + \frac{1}{4} \end{aligned} \tag{5.17}$$

at which point the identity (5.12) comes in handy to write

$$\begin{aligned} 0 &= \left(h + \frac{JD}{N_c}e^{\mu}\langle W\rangle\right)\left(\frac{\langle W\rangle}{N_c} - e^{-\mu}\right) + \frac{1}{4}e^{-\mu} \\ &= JDe^{\mu}\left(\frac{\langle W\rangle}{N_c}\right)^2 + (h-JD)\frac{\langle W\rangle}{N_c} + \left(\frac{1}{4} - h\right)e^{-\mu} \Leftrightarrow \end{aligned} \tag{5.18}$$

$$\begin{aligned} \frac{\langle W\rangle^{(\pm)}}{N_c} &= \frac{JD - h \pm \sqrt{(h-JD)^2 - 4JD\left(\frac{1}{4}-h\right)}}{2JDe^{\mu}} \\ &= \frac{1}{2}\left(1 - \frac{h}{JD} \pm \sqrt{\left(\frac{h}{JD}+1\right)^2 - \frac{1}{JD}}\right)e^{-\mu} \end{aligned} \tag{5.19}$$

from which the $\langle W^\dagger\rangle$ solutions can be found using the identity

$$\frac{\langle W^\dagger\rangle^{(\pm)}}{N_c} = \frac{1}{2}\left(1 - \frac{h}{JD} \pm \sqrt{\left(\frac{h}{JD}+1\right)^2 - \frac{1}{JD}}\right)e^{\mu} \tag{5.20}$$

Insertion into the self-consistency relations gives the $h_\pm$ expressions

$$h_+^{(\pm)} = \frac{1}{2}\left(JD + h \pm \sqrt{(h+JD)^2 - JD}\right)e^{\mu} \tag{5.21}$$

$$h_-^{(\pm)} = \frac{1}{2}\left(JD + h \pm \sqrt{(h+JD)^2 - JD}\right)e^{-\mu} \tag{5.22}$$

where the superscripted $(\pm)$ indicates the sign of the square root. As mentioned earlier the $h = 0$ solution is retrieved by setting $h = \mu = 0$ simultaneously.

5.2 Signs and Inequalities

At this point there are a few problems to address, namely expressing $\sqrt{h_+h_-} < \frac{1}{2}$ and $\sqrt{h_+h_-} \geq \frac{1}{2}$ in terms of h and μ, determining which of the $\pm$ solutions satisfy this condition and checking whether the square roots are real. The reality of the square roots is straightforward to check, since

$$(JD)^2 + (2h-1)JD + h^2 = 0 \Leftrightarrow \tag{5.23}$$

$$JD^{(\pm)} = \frac{1}{2}(1 - 2h \pm \sqrt{1-4h}) \tag{5.24}$$

From this we conclude that all is well for $h \geq \frac{1}{4}$, whereas for $h < \frac{1}{4}$ either $JD < \frac{1}{2}(1-2h-\sqrt{1-4h})$ or $JD > \frac{1}{2}(1-2h+\sqrt{1-4h})$ must be fulfilled. For the reexpression of $\sqrt{h_+h_-} < \frac{1}{2}$ then

$$\begin{aligned} &\frac{h}{|1-JD|} < \frac{1}{2} \\ &\quad \Leftrightarrow \;\; 2h < |1-JD| \\ &\quad \Leftrightarrow JD < 1-2h \vee JD > 1+2h \end{aligned} \tag{5.25}$$

Since the $JD > 1+2h$ solution results in negative $h_\pm$ only the $JD < 1-2h$ solution is valid. Continuing with $\sqrt{h_+h_-} \geq \frac{1}{2}$ then

$$\left| JD + h \pm \sqrt{(h+JD)^2 - JD} \right| \geq 1 \tag{5.26}$$

where the absolute value can be lifted in both cases, provided that the argument of the square root is positive. Proceeding gives

$$\pm\sqrt{(h+JD)^2 - JD} \geq 1 - JD - h \tag{5.27}$$

but here keeping track of the equality sign gets a bit tricky. Considering the case where both sides are positive (i.e. "+" and $JD \leq 1-h$) then

$$\begin{aligned} (h+JD)^2 - JD &\geq 1 + (JD+h)^2 - 2(JD+h) \\ &\Leftrightarrow JD \geq 1-2h \end{aligned} \tag{5.28}$$

meaning that this solution is valid for $JD \in [1-2h, 1-h]$. The case of $(-, JD > 1-h)$ leads to

$$\begin{aligned} (h+JD)^2 - JD &\leq 1 + (JD+h)^2 - 2(JD+h) \\ &\Leftrightarrow JD \leq 1-2h \end{aligned} \tag{5.29}$$

but since $JD > 1-h$ and $JD \leq 1-2h$ cannot both be fulfilled this case does not contain a solution. The $(-, JD \leq 1-h)$ case naturally does not have a solution, since

no negative number can be larger than a positive, so left is only the $(+, JD > 1-h)$ case, which depends on the absolute value of the right hand side as compared to the left:

$$JD + h - 1 \geq \sqrt{(h + JD)^2 - JD} \tag{5.30}$$

meaning that the inequality sign of eq. (5.27) needs to be flipped for $JD \leq 1 - 2h$. Considering $JD \geq 1 - 2h$ the conlusion is that of eq. (5.28), meaning $JD \geq 1 - h$. Flipping the inequality sign for $JD \leq 1-2h$ leads to eq. (5.29) meaning that, again, no solution exists. In conclusion for the whole $\sqrt{h_+ h_-} \geq \frac{1}{2}$ calculation then the requirement is that only the "+" solution is valid and only for $JD \geq 1-2h$. This also means that the expectation values are always real since $JD > \frac{1}{2}(1 - 2h + \sqrt{1 - 4h})$ is fulfilled by $JD \geq 1 - 2h$. As such the expectation values have a transition point between the two regions at $JD = 1 - 2h$. With this knowledge then the solutions are

$$\frac{\langle W \rangle}{N_c} = \begin{cases} \frac{h}{1-JD} e^{-\mu} & \text{for } JD < 1 - 2h \\ \frac{1}{2}\left(1 - \frac{h}{JD} + \sqrt{\left(\frac{h}{JD} + 1\right)^2 - \frac{1}{JD}}\right) e^{-\mu} & \text{for } JD \geq 1 - 2h \end{cases} \tag{5.31}$$

and

$$h_- = \begin{cases} \frac{h}{1-JD} e^{-\mu} & \text{for } JD < 1 - 2h \\ \frac{1}{2}\left(JD + h + \sqrt{(h + JD)^2 - JD}\right) e^{-\mu} & \text{for } JD \geq 1 - 2h \end{cases} \tag{5.32}$$

from which the $\langle W^\dagger \rangle$ and h_- solutions can be found by reversing the sign on μ. A noticable curiosity is that for $JD \geq 1 - 2h$ the limit $h \to 0$ does not result in the $h = 0$ solution - to retrieve $h = 0$ it is, as mentioned earlier, also necessary to set $\mu = 0$. To illustrate the behavior of the solutions at different values of h and μ they are plotted in fig. (5.1).

5.3 Numerical Evaluation

To see the convergence of the solutions as N_c is increasing a numerical evaluation is necessary. For this eq. (4.14) can be used to evaluate the partition function (5.5) in terms of Bessel functions for sets of (h_+, h_-) values, which then again can be used to calculate the expectation values as with difference quotients as described by eqs. (5.6-5.7). Plugging these expectation values into the self-consistency equations (5.4) allows for an iterative search for the correct (h_+, h_-) values. The iterative search was performed using the Newton-Rhapson method. It should be stressed that the it is the $U(N_c)$ case which have been solved for and not $SU(N_c)$; a choice which was made based on the poor convergence rate of the $SU(N_c)$ integrals.

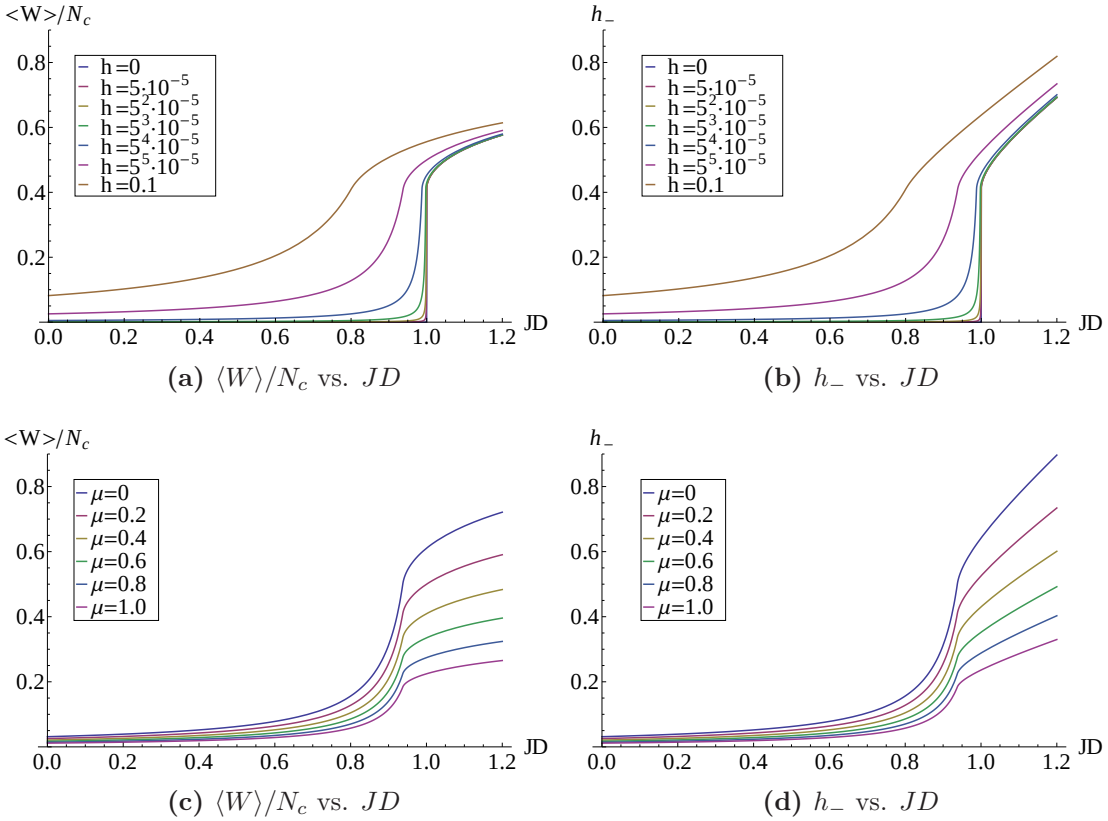

(a) $\langle W \rangle / N_c$ vs. JD **(b)** h_- vs. JD

(c) $\langle W \rangle / N_c$ vs. JD **(d)** h_- vs. JD

Figure 5.1: Plots of the analytical solutions for different values of h and μ. (a) and (b) have $\mu = 0.2$ and a varying range of h values, while (c) and (d) have $h = 5^5 \cdot 10^{-5}$ and a varying range of μ values.

5.3.1 The Newton-Rhapson Method

The Newton-Rhapson method is a straightforward algorithm for finding succesivly better approximations of roots based on a linear extrapolation from the current point. As such a simple 'first guess' for a root of a reasonably well-behaved function of one variable would be

$$x_1 = x_0 - \frac{f(x_0)}{f'(x_0)} \tag{5.33}$$

corresponding to a simple linear extrapolation from the starting point. Repeating the same procedure from this point means that the (n+1)'th point is found by

$$x_{n+1} = x_n - \frac{f(x_n)}{f'(x_n)} \tag{5.34}$$

The generalization of this procedure to functions of several variables is done by solving

$$J_f(x_n)(x_{n+1} - x_n) = -f(x_n) \tag{5.35}$$

for x_{n+1}. Here $J_f(x_n)$ is the Jacobian matrix at x_n defined by

$$J_f(x) \equiv \begin{bmatrix} \frac{\partial f_1}{\partial x_1} & \cdots & \frac{\partial f_1}{\partial x_n} \\ \vdots & \ddots & \vdots \\ \frac{\partial f_n}{\partial x_1} & \cdots & \frac{\partial f_n}{\partial x_n} \end{bmatrix} \tag{5.36}$$

as usual.

5.3.2 Application

Since the solutions that we seek are to the self-consistency equations, these need to be recast slightly:

$$f_+(h_+, h_-, h, \mu, N_c) = he^{\mu} + \frac{JD}{N_c}\langle W^\dagger\rangle(h_+, h_-, N_c) - h_+ \tag{5.37}$$

$$f_-(h_+, h_-, h, \mu, N_c) = he^{-\mu} + \frac{JD}{N_c}\langle W\rangle(h_+, h_-, N_c) - h_- \tag{5.38}$$

where $h_\pm$ are the roots we are going to iteratively solve for. The derivatives are

$$\frac{\partial f_+}{\partial h_+} = \frac{JD}{N_c}\frac{\partial\langle W^\dagger\rangle}{\partial h_+} - 1 \quad \frac{\partial f_+}{\partial h_-} = \frac{JD}{N_c}\frac{\partial\langle W^\dagger\rangle}{\partial h_-} \tag{5.39}$$

$$\frac{\partial f_-}{\partial h_+} = \frac{JD}{N_c}\frac{\partial\langle W\rangle}{\partial h_+} \qquad \frac{\partial f_-}{\partial h_-} = \frac{JD}{N_c}\frac{\partial\langle W\rangle}{\partial h_-} - 1 \tag{5.40}$$

where, due to eq. (5.6-5.7)

$$\frac{\partial\langle W^\dagger\rangle}{\partial h_+} = \frac{1}{N_c V_{\mathbf{x}}}\frac{\partial}{\partial h_+}\frac{\partial}{\partial h_-}\log(Z) = \frac{\partial\langle W\rangle}{\partial h_-} \tag{5.41}$$

$$\frac{\partial}{\partial h_+}\langle W\rangle(h_+, h_-) = \frac{1}{N_c V_{\mathbf{x}}}\frac{\partial^2}{\partial h_+^2}\log(Z(h_+, h_-)) = \frac{\partial}{\partial h_-}\langle W^\dagger\rangle(h_-, h_+) \tag{5.42}$$

implying that $\frac{\partial f_+}{\partial h_+} = \frac{\partial f_-}{\partial h_-}$. Since

$$J_f = \begin{bmatrix} \frac{\partial f_+}{\partial h_+} & \frac{\partial f_+}{\partial h_-} \\ \frac{\partial f_-}{\partial h_+} & \frac{\partial f_-}{\partial h_-} \end{bmatrix}, \quad J_f^{-1} = \frac{1}{\det J_f}\begin{bmatrix} \frac{\partial f_-}{\partial h_-} & -\frac{\partial f_+}{\partial h_-} \\ -\frac{\partial f_-}{\partial h_+} & \frac{\partial f_+}{\partial h_+} \end{bmatrix} \tag{5.43}$$

the next step in the iteration was found by

$$h_+^{(n+1)} = h_+^{(n)} - \frac{1}{\det J_f}\left(f_+\frac{\partial f_-}{\partial h_-} - f_-\frac{\partial f_+}{\partial h_-}\right)\Bigg|_{h_+^{(n)}, h_-^{(n)}} \tag{5.44}$$

$$h_-^{(n+1)} = h_-^{(n)} - \frac{1}{\det J_f}\left(f_-\frac{\partial f_+}{\partial h_+} - f_+\frac{\partial f_-}{\partial h_+}\right)\Bigg|_{h_+^{(n)}, h_-^{(n)}} \tag{5.45}$$

In practice all differentiations of the partition function were replaced with difference quotients with a fixed stepsize.

5.3.3 Results

Using a very small stepsize of 10^{-4} and a large numerical precision to increase the accuracy of the calculated differentials and solving the self-consistency relations in the range of $JD \in [0, 1.2]$ for $h = 0.2$ and $\mu = 0.4$ in the cases of $N_c = 1, 3, 7$ and 15 leads to the solutions which are displayed in fig. 5.2 together with the analytical solutions eqs. (5.31-5.32). As can be seen the convergence towards the $N_c \to \infty$ solution occurs rather rapidly.

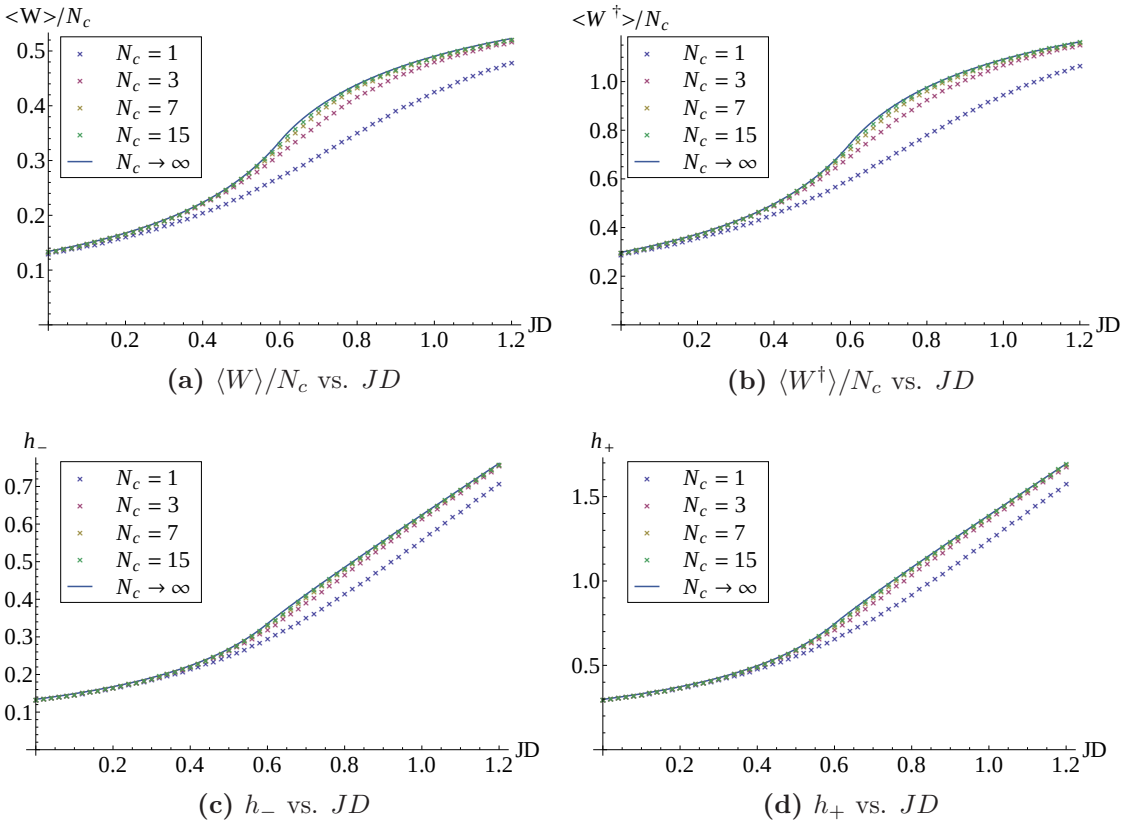

(a) $\langle W \rangle / N_c$ vs. JD **(b)** $\langle W^\dagger \rangle / N_c$ vs. JD

(c) h_- vs. JD **(d)** h_+ vs. JD

Figure 5.2: Plots of the numerical solutions to the self-consistency equations in the cases of $N_c = 1, 3, 7$ and 15 together with the analytical $N_c \to \infty$ solution in the case of $h = 0.2$ and $\mu = 0.4$.

5.4 Additional Calculations

Considering the free energy defined as

$$e^{-F} = Z \Leftrightarrow F = -\log(Z) \tag{5.46}$$

the differential expressions for the expectation values $\langle W \rangle$ and $\langle W^\dagger \rangle$ (eqs. (5.6) and (5.7)) can be used to calculate the free energy density $f = \frac{F}{N_c^2 V_{\mathbf{x}}}$ from eq. (5.14)

given that the normalization factor of $N(J) = \exp[-JD\sum_{\mathbf{x}}\langle W\rangle\langle W^\dagger\rangle]$ is kept. The two expressions are

$$\begin{aligned} f_+ &= JD\frac{\langle W\rangle\langle W^\dagger\rangle}{N_c^2} - \int dh_+\langle W\rangle \\ &= \begin{cases} JD\frac{\langle W\rangle\langle W^\dagger\rangle}{N_c^2} - h_+h_- + c_1^+(h_-) & \text{for } JD < 1-2h \\ JD\frac{\langle W\rangle\langle W^\dagger\rangle}{N_c^2} - 2\sqrt{h_+h_-} + \frac{1}{4}\log(h_+) + c_2^+(h_-) & \text{for } JD \geq 1-2h \end{cases} \end{aligned} \tag{5.47}$$

$$\begin{aligned} f_- &= JD\frac{\langle W\rangle\langle W^\dagger\rangle}{N_c^2} - \int dh_+\langle W\rangle \\ &= \begin{cases} JD\frac{\langle W\rangle\langle W^\dagger\rangle}{N_c^2} - h_+h_- + c_1^-(h_+) & \text{for } JD < 1-2h \\ JD\frac{\langle W\rangle\langle W^\dagger\rangle}{N_c^2} - 2\sqrt{h_+h_-} + \frac{1}{4}\log(h_-) + c_2^-(h_+) & \text{for } JD \geq 1-2h \end{cases} \end{aligned} \tag{5.48}$$

from which consistency of the two expressions can be reached by the choice

$$\begin{aligned} f &= JD\frac{\langle W\rangle\langle W^\dagger\rangle}{N_c^2} - \int dh_+\langle W\rangle \\ &= \begin{cases} JD\frac{\langle W\rangle\langle W^\dagger\rangle}{N_c^2} - h_+h_- & \text{for } JD < 1-2h \\ JD\frac{\langle W\rangle\langle W^\dagger\rangle}{N_c^2} - 2\sqrt{h_+h_-} + \frac{1}{2}\log(2\sqrt{h_+h_-}) + \frac{3}{4} & \text{for } JD \geq 1-2h \end{cases} \end{aligned} \tag{5.49}$$

found by setting $c_1^\pm = 0$ and insisting on a continuous transition between the solutions. This solution corresponds to that of Gross & Witten [23]. Inserting the solutions found simplifies the $JD < 1-2h$ solution to

$$f = -\frac{h^2}{1-JD} \tag{5.50}$$

whereas the $JD \leq 1-2h$ solution unfortunately does not get any prettier. A plot of the free energy density is shown in fig. 5.3 and displays an almost flat plateau near $f = 0$ at the lower values of JD and h, but drops at higher values of either parameter. The transition line is found by following the steps of Gross & Witten [23] and realizing that $g = \sqrt{h_+h_-}$ acts like an inverse coupling $\frac{1}{g^2}$ - writing $\lambda = \frac{1}{g}$ and disregarding equal terms in the expression of the free energy, gives

$$-f = \begin{cases} \frac{1}{\lambda^2} & \text{for } \lambda > 2 \\ \frac{2}{\lambda} + \frac{1}{2}\log(\frac{\lambda}{2}) - \frac{3}{4} & \text{for } \lambda \leq 2 \end{cases} \tag{5.51}$$

Differentiating with respect to λ leads to a discontinuity in the third derivative at $\lambda = 2$ i.e. a third order phase transition at $JD = 1-2h$ which is the line displayed in fig. 5.3.

Another interesting consequence is that the expectation value of the quark density operator, which can be found by derivation with respect to μ, is seen to be zero

$$\langle\psi^\dagger\psi\rangle = -\frac{\partial F}{\partial\mu} = 0 \tag{5.52}$$

due to the complete lack of μ dependence in (5.49). This means that the average number of expected quarks and antiquarks are equal within the effective theory of Polyakov loops, despite the chemical potential which treats them differently.

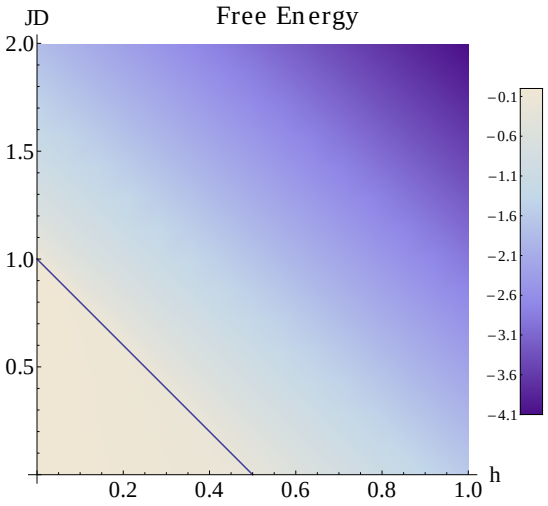

Figure 5.3: Plot of the free energy density calculated in eq. 5.49 with the third order transition line drawn.

Appendix A

Recovering the Continuum

This section has the explicit purpose of verifying (3.5): To start off consider a plaquette with center in x_μ and oriented in the (ν', η') plane. Then eq. (3.4) takes the form

$$S_\Box = \beta\Big(1 - \frac{1}{n}\,\mathrm{Re}\,\mathrm{Tr}\exp\big[iagA_{\nu'}(x_\mu - \frac{1}{2}a\delta_{\mu\eta'})\big] \times \exp\big[iagA_{\eta'}(x_\mu + \frac{1}{2}a\delta_{\mu\nu'})\big] \\ \times \exp\big[-iagA_{\nu'}(x_\mu + \frac{1}{2}a\delta_{\mu\eta'})\big] \times \exp\big[-iagA_{\eta'}(x_\mu - \frac{1}{2}a\delta_{\mu\nu'})\big]\Big) \quad \text{(A.1)}$$

Adapting the shorthand notations $A^{\pm}_{\nu'} = A_{\nu'}(x_\mu \pm \frac{1}{2}a\delta_{\mu\eta'})$ and $a \to -\frac{ia}{g}$ for brevity the expression can be written as

$$S_\Box = \beta(1 - \frac{1}{n}\,\mathrm{Re}\,\mathrm{Tr}\exp(aA^-_{\nu'})\exp(aA^+_{\eta'})\exp(-aA^+_{\nu'})\exp(-aA^-_{\eta'})) \quad \text{(A.2)}$$

from which the two first exponentials can be written as one using the Baker-Campbell-Hausdorff formula

$$\exp\Big(a(A^-_{\nu'} + A^+_{\eta'}) + \frac{1}{2}a^2[A^-_{\nu'}, A^+_{\eta'}] + \frac{1}{12}a^3\left[A^-_{\nu'} - A^+_{\eta'}, [A^-_{\nu'}, A^+_{\eta'}]\right] \\ - \frac{1}{24}a^4\left[A^+_{\eta'}, \left[A^-_{\nu'}, [A^-_{\nu'}, A^+_{\eta'}]\right]\right] + O(a^5)\Big) \quad \text{(A.3)}$$

and likewise for the last two

$$\exp\Big(-a(A^+_{\nu'} + A^-_{\eta'}) + \frac{1}{2}a^2[A^+_{\nu'}, A^-_{\eta'}] - \frac{1}{12}a^3\left[A^+_{\nu'} - A^-_{\eta'}, [A^+_{\nu'}, A^-_{\eta'}]\right] \\ - \frac{1}{24}a^4\left[A^-_{\eta'}, \left[A^+_{\nu'}, [A^+_{\nu'}, A^-_{\eta'}]\right]\right] + O(a^5)\Big) \quad \text{(A.4)}$$

Combining it all into just one exponential leads to the argument

$$
\begin{aligned}
& a\left(A^-_{\nu'} + A^+_{\eta'} - A^+_{\nu'} - A^-_{\eta'}\right) \\
+ & \frac{a^2}{2}\left([A^-_{\nu'}, A^+_{\eta'}] + [A^+_{\nu'}, A^-_{\eta'}] - \left[A^-_{\nu'} + A^+_{\eta'}, A^+_{\nu'} + A^-_{\eta'}\right]\right) \\
+ & \frac{a^3}{4}\left(\left[A^-_{\nu'} + A^+_{\eta'}, [A^+_{\nu'}, A^-_{\eta'}]\right] + \left[A^+_{\nu'} + A^-_{\eta'}, [A^-_{\nu'}, A^+_{\eta'}]\right]\right) \\
+ & \frac{a^3}{12}\left(\left[A^-_{\nu'} - A^+_{\eta'}, [A^-_{\nu'}, A^+_{\eta'}]\right] - \left[A^+_{\nu'} - A^-_{\eta'}, [A^+_{\nu'}, A^-_{\eta'}]\right]\right) \\
+ & \frac{a^4}{24}\left(\left[A^-_{\nu'} + A^+_{\eta'}, \left[A^+_{\nu'} - A^-_{\eta'}, [A^+_{\nu'}, A^-_{\eta'}]\right]\right]\right) \\
- & \frac{a^4}{24}\left(\left[A^+_{\nu'} + A^-_{\eta'}, \left[A^-_{\nu'} - A^+_{\eta'}, [A^-_{\nu'}, A^+_{\eta'}]\right]\right]\right) + \frac{a^4}{8}\left[[A^-_{\nu'}, A^+_{\eta'}], [A^+_{\nu'}, A^-_{\eta'}]\right] \\
- & \frac{a^4}{24}\left(\left[A^+_{\eta'}, \left[A^-_{\nu'}, [A^-_{\nu'}, A^+_{\eta'}]\right]\right] + \left[A^-_{\eta'}, \left[A^+_{\nu'}, [A^+_{\nu'}, A^-_{\eta'}]\right]\right]\right) + O(a^5) \qquad \text{(A.5)} \\
\rightarrow & ia^2 g\left(\partial_{\nu'} A_{\eta'} - \partial_{\eta'} A_{\nu'} - ig[A_{\nu'}, A_{\eta'}]\right) + O(a^3) \qquad \text{(A.6)}
\end{aligned}
$$

where in the last term $a \to iag$ has been taken and a Taylor expansions around x has been performed:

$$A_{\nu'}(x_\mu - \frac{1}{2}a\delta_{\mu\eta'}) = (1 - \frac{1}{2}a\partial_{\eta'})A_{\nu'}(x_\mu) + O(a^2) \qquad \text{(A.7)}$$

At this point it is worth noticing that the $\mathcal{O}(a^3)$ term is a sum of Hermitian matrices and that the action can be written as:

$$S_\Box = \beta\left(1 - \frac{1}{n}\operatorname{Re}\operatorname{Tr}[\exp(iga^2 F_{\mu\nu} + \mathcal{O}(a^3))]\right) \qquad \text{(A.8)}$$

which is exactly the result postulated in eq. (3.5).

Appendix B

Mathematica Code

Below are the copies of the Mathematica codes used for the project. They are copied directly and works if plugged into Mathematica 8.0.1.0 - subsections rely on the prior execution of the section they are part of. Notice that the lone \-lines were not a orinal part of the code but added upon copying to avoid lines that were too long.

B.1 Plot 4.1: Numerical and Bessel Evaluation of $U(N)$-integral

```
h1 = 1;
DataTable =
  Table[{h2,
    Log10[Abs[
      Integrate[
          Abs[Sin[2*y]]*
           Exp[2*Cos[y]*Cos[z]*(h1*Exp[x*I] + h2*Exp[-x*I])], {x, -Pi,
            Pi}, {y, 0, Pi}, {z, 0, Pi}]/(2^2*
           Pi^2)/(BesselI[0, 2*Sqrt[h1*h2]]*
           BesselI[0, 2*Sqrt[h1*h2]] -
          BesselI[-1, 2*Sqrt[h1*h2]]*BesselI[1, 2*Sqrt[h1*h2]]) -
       1]]}, {h2, 0, 10, 0.1}];
ListPlot[DataTable, PlotMarkers -> Automatic,
 AxesLabel -> {"\!\(\*SubscriptBox[\(h\), \(+\)]\)",
   "\!\(\*SubscriptBox[\(Log\), \(10\)]\)|\!\(\*SubscriptBox[\(Z\), \
\(U\)]\)/\!\(\*SubscriptBox[\(Z\), \(B\)]\)-1|"}]
Export["Out.dat", DataTable]
```

B.2 Plot 5.1: Varying h and μ for the Analytical Solution

```
Needs["PlotLegends`"]
f[x_, h_, mu_] :=
 If[x <= 1 -
    2*h, (h*Exp[-mu])/(1 - x), ((x + h + Sqrt[(x + h)^2 - x])*
     Exp[-mu])/2]
g[x_, h_, mu_] :=
 If[x <= 1 -
    2*h, (h*Exp[-mu])/(1 - x), ((1 - h/x + Sqrt[(1 + h/x)^2 - 1/x])*
     Exp[-mu])/2]
mu = 2/10;
Plot[Evaluate[
  Table[f[x, h,
    mu], {h, {0, 0.00005, 0.00025, 0.00125, 0.00625, 0.03125,
     0.10}}]], {x, 0, 12/10}, PlotStyle -> Thick,
 PlotLegend -> {Style["h=0", FontSize -> 30],
   Style["h=5\[CenterDot]\!\(\*SuperscriptBox[\(10\), \(-5\)]\)",
    FontSize -> 30],
   Style["h=\!\(\*SuperscriptBox[\(5\), \
\(2\)]\)\[CenterDot]\!\(\*SuperscriptBox[\(10\), \(-5\)]\)",
    FontSize -> 30],
   Style["h=\!\(\*SuperscriptBox[\(5\), \
\(3\)]\)\[CenterDot]\!\(\*SuperscriptBox[\(10\), \(-5\)]\)",
    FontSize -> 30],
   Style["h=\!\(\*SuperscriptBox[\(5\), \
\(4\)]\)\[CenterDot]\!\(\*SuperscriptBox[\(10\), \(-5\)]\)",
    FontSize -> 30],
   Style["h=\!\(\*SuperscriptBox[\(5\), \
\(5\)]\)\[CenterDot]\!\(\*SuperscriptBox[\(10\), \(-5\)]\)",
    FontSize -> 30], Style["h=0.1", FontSize -> 30]},
 LegendPosition -> {-.75, -.075}, LegendSize -> {0.5, 0.50},
 LegendShadow -> None, LegendTextSpace -> 6, ImageSize -> 750,
 TicksStyle -> Directive[30],
 AxesLabel -> {" JD", "\!\(\*SubscriptBox[\(h\), \(-\)]\)"},
 LabelStyle -> Directive[30], PlotRange -> {0, 0.9}]
Plot[Evaluate[
  Table[g[x, h,
    mu], {h, {0, 0.00005, 0.00025, 0.00125, 0.00625, 0.03125,
     0.10}}]], {x, 0, 12/10}, PlotStyle -> Thick,
 PlotLegend -> {Style["h=0", FontSize -> 30],
   Style["h=5\[CenterDot]\!\(\*SuperscriptBox[\(10\), \(-5\)]\)",
```

```
    FontSize -> 30],
   Style["h=\!\(\*SuperscriptBox[\(5\), \
\(2\)]\)\[CenterDot]\!\(\*SuperscriptBox[\(10\), \(-5\)]\)",
    FontSize -> 30],
   Style["h=\!\(\*SuperscriptBox[\(5\), \
\(3\)]\)\[CenterDot]\!\(\*SuperscriptBox[\(10\), \(-5\)]\)",
    FontSize -> 30],
   Style["h=\!\(\*SuperscriptBox[\(5\), \
\(4\)]\)\[CenterDot]\!\(\*SuperscriptBox[\(10\), \(-5\)]\)",
    FontSize -> 30],
   Style["h=\!\(\*SuperscriptBox[\(5\), \
\(5\)]\)\[CenterDot]\!\(\*SuperscriptBox[\(10\), \(-5\)]\)",
    FontSize -> 30], Style["h=0.1", FontSize -> 30]},
 LegendPosition -> {-.75, -.075}, LegendSize -> {0.5, 0.50},
 LegendShadow -> None, LegendTextSpace -> 6, ImageSize -> 750,
 TicksStyle -> Directive[30],
 AxesLabel -> {" JD", "<W>/\!\(\*SubscriptBox[\(N\), \(c\)]\)"},
 LabelStyle -> Directive[30], PlotRange -> {0, 0.9}]
h = 3125/10^5;
Plot[Evaluate[Table[f[x, h, mu], {mu, 0, 1.0, 0.2}]], {x, 0, 12/10},
 PlotStyle -> Thick,
 PlotLegend -> {Style["\[Mu]=0", FontSize -> 30],
   Style["\[Mu]=0.2", FontSize -> 30],
   Style["\[Mu]=0.4", FontSize -> 30],
   Style["\[Mu]=0.6", FontSize -> 30],
   Style["\[Mu]=0.8", FontSize -> 30],
   Style["\[Mu]=1.0", FontSize -> 30]},
 LegendPosition -> {-.75, -.075}, LegendSize -> {0.3, 0.50},
 LegendShadow -> None, LegendTextSpace -> 5.8, ImageSize -> 750,
 TicksStyle -> Directive[30],
 AxesLabel -> {" JD", "\!\(\*SubscriptBox[\(h\), \(-\)]\)"},
 LabelStyle -> Directive[30], PlotRange -> {0, 0.9}]
Plot[Evaluate[Table[g[x, h, mu], {mu, 0, 1.0, 0.2}]], {x, 0, 12/10},
 PlotStyle -> Thick,
 PlotLegend -> {Style["\[Mu]=0", FontSize -> 30],
   Style["\[Mu]=0.2", FontSize -> 30],
   Style["\[Mu]=0.4", FontSize -> 30],
   Style["\[Mu]=0.6", FontSize -> 30],
   Style["\[Mu]=0.8", FontSize -> 30],
   Style["\[Mu]=1.0", FontSize -> 30]},
 LegendPosition -> {-.75, -.075}, LegendSize -> {0.3, 0.50},
 LegendShadow -> None, LegendTextSpace -> 5.8, ImageSize -> 750,
 TicksStyle -> Directive[30],
```

```
 AxesLabel -> {" JD", "<W>/\!\(\*SubscriptBox[\(N\), \(c\)]\)"},
 LabelStyle -> Directive[30], PlotRange -> {0, 0.9}]
```

B.3 Self-Consistency Solving for $U(N)$

```
(*Function calculating the determinant of a matrix consisting of \
Bessel functions:*)
DetBes[a_, b_, dim_, nu_] := (
  M = ConstantArray[0, {dim, dim}];
  For[iDB = 1, iDB <= dim, iDB++,
   For[jDB = 1, jDB <= dim, jDB++,
     M[[iDB, jDB]] = BesselI[nu + jDB - iDB, 2*Sqrt[a*b]];
     ];
   ];
  Det[M])

(*Function calculating the once a-differentiated DetBes-value i.e. \
<W>/Nc:*)
Expect[a_, b_, dim_, nu_, step_] := (
  (DetBes[a*dim + step, b*dim, dim, nu]/
      DetBes[a*dim, b*dim, dim, nu] - 1)/(step*dim)
  )

(*Function calculating the twice a-differentiated DetBes-value i.e. \
d(<W>/Nc)\.b2/d\.b2a:*)
DaExpect[a_, b_, dim_, nu_, step_] := (
  (DetBes[a*dim + step, b*dim, dim, nu]/
      DetBes[a*dim, b*dim, dim, nu] -
     DetBes[a*dim, b*dim, dim, nu]/
      DetBes[a*dim - step, b*dim, dim, nu])/(step^2)
  )

(*Function calculating the once a, once b differentiated DetBes-value \
i.e. d(<W>/Nc)/dadb:*)
DbExpect[a_, b_, dim_, nu_, step_] := (
  (DetBes[a*dim + step, b*dim + step, dim, nu]/
      DetBes[a*dim, b*dim + step, dim, nu] -
     DetBes[a*dim + step, b*dim, dim, nu]/
      DetBes[a*dim, b*dim, dim, nu])/(step^2)
  )

CompPrec = 200; (*Computation precision - must be high due to \
```

```
sensitivity of the derivatives*)

h = 2/10;
mu = 4/10; (*Chemical potential*)

a = N[h*Exp[mu], CompPrec];
b = N[h*Exp[-mu], CompPrec];
aEff = N[15/10, CompPrec]; (*Self-consist h+*)
bEff =
 N[12/10, CompPrec];(*Self-consist h-*)
(*Nc = 15; *)
nu = 0;  \
(*Largely redundant parameter*)
DStep =
 N[1/10000,
  CompPrec]; (*Step-size for difference quotients*)
NIter = 200; \
(*Number of iteration steps*)

(*JD = 1;*)
JDMax =
 12/10; (*Maximum value of JD*)
JDMin = 0;          (*Minimum value \
of JD*)
NJD =
 60 + 1;     (*Number of points in which to solve the \
self-consistency equations*)

(*
NcMin = 1;
NcMax = 7;
NcStep =2;
NNc = (NcMax-NcMin)/NcStep+1;*)

NcArray = {1, 3, 7, 15};          (*Number of colours to run code with*)
NNc = Dimensions[NcArray][[1]];   (*Number of number of colours*)

Data = ConstantArray[0, {10, NJD, NNc + 1}]; (*Array for data*)

(*A few hints;
Expect[a,b,Nc,nu,DStep] is <W>/Nc;
Expect[b,a,Nc,nu,DStep] is <Wdagger>/Nc;
DaExpect[a,b,Nc,nu,DStep] is d (<W>/Nc)/da;
```

```
DaExpect[b,a,Nc,nu,DStep] is d (<Wdagger>/Nc)/db;
DbExpect[a,b,Nc,nu,DStep] is d (<W>/Nc)/db;
DbExpect[b,a,Nc,nu,DStep] is d (<Wdagger>/Nc)/da;*)

(*a+(JD/Nc)*Expect[b,a,Nc,nu,DStep]-aEff;*)

For[iNc = 1, iNc <= NNc, iNc++,
 Nc = NcArray[[iNc]];
 Print[Nc];

 For[iJD = 0, iJD < NJD, iJD++,
  JD = JDMin + (iJD*(JDMax - JDMin))/(NJD - 1);

  (*Print[JD];*)

  Data[[1, iJD + 1, iNc]] = JD;

  F1 = 2;
  F2 = 2;
  aEff = If[JD <= 1 - 2*Sqrt[a*b],
    a/(1 - JD), (a + JD*Sqrt[a/b] +
       Sqrt[(a + JD*Sqrt[a/b])^2 - JD*(a/b)])/2];
  bEff = (b/a)*aEff;

  For[iIter = 1, (Abs[F1] + Abs[F2] >= 0.00001) && iIter <= NIter,
   iIter++,

   F1 = (a + JD*Expect[bEff, aEff, Nc, nu, DStep] - aEff);
   F2 = (b + JD*Expect[aEff, bEff, Nc, nu, DStep] - bEff);

   DaF1 = JD*DbExpect[bEff, aEff, Nc, nu, DStep] - 1;
   DbF1 = JD*DaExpect[bEff, aEff, Nc, nu, DStep];
   DaF2 = JD*DaExpect[aEff, bEff, Nc, nu, DStep];
   DbF2 = DaF1; (*Allowed due to identity;
   might suffer small accuracy loss*)
   (*DbF2 = JD*DbExpect[aEff,
   bEff,Nc,nu,DStep]-1;*)

   DetDF = DaF1*DbF2 - DaF2*DbF1;

   aEff = (-F1*DbF2 + F2*DbF1)/DetDF + aEff;
   bEff = (F1*DaF2 - F2*DaF1)/DetDF + bEff;
   ];
```

```
  (*Print[iIter];*)

  Data[[2, iJD + 1, iNc]] = aEff;
  Data[[3, iJD + 1, iNc]] = bEff;
  Data[[4, iJD + 1, iNc]] = Expect[aEff, bEff, Nc, nu, DStep];
  Data[[5, iJD + 1, iNc]] = Expect[bEff, aEff, Nc, nu, DStep];
  Data[[6, iJD + 1, iNc]] = F1;
  Data[[7, iJD + 1, iNc]] = F2;
  Data[[8, iJD + 1, iNc]] = Nc;

  (*Print[N[F1,10]];
  Print[N[F2,10]];

  Print[aEff];
  Print[bEff];*)
  ]
 ]
```

B.3.1 Plot 5.2a: $\langle W \rangle$ vs. JD

```
(*<W>*)
Needs["PlotLegends`"]
AnalytList =
  Table[{i,
    If[i <= 1 - 2*h,
     b/(1 - i), ((1 - h/i + Sqrt[(1 + h/i)^2 - 1/i])*Exp[-mu])/
      2]}, {i, JDMin, JDMax, (JDMax - JDMin)/100}];
NumList =
  Table[If[j <= NNc,
    Table[{Data[[1, i, j]], Data[[4, i, j]]}, {i, NJD}],
    AnalytList], {j, 1, NNc + 1}];
ListPlot[NumList, Joined -> {False, False, False, False, True},
 PlotStyle -> {Thick},
 PlotMarkers -> {Style["\[Cross]", FontSize -> 15, Bold],
   Style["\[Cross]", FontSize -> 15, Bold],
   Style["\[Cross]", FontSize -> 15, Bold],
   Style["\[Cross]", FontSize -> 15, Bold], ""},
 PlotLegend -> {Style["\!\(\*SubscriptBox[\(N\), \(c\)]\) = 1",
    FontSize -> 30],
   Style["\!\(\*SubscriptBox[\(N\), \(c\)]\) = 3", FontSize -> 30],
   Style["\!\(\*SubscriptBox[\(N\), \(c\)]\) = 7", FontSize -> 30],
   Style["\!\(\*SubscriptBox[\(N\), \(c\)]\) = 15", FontSize -> 30],
```

```
   Style["\!\(\*SubscriptBox[\(N\), \(c\)]\) \[RightArrow] \
\[Infinity]", FontSize -> 30]}, LegendPosition -> {-.8, -.0},
 LegendSize -> {0.5, 0.50}, LegendShadow -> None,
 AxesLabel -> {"JD", "<W>/\!\(\*SubscriptBox[\(N\), \(c\)]\)"},
 LabelStyle -> Directive[30], ImageSize -> 750,
 TicksStyle -> Directive[30]]
```

B.3.2 Plot 5.2b: $\langle W^{\dagger} \rangle$ vs. JD

```
(*<(W^\[Dagger])>*)
Needs["PlotLegends`"]
AnalytList =
  Table[{i,
    If[i <= 1 - 2*h,
     a/(1 - i), ((1 - h/i + Sqrt[(1 + h/i)^2 - 1/i])*Exp[mu])/2]}, {i,
     JDMin, JDMax, (JDMax - JDMin)/100}];
NumList =
  Table[If[j <= NNc,
    Table[{Data[[1, i, j]], Data[[5, i, j]]}, {i, NJD}],
    AnalytList], {j, 1, NNc + 1}];
ListPlot[NumList, Joined -> {False, False, False, False, True},
 PlotStyle -> {Thick},
 PlotMarkers -> {Style["\[Cross]", FontSize -> 15, Bold],
   Style["\[Cross]", FontSize -> 15, Bold],
   Style["\[Cross]", FontSize -> 15, Bold],
   Style["\[Cross]", FontSize -> 15, Bold], ""},
 PlotLegend -> {Style["\!\(\*SubscriptBox[\(N\), \(c\)]\) = 1",
    FontSize -> 30],
   Style["\!\(\*SubscriptBox[\(N\), \(c\)]\) = 3", FontSize -> 30],
   Style["\!\(\*SubscriptBox[\(N\), \(c\)]\) = 7", FontSize -> 30],
   Style["\!\(\*SubscriptBox[\(N\), \(c\)]\) = 15", FontSize -> 30],
   Style["\!\(\*SubscriptBox[\(N\), \(c\)]\) \[RightArrow] \
\[Infinity]", FontSize -> 30]}, LegendPosition -> {-.8, -.0},
 LegendSize -> {0.5, 0.50}, LegendShadow -> None,
 AxesLabel -> {"JD",
   "<\!\(\*SuperscriptBox[\(W\), \
\(\[Dagger]\)]\)>/\!\(\*SubscriptBox[\(N\), \(c\)]\)"},
 LabelStyle -> Directive[30], ImageSize -> 750,
 TicksStyle -> Directive[30]]
```

B.3.3 Plot 5.2d: h_{+} vs. JD

```
(*<Subscript[h, +]>*)
```

```
Needs["PlotLegends`"]
AnalytList =
  Table[{i,
    If[i <= 1 - 2*h,
     a/(1 - i), ((i + h + Sqrt[(i + h)^2 - i])*Exp[mu])/2]}, {i,
    JDMin, JDMax, (JDMax - JDMin)/100}];
NumList =
  Table[If[j <= NNc,
    Table[{Data[[1, i, j]], Data[[2, i, j]]}, {i, NJD}],
    AnalytList], {j, 1, NNc + 1}];
ListPlot[NumList, Joined -> {False, False, False, False, True},
 PlotStyle -> {Thick},
 PlotMarkers -> {Style["\[Cross]", FontSize -> 15, Bold],
   Style["\[Cross]", FontSize -> 15, Bold],
   Style["\[Cross]", FontSize -> 15, Bold],
   Style["\[Cross]", FontSize -> 15, Bold], ""},
 PlotLegend -> {Style["\!\(\*SubscriptBox[\(N\), \(c\)]\) = 1",
    FontSize -> 30],
   Style["\!\(\*SubscriptBox[\(N\), \(c\)]\) = 3", FontSize -> 30],
   Style["\!\(\*SubscriptBox[\(N\), \(c\)]\) = 7", FontSize -> 30],
   Style["\!\(\*SubscriptBox[\(N\), \(c\)]\) = 15", FontSize -> 30],
   Style["\!\(\*SubscriptBox[\(N\), \(c\)]\) \[RightArrow] \
\[Infinity]", FontSize -> 30]}, LegendPosition -> {-.8, -.0},
 LegendSize -> {0.5, 0.50}, LegendShadow -> None,
 AxesLabel -> {"JD", "\!\(\*SubscriptBox[\(h\), \(+\)]\)"},
 LabelStyle -> Directive[30], ImageSize -> 750,
 TicksStyle -> Directive[30]]
```

B.3.4 Plot 5.2c: h_- vs. JD

```
(*<Subscript[h, -]>*)
Needs["PlotLegends`"]
AnalytList =
  Table[{i,
    If[i <= 1 - 2*h,
     b/(1 - i), ((i + h + Sqrt[(i + h)^2 - i])*Exp[-mu])/2]}, {i,
    JDMin, JDMax, (JDMax - JDMin)/100}];
NumList =
  Table[If[j <= NNc,
    Table[{Data[[1, i, j]], Data[[3, i, j]]}, {i, NJD}],
    AnalytList], {j, 1, NNc + 1}];
ListPlot[NumList, Joined -> {False, False, False, False, True},
 PlotStyle -> {Thick},
```

```
 PlotMarkers -> {Style["\[Cross]", FontSize -> 15, Bold],
   Style["\[Cross]", FontSize -> 15, Bold],
   Style["\[Cross]", FontSize -> 15, Bold],
   Style["\[Cross]", FontSize -> 15, Bold], ""},
 PlotLegend -> {Style["\!\(\*SubscriptBox[\(N\), \(c\)]\) = 1",
    FontSize -> 30],
   Style["\!\(\*SubscriptBox[\(N\), \(c\)]\) = 3", FontSize -> 30],
   Style["\!\(\*SubscriptBox[\(N\), \(c\)]\) = 7", FontSize -> 30],
   Style["\!\(\*SubscriptBox[\(N\), \(c\)]\) = 15", FontSize -> 30],
   Style["\!\(\*SubscriptBox[\(N\), \(c\)]\) \[RightArrow] \
\[Infinity]", FontSize -> 30]}, LegendPosition -> {-.8, -.0},
 LegendSize -> {0.5, 0.50}, LegendShadow -> None,
 AxesLabel -> {"JD", "\!\(\*SubscriptBox[\(h\), \(-\)]\)"},
 LabelStyle -> Directive[30], ImageSize -> 750,
 TicksStyle -> Directive[30]]
```

B.4 Plot 5.3: The Free Energy

```
Needs["PlotLegends`"]
DenAndLine =
  Show[DensityPlot[
    If[JD < 1 -
       2 h, -h^2/(1 -
        JD), (JD/4)*(1 - h/JD + Sqrt[(1 + h/JD)^2 - 1/JD])^2 - (JD +
        h + Sqrt[(JD + h)^2 - JD]) -
      Log[(JD + h + Sqrt[(JD + h)^2 - JD])]/2 + 3/4], {h, 0, 1}, {JD,
     0, 2}, ColorFunction -> "LakeColors"(*ColorData[{"SunsetColors",
    "Reverse"}]*)], Plot[1 - 2*h, {h, 0, 0.5}, PlotStyle -> Thick],
   ImageSize -> 750, AxesLabel -> {" h", "JD"},
   LabelStyle -> Directive[30], Frame -> False, Axes -> True,
   TicksStyle -> Directive[30]];
DenAndLineLegend =
  DensityPlot[y, {x, 0, 1}, {y, -4.1, 0},
   ColorFunction -> "LakeColors", PlotPoints -> 51,
   AspectRatio -> Full, PlotRange -> {{0, 1}, {-4.1, 0}},
   Background -> None, Frame -> True,
   FrameTicks -> {None, Range[-4.1, 0, 0.5], None, None},
   ImagePadding -> {{45, 2}, {10, 5}}, BaseStyle -> {FontSize -> 20},
   ImageSize -> {50, 250}];
Graphics[{Inset[
   DenAndLine, {4.4, 4.7}, {Center, Center}, {400, 450} 0.022],
  Inset[DenAndLineLegend, {9.0, 4.7}, {Center, Center}, {6, 35} 0.17],
```

```
  Text[Style["Free Energy", 35], {5, 8.9}]},
 PlotRange -> {{0, 10}, {0, 9.2}}, Frame -> False, ImageSize -> 750]
```

Bibliography

[1] J. Ambjørn and J. L. Petersen, *Quantum Field Theory*. The Niels Bohr Institute, 1999. Lecture notes.

[2] J. F. Cornwell, *Group Theory in Physics, Vol. 1*. Techniques of Physics, Academic Press, London, 1984.

[3] K. F. Riley, M. P. Hobson, and S. Bence, *Mathematical Methods for Physics and Engineering*. Cambridge, UK: Univ. Pr., 4th ed., 2010.

[4] I. Montvay and G. Munster, *Quantum Fields on a Lattice*. Cambridge Monographs On Mathematical Physics, Cambridge, UK: Univ. Pr., paperback ed., 1997.

[5] M. Creutz, *Quarks, Gluons and Lattices*. Cambridge Monographs On Mathematical Physics, Cambridge, UK: Univ. Pr., 1983.

[6] M. Srednicki, *Quantum Field Theory*. Cambridge, UK: University Press, 4th ed., 2010. Chap. 69.

[7] K. G. Wilson, "Confinement of Quarks," *Phys. Rev.*, vol. D10, pp. 2445–2459, 1974.

[8] M. Creutz, "Feynman Rules for Lattice Gauge Theory," *Rev. Mod. Phys.*, vol. 50, p. 561, 1978.

[9] M. Creutz, "On Invariant Integration over SU(N)," *J. Math. Phys.*, vol. 19, p. 2043, 1978.

[10] M. E. Peskin and D. V. Schroeder, *An Introduction to Quantum Field Theory*. Westview Press, 1995.

[11] M. Maggiore, *A Modern introduction to quantum field theory*. Oxford Series in Physics, 12, Oxford University Press, 2005. ISBN 0 19 852073 5.

[12] J. Smit, *Introduction to Quantum Fields on a Lattice: A Robust Mate*, vol. 15 of *Cambridge Lecture Notes in Physics*. Cambridge, UK: Univ. Pr., 2002.

[13] M. Creutz, *Quarks, Gluons and Lattices*. Cambridge Monographs On Mathematical Physics, Cambridge, UK: Univ. Pr., 1983. Chap. 7.

[14] M. Creutz, *Quarks, Gluons and Lattices*. Cambridge Monographs On Mathematical Physics, Cambridge, UK: Univ. Pr., 1983. Chap. 5.

[15] J. Smit, *Introduction to Quantum Fields on a Lattice: A Robust Mate*, vol. 15 of *Cambridge Lecture Notes in Physics*. Cambridge, UK: Univ. Pr., 2002. Chap. 6.

[16] I. Montvay and G. Munster, *Quantum Fields on a Lattice*. Cambridge Monographs On Mathematical Physics, Cambridge, UK: Univ. Pr., paperback ed., 1997. Sec. 5.4.3.

[17] J. Bartholomew, D. Hochberg, P. H. Damgaard, and M. Gross, "Effect of Quarks on SU(N) Deconfinement Phase Transitions," *Phys. Lett.*, vol. B133, p. 218, 1983.

[18] J. Langelage, S. Lottini, and O. Philipsen, "Centre symmetric 3d effective actions for thermal SU(N) Yang-Mills from strong coupling series," *JHEP*, vol. 02, p. 057, 2011.

[19] M. Fromm, J. Langelage, S. Lottini, and O. Philipsen, "The QCD deconfinement transition for heavy quarks and all baryon chemical potentials," *JHEP*, vol. 01, p. 042, 2012.

[20] B. Schlittgen and T. Wettig, "Generalizations of some integrals over the unitary group," *J.Phys.A*, vol. A36, pp. 3195–3202, 2003.

[21] A. Balantekin, "Character expansions, Itzykson-Zuber integrals, and the QCD partition function," *Phys.Rev.*, vol. D62, p. 085017, 2000.

[22] P. H. Damgaard and A. Patkos, "Analytic Results for the Effective Theory of Thermal Polyakov Loops," *Phys. Lett.*, vol. B172, p. 369, 1986.

[23] D. J. Gross and E. Witten, "Possible Third Order Phase Transition in the Large N Lattice Gauge Theory," *Phys. Rev.*, vol. D21, pp. 446–453, 1980.